CRANFIELD UNIVERSITY
&
UNIVERSITY OF AVEIRO

Eliana Marisa dos Santos Cavaleiro

Development of Polymeric Materials to Inhibit Bacterial Quorum Sensing

Faculty of Medicine and Biosciences & Department of Biology

PhD Thesis
Academic Year: 2010 - 2014

Supervisors: Dr. Iva Chianella
Dr. Ana Sofia Duarte
Prof. Dr. António Correia

July 2014

CRANFIELD UNIVERSITY

Faculty of Medicine and Biosciences

Doctor of Philosophy (PhD)

Academic Year 2013- 2014

Eliana Marisa dos Santos Cavaleiro

Development of polymeric materials to inhibit Quorum Sensing

Supervisors: Dr. Iva Chianella
Dr. Ana Sofia Duarte
Prof. Dr. António Correia

This thesis is submitted in partial fulfilment of the requirements for the degree of Doctor of Philosophy

ABSTRACT

Bacterial infections are an increasing problem for human health. In fact, an increasing number of infections are caused by bacteria that are resistant to most antibiotics and their combinations. A new solution to fight bacteria and infectious diseases, without promoting antimicrobial resistance, is required. A promise strategy is the disruption or attenuation of bacterial Quorum Sensing (QS), a refined system that bacteria use to communicate. In a QS event, bacteria produce and release specific small chemicals, signal molecules - autoinducers (AIs) - into the environment. AIs regulate gene expression as a function of cell population density. Phenotypes mediated by QS (QS-phenotypes) include virulence factors, toxin production, antibiotic resistance and biofilm formation. In this work, two polymeric materials (linear polymers and molecularly imprinted nanoparticles) were developed and their ability to attenuate QS was evaluated. Both types of polymers should be able to adsorb bacterial signal molecules, limiting their availability in the extracellular environment, with expected disruption of QS. Linear polymers were composed by methyl methacrylate as backbone and itaconic acid or methacrylic acid as functional monomer. IA and MAA monomers were identified by computer modelling to have strong interactions with the AIs produced by Gram-negative bacteria. Molecularly imprinted polymer nanoparticles (MIP NPs), which also contained MAA, have recognition capability for the analyte of interest. Both the linear polymers and MIP NPs, tested free in solutions and coated to surfaces, showed ability to disrupt QS by decreasing bioluminescence of *Vibrio fischeri* and biofilm formation of *Aeromonas hydrophila*. No significant effect on bacterial growth was detected. Cytotoxicity in fibroblast-like Vero cell line showed no cytotoxic effect either by the linear polymers or by MIP NPs. The cellular viability was not affected during the 48 hours exposition to the polymers (linear polymers and MIP NPs). The biofilm formation of *A. hydrophila* was significantly affected in the presence of the linear polymers, pIA_{25}-*co*-$pMMA_{75}$ and $pMAA_{25}$-*co*-$pMMA_{75}$. The MIP NPs coated in cover slips also had an effect on biofilm formation of *A. hydrophila.* The bioluminescence of *V. fischeri*, in presence of

pIA$_{25}$-co-pMMA$_{75}$ had a significant delay and a reduction compared to the *V. fischeri* without the linear polymer. The *pIA$_{25}$-co-pMMA$_{75}$* showed to be more efficient then *pMAA$_{25}$-co-pMMA$_{75}$* in terms of interfering with bioluminescence. A solution of MIP NPs also had an effect (reduction) on biofilm formation of *A. hydrophila* and produced a bioluminescence delay during the exponential phase *V. fischeri*. In conclusion, the results reported in this thesis, show that the polymers developed are a promising strategy to disrupt QS and reduce bacterial infection and resistance. In addition, due to their low toxicity, solubility and easy integration by surface coating, the polymers have potential for applications in scenarios where bacterial infection is a problem: medicine, pharmaceutical, food industry and in agriculture or aquaculture.

Keywords: Quorum Sensing, Linear Polymers, Molecularly Imprinted Nanoparticles, *Vibrio fischeri*, *Aeromonas hydrophila*

ACKNOWLEDGEMENTS

This work was developed at the Department of Biology/CESAM at the University of Aveiro and at the Cranfield Health Department (?) of Cranfield University. I would like to thank to both Institutions and all their staff, for providing me with the technical support necessary to perform this work, as well as to FCT (Foundation of Science and Technology) for funding this work, with the PhD grant BD/47502/2008.

I would like to thank my supervisors, Prof. António Correia, Dr. Ana Sofia Duarte and Dr. Iva Chianella for their support, encouragement and guidance through this pathway. Thank you professor António Correia for introducing me to microbiology, for sharing your enthusiasm and passion for the micro-world. Thank you Dr. Ana Sofia Duarte for all the moments, all the situations, all the teachings, for all your patience and friendship. I'm deeply grateful to Dr. Iva Chianella, for receiving me so well in Cranfield, with so much kindness and gentleness, for being so helpful in all the situations, for the teaching, for the talks, for making me a better person, and for the friendship for the life: thank you so very much!!!

I would like to thank Prof. Sergey Piletsky, for integrating me so well in the group. I would like to thank to Dr. Mike Whitcombe for his incredible help and teaching of polymers. To Dr. Elena Piletska for her constant help, support and availability with the HPCL thank you!! I would also like to thank Dr. Kal Karim and Dr. Dhana Lakshmi, for having contribute to my integration within the group. To all my lab-colleagues, Alessandro, Luismi, Francesco, Isabel, Ewa, for the amusing and pleasant moments spent in the lab. To Dr. António Guerreiro, I would like to thank his patience, teaching on MIP NPs, support and friendship.

I would like to thank all the amazing people that I met in Cranfield, who contributed to me feeling welcomed and at home from the very first day; I will carry them in my memories and thoughts forever. Especially to the "tugas": Gonçalo, António, Francisco, João, Carla, Cátia Sousa, thank you for making my life happier.

To professor Paula Gonçalves, I would like to thank for the lab facilities on cell culture. To Virgilia and Ana a very especial thanks for sharing good and bad moments alike.

I would like to acknowledge Dr. Ana Cristina Esteves for all the support on the data statistics and on the writing, for being so helpful, thank you for believing!

I would like to acknowledge all the people from the MicroLab that during all these years, allowed an amazing environment and to all good moments (inside and outside the lab), thank you my people!

A very deep, heartfelt and especial thanks to Juliana, Susana and Nádia that were my grounding when things were not so optimistic. You are in my heart for ever! Love you my girls! Also, a special acknowledgement to Luisa and Tânia, for being there for me when I needed.

I also would like to thank to my dear friends Gonçalo, Mónica, Korrodi, and Rita that have accompanied me during these years, encouraging me and supporting me. Thanks a lot everyone!

And last but not least, I would like to thank my entire family but especially my parents and my lovely sister Tânia, for their support and encouragement, for understanding my prolonged absences and missing important dates, for always being there when I needed it. I love you all.

The most especial thanks is to my dear husband for his endless love, enduring support, encouragement and understanding through all these years together. Love you!!

TABLE OF CONTENTS

LIST OF FIGURES

LIST OF TABLES

LIST OF ABBREVIATIONS

3-oxo-C_6-AHL	N-(β-ketocapryloyl)-DL-Homoserine Lactone
ACN	Acetonitrile
AHL	Acyl-homoserine lactone
AIs	Autoinducers
AI-2	Autoinducer 2
AIBN	2,2'-azobis-(2-isobutyronitrile)
APTMS	3-aminopropyltrimethyloxysilane
ATCC	American Type Culture Collection
Butyrolactone hydrobromide	[(S)-(−)-α-Amino-γ-butyrolactone hydrobromide
C_4-AHL	N-Butyryl-L-Homoserine Lactone
C_6-AHL	N-Hexanoyl-DL-Homoserine Lactone
CD_3OD	Methanol-D4
$CDCl_3$	Chloroform-D
CECT	Spanish Type Culture Collection
CFU	Colony Forming Unit
CTA	Chain Transfer Agent
DLS	Dynamic Light Scattering
DMEM	Dulbecco's Modified Eagle's Medium
DMF	Dimethylformamide
DPD	4,5-dihydroxy-2,3-pentandione
ECACC	European Collection of Cell Culture
EDC	N-(3-Dimethylaminopropyl)-N′-ethylcarbodiimide hydrochloride
EGDMA	Ethylene Glycol Dimethacrylate
EPS	Extracellular Polymeric Substances
ESI	Electrospray Ionization
FBS	Fetal Bovine Serum
GPC	Gel Permeation Chromatography

HPLC-MS	High Performance Liquid Chromatography-Mass Spectrometry
HSL	Homoserine Lactone
INIFERTER	*Ini*tiator, Trans*fer* Agent, *Ter*minator
IA	Itaconic Acid
K_a	Association Rate Constant
K_A	Equilibrium Association Constant
K_d	Dissociation Rate Constant
K_D	Equilibrium Dissociation Constant
LB	Luria - Bertani
M	Molar
MAA	Methacrylic Acid
MB	Marine Broth
MES	2-[morpholino]ethanesulfonic Acid
MHz	Megahertz
MIPs	Molecularly Imprinted Polymers
MIP NPs	Molecularly Imprinted Polymer Nanoparticles
MM	Molecular Modelling
MMA	Methyl Methacrylate
Mn	Molecular Number
Mw	Molecular Weight
MTT	3-(4,5-dimethylthiazol-2-yl)-2,5-diphenyltetrazolium bromide
NaCl	Sodium Chloride
Na_2CO_3	Sodium Carbonate
NaOH	Sodium Hydroxide
NB	Nutrient Broth
NHS	N-hydroxysuccinimide
NMR	Nuclear Magnetic Resonance
NPs	Nanoparticles
ON	OverNight Conditions

PBS	Phosphate Buffered Saline
PDI	Polydispersity Index
PEG	Polyethylene Glycol
PMMA	Poly-(Methyl Methacrylate)
ppm	Parts Per Million
QS	Quorum Sensing
RLU	Relative Light Units
RT	Room Temperature
SPR	Surface Plasmon Resonance
SSP	Signal Sequestering Polymer
TEM	Transmission Electron Microscopy
TRIM	Trimethylolpropane Trimethacrylate
UV	Ultraviolet

Chapter 1

Introduction and Aim and Objectives

1 Introduction

After Alexander Fleming discovered in the late 1920s penicillin - the first of many antibiotics that are still used today - the general feeling was that infectious diseases were under control and that pathogenic bacteria were no longer a major threat. Unfortunately, nowadays the number of organisms showing resistance to antimicrobial drugs is on the increasing and showing increasingly less effectiveness. The ability of bacteria to evolve quickly, combined with the intensive use of antibiotics (and other antimicrobial drugs) in human and veterinary medicine as well as in agriculture or aquaculture, have been appointed as factors leading to the spread of antibiotic resistance in bacteria.

The scientific community and the pharmaceutical industries are actively searching for new solutions to avoid bacterial infections without inducing resistance mechanisms. Nonetheless, many studies focus in the identification of new cell targets or new families of drugs capable to fight bacteria, which may reveal to be a short term solution to the problem, mainly because bacteria might become resistant to the developed drugs.

One of the most promising strategies is the disruption or attenuation of bacterial Quorum Sensing (QS) (Finch *et al.* 1998, Williams 2002). Bacterial virulence, resistance to antibiotics and biofilm formation are linked to QS. QS is the ability of microorganisms to regulate their gene expression according to fluctuations in cell population density. In a QS event, bacteria release specific small chemicals (signal molecules/autoinducers) into the environment (Bassler 1999, Miller and Bassler 2001). Microorganisms are able to respond to the total quantity of the autoinducer in the environment and therefore are able to sense population density (Fuqua *et al.* 1994, Swift *et al.* 1996). Using this information microorganisms communicate and coordinate their behaviour accordingly, expressing virulence factors or antibiotics resistance determinants and/or creating biofilms. The type of autoinducers released into the environment depends on bacterial species. Whereas the most common signal molecules for Gram-negative bacteria are N-acyl-L-homoserine lactones (AHLs) (Fuqua *et al.*

1996), Gram-positive bacteria release a variety of small peptides (Reading and Sperandio 2006).

There are a number of methods currently being evaluated, to attenuate QS and consequently to moderate QS related phenotypes. They include use of antibodies, vaccines or enzymes/catalysts directed against the signal molecules, or the application of agonists or antagonists based on the similarity with molecular structures of the signal molecules (Cámara *et al.* 2002, Pan and Ren 2009, Tsao *et al.* 2012). Unfortunately most of these methods rely either on toxic chemicals (which cannot be considered for example as therapeutics) or on compounds too difficult to produce and manufacture in large scale.

This thesis describes the development of materials able to attenuate QS in Gram-negative bacteria. The method proposed involves sequestering bacterial signal molecules, N-acyl-L-homoserine lactones (AHLs), using two types of polymers: linear polymers and molecularly imprinted polymer nanoparticles (MIP NPs). The linear polymers are synthesised using monomers that are known to create strong non covalent interactions with AHLs. Molecularly imprinted polymers are cross-linked polymers, that possess recognition capabilities for the analyte of interest (Alexander *et al.* 2006). The MIPs can be prepared with many different formats such as bulk (powder) (Pérez-Moral and Mayes 2006), membranes, films for sensors (Haupt *et al.* 1999, Pichon and Haupt 2006, Sergeyeva *et al.* 2010) and nanoparticles (Pérez-Moral and Mayes 2006, Poma 2012). Nanoparticles, due to the high ratio of surface area over volume of this format, have a great potential for a variety of applications, such as Elisa-like assays (Chianella *et al.* 2013, Korposh *et al.* 2014, Shutov *et al.* 2014).

The use of MIPs (in bulk form) and of cross-linked polymers for the attenuation of QS has been tried before for *Vibrio fischeri* (Piletska *et al.* 2010) and *Pseudomonas aeruginosa* (Piletska *et al.* 2011). Linear polymers and MIP NPs were never tested before.

Synthetic polymers are known for their robustness that makes them ideal for environmental and clinical applications. Polymers designed with specific recognition capabilities can adsorb and remove signal molecules from a system, reducing their concentration below the threshold necessary for the activation of QS. This would disrupt the communication between bacterial cells, thus avoiding the activation genes involved in the expression of QS phenotypes. One of the advantages of polymers in QS attenuation strategies is that it is not expected that the removal of signal molecules from the system induce mutagenesis or the development of bacterial resistance. Another advantage is the wide range of convenient formats that polymers can adopt such as films, injection moulds and nanoparticles, offering the possibility to reduce QS-based infections in many different settings.

In this work linear polymers and the MIP NPs were used to attenuate QS of *V. fischeri* and *A. hydrophila*. *Vibrio fischeri* was selected as model microorganism due to its QS related phenotype. In fact, in *V. fischeri* bioluminescence is a QS process dependent that can be easily measured. In addition, since this bacterium was studied before, the results obtained here can be compared with those obtained in the past for an evaluation of the efficacy of the material produced in this work.

Aeromonas hydrophila is a Gram-negative bacterium whose production of biofilms is regulated by QS. *Aeromonas hydrophila* is widely spread in aquatic environments such as estuarine and marine waters, wastewater and drinking water (Holmes and Nicolls 1995, EPA 2006). The major impact of *Aeromonas* pathogenicity is in the aquaculture industry and in clinical settings (EPA 2006). In fact, *A. hydrophila* causes wound infections in humans and haemorrhagic septicaemia in fish (Vivas *et al.* 2004, Chen *et al.* 2010). This last feature makes this microorganism one among others responsible for significant economic losses in farm raised fish.

In the aquaculture industry, infectious diseases are one of the major limiting factors and control of diseases has become a key to successful fish farming

management (Rasch *et al.* 2004, Vivas *et al.* 2004). Currently, infectious diseases in aquacultures are controlled through heavy (and sometimes unjustified) use of antibiotics and chemical compounds like disinfectants, which largely contribute to the increase in bacterial resistance (Williams 2002, Chen *et al.* 2010).

A few researchers have reported the use of vaccines as an alternative to antibiotics to control the extent of infectious diseases in farmed fish, with reduction in economic losses (Defoirdt *et al.* 2004). However, vaccines seem to work against a limited type of bacteria and their efficacy and safety is still not completely understood (Poobalane *et al.* 2010). Therefore, the need for developing alternative or complementary methods to control bacterial diseases without inducing bacterial resistance is urgent.

1.1 Aim and Objectives

The thesis is structured in six chapters. Chapter 1 presents an introduction relating the main topic of this thesis - infectious diseases caused by bacteria, and briefly explaining the actual strategies to control this issue. Chapter 2 contains a review of the literature, providing relevant information for the understanding of communication mechanisms of bacteria. It also presents a current understanding of the synthetic materials (Linear Polymers and MIP NPs) used in this project. Chapter 3, one of the experimental chapters, is presented in a manuscript format. It describes the results obtained by interrupting bacterial communication by using Linear Polymers. Chapter 4, presented also in a manuscript format, describes the results obtained by testing the MIP NPs in the bacterial communication. Chapter 5 reports a final discussion and Chapter 6 gives a general conclusion and some perspectives of future work.

The main aim of this project is the development of non-toxic polymers (linear polymers and MIP NPs) capable to disrupt or attenuate Quorum Sensing in Gram-negative bacteria by selectively sequestration of the signal molecules released from bacteria. In the future, such polymers may be used to reduce

bacterial infections, without inducing the development of antimicrobial resistance.

In order to evaluate the performance of the polymers in QS disruption, two model bacteria will be used: *Vibrio fischeri* ATCC 7744 and *Aeromonas hydrophila* IR-13.

To achieve the main aim of this project, the objectives of this work have been:

1. The synthesis and optimisation of linear polymers based on functional monomers (methacrylic acid or itaconic acid) and an inert monomer (methyl methacrylate), by free radical polymerisation technique;

2. The chemical and physical evaluation of the produced polymers (molecular weight, composition and binding capacity) by NMR, GPC, HPLC-MS and optical microscopy;

3. The evaluation of biological properties of the linear polymers: the cytotoxicity using the mammalian Vero cell line. The ability to attenuate QS-phenotypes of *V. fischeri* (bioluminescence) and *A. hydrophila* (biofilm) through RLU measurements and resazurin methodology, respectively;

4. The synthesis of molecularly imprinted polymer nanoparticles (MIP NPs) using the solid-phase approach methodology;

5. The characterisation of MIP NPs by dynamic light scattering (DLS), surface plasmon resonance (SPR) and transmission electron microscopy (TEM);

6. The evaluation of MIP NPs cytotoxicity using the mammalian Vero cell line; and the ability to attenuate QS-phenotypes of *V. fischeri* (bioluminescence) and *A. hydrophila* (biofilm) through RLU measurements and resazurin methodology, respectively;

The objectives 1-3 linked with the disruption of QS, in *V. fischeri* and *A. hydrophila*, by the linear polymers are described in chapter 3. Chapter 4 described the effect of the MIP NPs in QS-phenotypes of *V. fischeri* and *A. hydrophila*.

Chapter 2

Literature Review

2 Literature Review

This chapter includes a detailed description of the scientific background necessary to understand the rest of the thesis. This includes explanation of Quorum Sensing and its mechanism in the two bacteria used in the project. In addition to this, a general description of polymers production including synthesis of molecularly imprinted polymers is reported. Furthermore, each section is enriched with the latest research findings available in the scientific literature.

2.1 Quorum Sensing

Specific bacterial phenotypes are responsible for the growth and proliferation of microorganisms in different environments (Fuqua *et al.* 1994, Swift *et al.* 1996). Gram-negative and Gram-positive microorganisms use cell-to-cell communication systems to regulate some of their phenotypes (Bassler 1999, Gera and Srivastava 2006). The majority of these phenotypes are density-depend and consequently influenced by the increase of microbial population (Fuqua *et al.* 1994, Swift *et al.* 1996, Waters and Bassler 2005a).

In a specific environment, once the appropriate population density is attained and cross-communication is established, these phenotypes provide a successful microbial community function: antibiotic production, bioluminescence, nodulation, conjugation, sporulation, biocorrosion, swarming, biofilm production and expression of several virulence factors such as toxins, which are phenotypes correlated with QS. Figure 2-1 shows how phenotypic diversity can be modulated by QS (Finch *et al.* 1998, Williams *et al.* 2000, Whitehead *et al.* 2001, Camilli and Bassler 2006, Dobretsov *et al.* 2009, Defoirdt *et al.* 2010). Hence, bacterial populations are able to coordinate activities as a multicellular organism (Bassler 1999); they act as a group using a cell-to-cell communication system as an exceptional tool to proliferate (Miller and Bassler 2001).

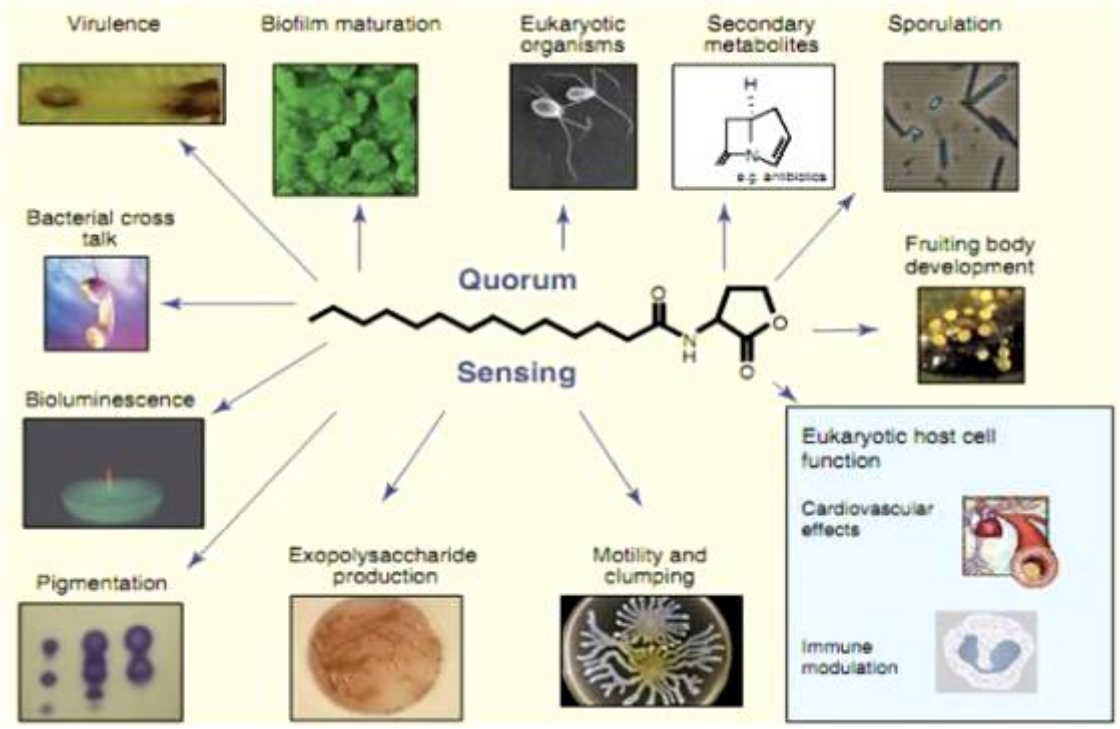

Figure 2-1 Illustration of several phenotypes regulated by Quorum Sensing in Gram-negative and Gram-positive bacteria (*adapted from* Diggle *et al.* 2007)**.**

The term Quorum Sensing, introduced by Fuqua and co-workers (1994), describes a refined system of communication that consists on emitting and receiving chemical messages, to and from bacteria, in a cell-density-dependent manner. The communication between bacteria is mediated by small diffusible molecules called autoinducers (AIs) (Bassler 1999). AIs are produced inside the cell at low levels and diffuse outside through cell membrane. Whenever the outside concentration of signal molecules reaches a critical value these molecules re-enter the cells as Figure 2-2 illustrates (Fuqua *et al.* 1994, Miller and Bassler 2001). As bacterial population grows, extracellular signal molecules also increase. When a critical concentration is reached, cells respond by altering their gene expression. Consequently, autoinducers are linked to gene expression as a function of cell population density (Bassler and Losick 2006, Williams 2007a).

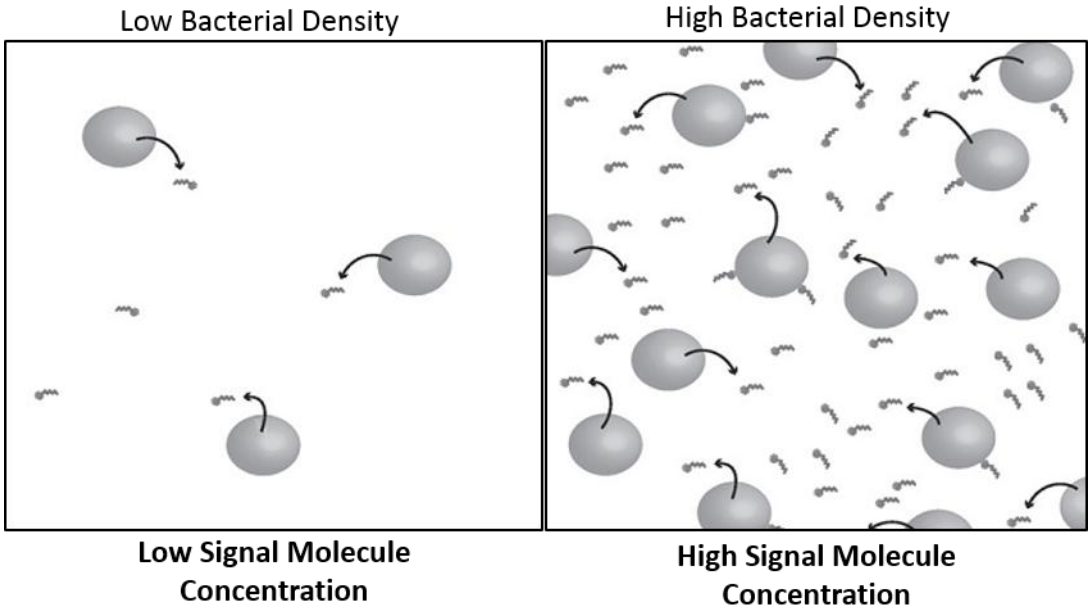

Figure 2-2 Principle of Quorum Sensing: at low bacterial density (left), the signal molecule concentration is also low and no threshold it exceed. When the bacterial density becomes high (right), the signal molecule concentration is also high and a threshold is reached. Consequently, gene expression is changed by connection between signal molecule and receptor (*adapted from* Boyen *et al.* 2009)**.**

The specificity of QS is very high due to the specificity of the interactions between the signal molecules and their receptors. The signal molecules are different in Gram-negative and Gram-positive bacteria (Waters and Bassler 2005a). Depending on environmental stimuli, several bacterial genes that are involved in pathogenicity are also regulated by QS (Asad and Opal 2008). Some examples are the motility in *Yersinia*, the production of antibiotics in *Erwinia* and biofilm formation in *Pseudomonas aeruginosa* (Williams *et al.* 2000, Smith and Iglewski 2003).

2.1.1 Quorum Sensing Intercellular Signals

Bacteria use different QS systems. The LuxR/LuxI-type system is used by Gram-negative bacteria with N-acyl-homoserine lactone (AHL) (Figure 2-3) being the signalling molecule (Fuqua *et al.* 1996). In Gram-positive bacteria the QS systems use peptides as signal molecules. For interspecies communication the LuxS/AI-2 signalling system is used with AI-3/epinephrine/norepinephrine as signalling molecules (Reading and Sperandio 2006). Signal molecules are small and diffusible, which allow an easy communication between cells. Autoinducers molecules have the specific characteristics:

i) Their production occurs during precise stages of cell growth and under specific conditions or in response to alterations of the extracellular environment;
ii) They recognise a specific cell receptor and have specific response production, once a threshold is reached outside cell;
iii) Bacterial cellular response increases due to autoinducers physiological alterations (Winzer *et al.* 2002, Atkinson and Williams 2009).

Signal molecules can be small organic molecules (<1000Da) or peptides with 5-10 amino acids (Williams 2007b). Gram-negative bacteria can also use other molecules such as long-chain fatty acid derivatives and fatty acid methyl esters, or, as Gram-positive bacteria, even peptides such as the 4,5-dihydroxy-2,3-pentandione (DPD), collectively referred to as autoinducer 2 (AI-2) and autoinducer 3 (AI-3) (Williams 2007b, Atkinson and Williams 2009). Gram-positive bacteria can also produce AI-2, though these bacteria prefer to use other types of peptides (Bassler and Losick 2006).

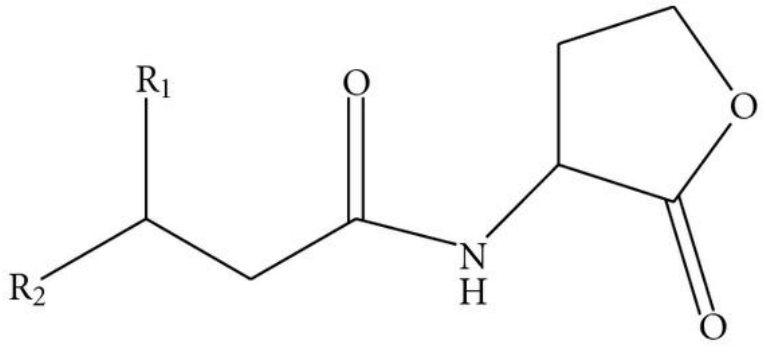

Figure 2-3 Schematic structure of an acyl-HSL (homoserine lactone): where R1 can be H, OH or O; and R2 can be (CH) or (CH-CH-CH=CH-CH-CH). The acylated acyl carrier protein (Acyl-ACP) and the S-adenosylmethionine (SAM) are the substrates (*adapted from* Greenberg 2000)**.**

2.1.2 Quorum Sensing in Gram-Negative Bacteria

Gram-negative bacteria produce and use N-acyl-L-homoserine lactones (AHLs) as intercellular signal molecules for cell-to-cell communication (Fuqua *et al.* 2001). The N-(3-oxohexanoyl)-L-homoserine lactone (3-oxo-C_6-AHL) used by *V. fischeri* was the first AHL identified as autoinducer (Engebrecht *et al.* 1983). AHL (Figure 2-3) has a conserved homoserine lactone ring that can be linked to a variable length acyl side chain (4-18 carbon atoms). This chain can undergo variable and extra modifications (Greenberg 2000). Short chain AHLs can pass freely in and out of the bacterial cell. Long chain AHLs need an activation mechanism for their transport across the cell membrane (Fuqua *et al.* 2001, Boyen *et al.* 2009).

The AHLs signal molecules are synthesised by the LuxI/LuxR system. The LuxI protein, also known as AHL synthase, is responsible for the synthesis of AHLs while the LuxR homologues are proteins belonging to a family of transcriptional regulators. The LuxI synthase uses S-adenosylmethionine (SAM) as substrate and acyl-acyl carrier proteins (Bassler 1999, Parsek *et al.* 1999). After synthesis, the AHLs are released outside the cell. When a specific

concentration threshold is reached, the cytoplasmic proteins, such as LuxR protein (AHL receptor), detect and bind AHLs (Fuqua *et al.* 1996, Cámara *et al.* 2002, Atkinson and Williams 2009). This interaction induces LuxR protein dimerization leading to signal detection. The LuxR proteins have in fact two functions: binding the signal molecule (autoinducer) and binding the promoter of target genes inducing their expression and the consequent manifestation of several phenotypes (Fuqua *et al.* 2001). A representation of the mechanism is reported in Figure 2-4.

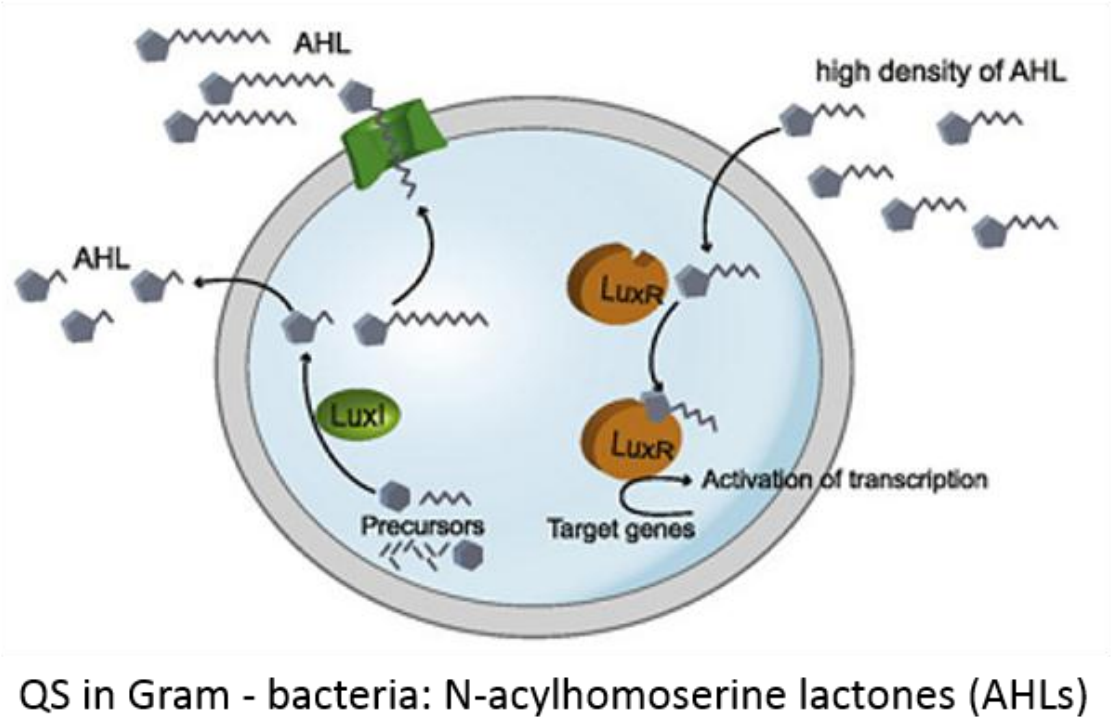

Figure 2-4 Quorum Sensing mechanism in Gram-Negative bacteria (*adapted from* Boyen et al. 2009)**.**

Proteins as LuxR-type frequently bind only to one specific AHL. However they can bind to different AHLs, making them responsible for interspecies communication (Reading and Sperandio 2006). The LuxI/LuxR homologues

show diversity in their mechanism, with variations between different bacterial species. Gram-negative autoinducers have similar structural elements, nevertheless the main difference is essentially in the 3-position of the N-acyl chain, which in some cases can assume the 3-oxo function, as happens in *P. aeruginosa* (Dickschat 2010). The LuxR/LuxI system was identified and described for the first time in the marine species *V. fischeri* and *Vibrio harveyi* (Nealson 1978, Bassler 1999).

In *V. fischeri* bioluminescence is a phenotype resultant of QS intervention. The LuxI/LuxR system is essential in this mechanism. As mentioned before, LuxI protein is responsible for synthesis of acyl-HSL, and LuxR protein for binding autoinducer and promoting transcription of luciferase operon lux*CDABE* (Fuqua *et al.* 1994, Lupp *et al.* 2003).

Pseudomonas aeruginosa is an opportunistic pathogen. Its QS mechanism relies on two signalling systems: the LasI/LasR and the RhII/RhIR (with C_4-homoserine lactone). Both systems are linked to the expression of virulence factors (Bassler 1999, Parsek *et al.* 1999) and biofilm formation (Smith and Iglewski 2003). Similar to *V. fischeri,* in *P. aeruginosa* LasI syntheses 3-oxo-C_{12}-homoserine lactone and LasR regulates the expression of target genes. The RhII/RhIR system has a similar function and also regulates gene expression of the bacterium. Some of the genes involved encode virulence genes, like elastases and proteases, important for the infection process (Jahid *et al.* 2013).

2.1.3 Quorum Sensing in Gram-Positive Bacteria

Gram-positive bacteria do not use the LuxI/LuxR QS system or AHLs as signal molecules; instead, they produce small peptides as autoinducers through the ATP-binding cassette (ABC) exporter protein (Novick and Muir 1999). The mechanism can be seen in Figure 2-5

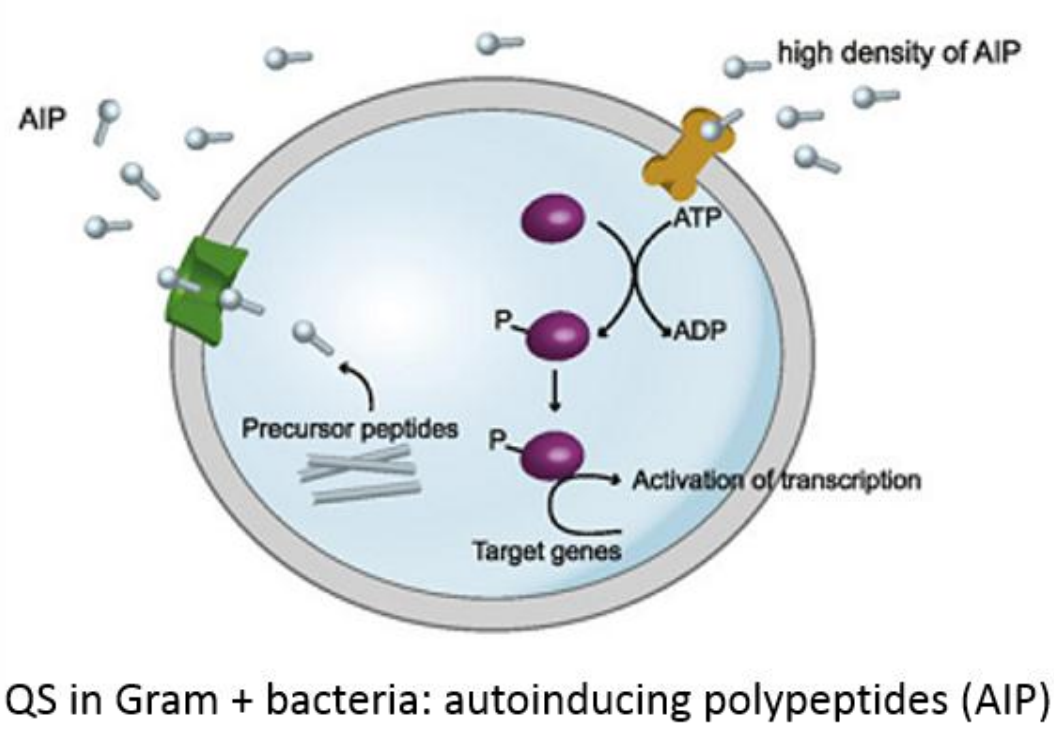

Figure 2-5 Quorum Sensing in Gram-Positive bacteria (*adapted from* Boyen *et al.* 2009)**.**

These autoinducers are known as Auto-Inducing Polypeptides (AIPs). They contain between 5-17 amino acids and they have modifications on side chain such as isoprenyl groups (in *Bacillus* spp.) or thiolactone rings (in *Staphylococcus* spp.). In the cytoplasm, the synthesises of AIPs as precursor peptides occurs; they then are cleaved, modified and transported to the extracellular environment of the bacterium (Lyon and Novick 2004, Boyen *et al.* 2009). At a critical extracellular peptide concentration, kinases (two component system) in cell membranes detect and bind these peptides. Some peptides are transported directly into the cytoplasm to their receptors. These small signal peptides are commonly specific to the corresponding cognate receptor (Bassler 1999, Novick and Geisinger 2008). This type of QS is known to control the development of several bacterial skills in *Bacillus subtilis* and *Streptococcus pneumoniae*, virulence in *Staphylococcus aureus*, conjugation in *Enterococcus*

faecalis and microcin production both in *Lactobacillus sake* and in *Carnobacterium piscicola* (Gera and Srivastava 2006).

Staphylococcus aureus is frequently associated with pneumonia, wound infections and other human diseases; its QS system has been studied. Secretion of toxins, haemolysins, enzymes, enterotoxins and proteases are regulated by the *agr* (accessory gene regulator) system (Novick 2003). Several functions in *S. aureus* pathogenesis have been assigned to these genes. The short peptides (5-9 amino acids) are cyclic and have a thiolactone ring structure at the terminal carboxylic group. The linkage between the carboxyl terminus and a conserved cysteine moiety within the peptide sequences generate the formation of the ring (Lyon and Novick 2004). The peptides are recognised by receptors in the cell surface, activating a histidine kinase that causes the transcriptional activation of multiple gene loci. At low densities, *S. aureus* expresses proteins required for attachment and colonisation. When cell density increases, the protein expression profile changes, with proteins such as proteases and toxins being synthesised (Novick 2003, Novick and Geisinger 2008).

The LuxS protein produces the furanosyl borate ester AI-2 (autoinducer 2). The AI-2 was described in Gram-positive and Gram-negative bacteria, and the mechanism of its production is reported in Figure 2-6 (Schauder *et al.* 2001, Waters and Bassler 2005a). The AI-2 binds a periplasmic protein, interacting with a two-component system or other kind of transporter. After the ligation, a phosphorelay cascade that culminates in activation or repression of gene expression is activated (Novick and Geisinger 2008, Ng and Bassler 2009). The enzymes Pfs and LuxS activate reactions for AI-2 synthesis. SAM (S-adenosylmethionine), in the bacterial cells, operates like a methyl donor resulting in SAH (S-adenosylhomocysteine). However, as SAH is toxic to the cell, bacteria have a mechanism to recycle it. This mechanism takes place with the enzyme Pfs converting SAH to S-rybosylhomocysteine (SHR). AI-2 and homocysteine are produced from SHR by the enzyme LuxS (Schauder *et al.* 2001, Jayaraman and Wood 2008).

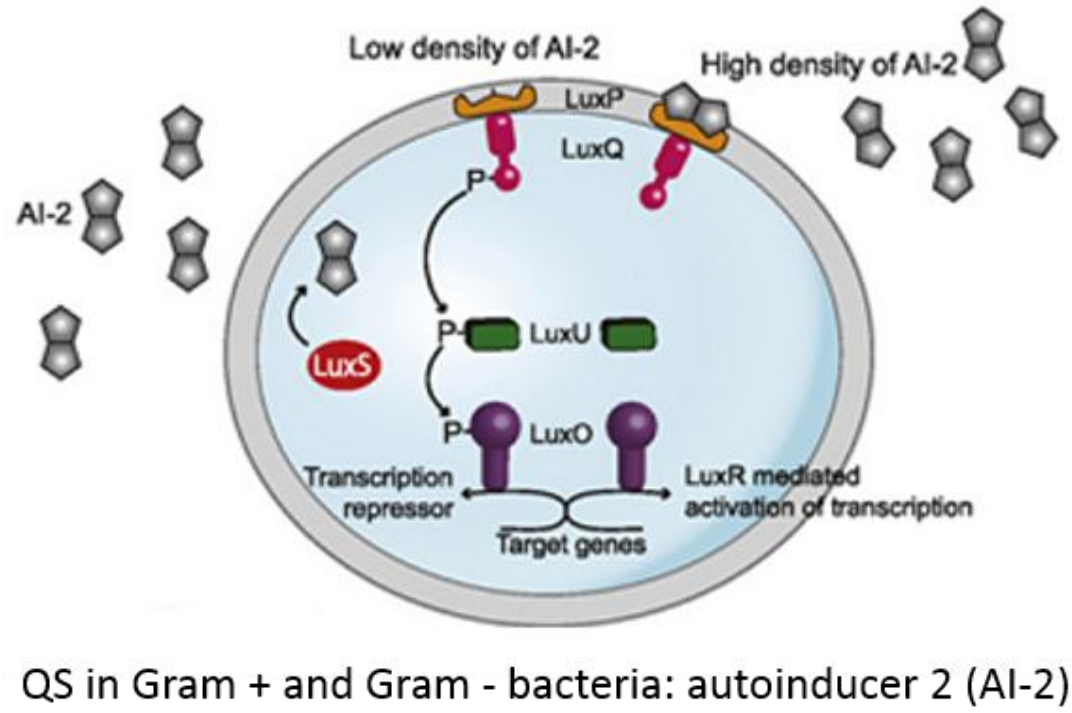

Figure 2-6 Quorum Sensing in Gram-Positive and Gram-Negative bacteria (*adapted from* Boyen *et al.* 2009)**.**

There seems to be several reasons for the synthesis of AI-2 in bacterial cells. One of the most important is that the AI-2 precursor is a main methyl donor in bacterial cells, and therefore activates several metabolic processes. LuxS is also implicated in the detoxification of a metabolic intermediate (Winzer *et al.* 2002). To clarify the role of AI-2 several studies were carried out in organisms like *E. coli* and *V. harveyi*. Researchers believe that production of AI-2 is mainly an effect of SAM utilisation and SAH detoxification (Rezzonico and Duffy 2008). Autoinducer AI-2 is now recognised as one ubiquitous signalling system used by Gram-negative and Gram-positive bacteria. Xavier and Bassler (2003) have described the auto-inducer AI-2 as a “universal signal” for interspecies communication.

The marine bacterium *V. harveyi* uses QS system to control bioluminescence. *V. harveyi* QS mechanism is a mix between components of Gram-positive and

Gram-negative systems (Xavier and Bassler 2003). *Vibrio harveyi* has a second QS pathway, which is controlled by luxS gene locus and associated homologues. However many bacteria contains AI-2 receptor and apparently they do not express luxS gene (Miller and Bassler 2001, Waters and Bassler 2005a, Reading and Sperandio 2006). In *V. harveyi* the periplasmatic LuxP protein is the receptor for AI-2. After the interaction between LuxP and AI-2, the complex binds the LuxQ, a two-component protein that has a sensor kinase domain and a response regulator domain (Neiditch *et al.* 2005).

The Autoinducer type 3 (AI-3) system has many similarities to the AI-2 system as can be seen in Figure 2-7 (Atkinson and Williams 2009). Both use a two-component receptor kinase-intracellular signalling complex to activate gene expression. However, AI-3 system is able to use as signal molecules epinephrine or norepinephrine, two compounds also known as human stress hormones (Fuqua *et al.* 2001). It is still not very clear which molecule can activate AI-3 autoinducers, but there is indication that it might be some type of catecholamines. Nevertheless, in *E. coli* the α-adrenergic receptor can block AI-3 signalling (Reading and Sperandio 2006, Kendall and Sperandio 2007). *Escherichia coli* is responsible for several diseases in humans such as intestinal diseases or haemolytic uremic syndrome. The virulence genes in *E. coli* are also regulated by QS mechanism. The AI-3 autoinducer seems to be related and involved in this regulation (Moxley 2004). The two-component system QseB/C has been identified in numerous bacterial species as the receptor/response regulator of AI-3 and epinephrine/norepinephrine. Despite the incomplete knowledge about this QS system, it has been recognised that it is very important for inter-kingdom communication (Kendall and Sperandio 2007, Boyen *et al.* 2009).

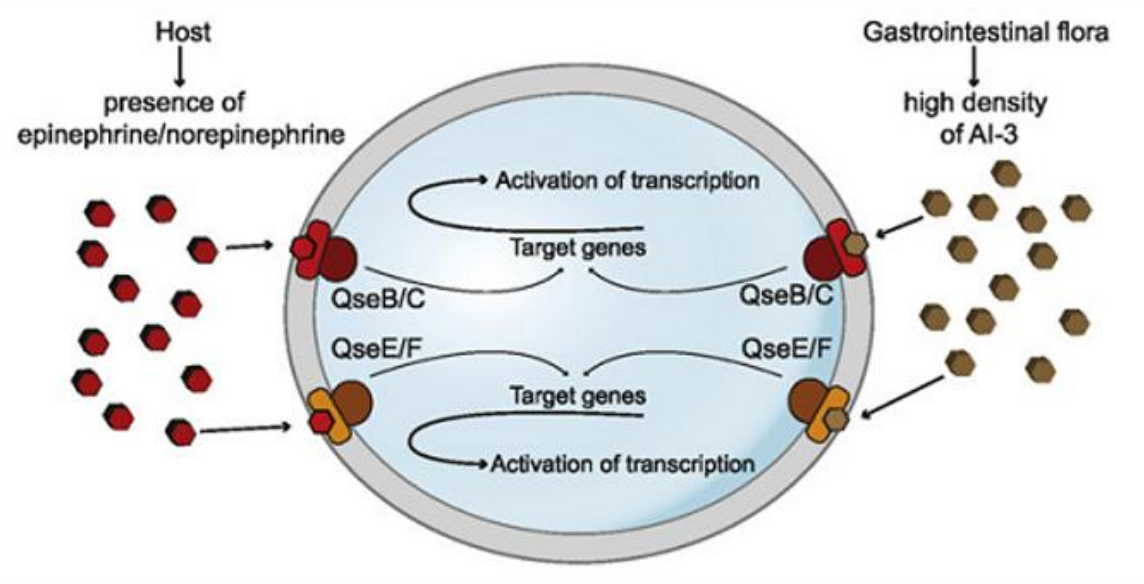

Figure 2-7 Quorum Sensing mechanism using autoinducer 3 (*adapted from* Boyen *et al.* 2009)**.**

2.1.4 Bacterial Behaviours Controlled by QS

2.1.4.1 Bioluminescence

Several marine Gram-negative bacteria, such as *V. fischeri,* emit light, a behaviour regulated by QS. Organisms like squids have evolved organs to house such bacteria and use their bioluminescence during particular nocturnal behaviours (Miyashiro and Ruby 2012).

The mechanisms regulating bacterial bioluminescence are well understood particularly in what concerns the *Vibrionaceae* family (Meighen 1993). The LuxCDABEG genes, that encode all of the structural components necessary for light production, are regulated by the LuxR-LuxI Quorum Sensing. The enzyme luciferase is at the core of light production. Luciferase is a heterodimer

composed of alpha and beta subunits encoded by LuxA and LuxB respectively. The enzyme produces light by oxidising a long chain aldehyde and at the same time reducing a flavin mononucleotide ($FMNH_2$) as described in Figure 2-8. LuxD diverts fatty acids from their biosynthesis pathway and makes them available for luminescence production (Boylan *et al.* 1989). LuxC activates the acyl group within AMP and LuxE reduces it to the long chain aldehyde. LuxC and LuxE use the same mechanism to recycle the long chain fatty acids, produced by the luciferase reaction. Finally LuxG was shown to reduce FMN, also a product of the luciferase reaction (Nijvipakul *et al.* 2008)

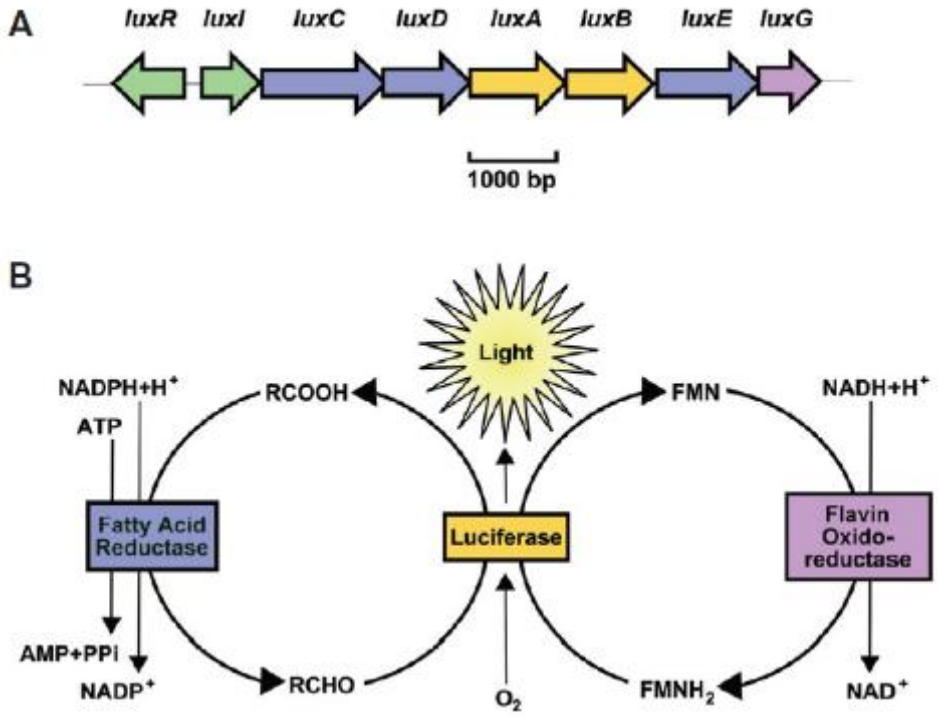

Figure 2-8 Schematic representation of the genes encoding proteins involved in regulating (LuxR and LuxI) and in the production (LuxA-G) of bioluminescence in A); Schematic representation of the enzymatic reaction of luciferase in B) (*adapted from* Miyashiro and Ruby 2012)**.**

2.1.4.2 Biofilm Formation

Most bacteria can be present in nature either as single free suspended cells or associated with a solid surface – a biofilm (Costerton 1995). Physiology, morphology and gene expression patterns are the differences between these two bacterial forms (Miller and Bassler 2001, Landini *et al.* 2010). Biofilms are sessile microbial communities characterised by adhesion to each other and/or to a solid surface producing a hydrated exopolysaccharide matrix. Usually the structure is present as microcolonies enclosed in a matrix (Annous *et al.* 2009). The matrix is constituted by extracellular polysaccharides (EPS), proteins and nucleic acids (DNA), and can assume different structures such as monolayers or multilayer's (Costerton *et al.* 1999). The matrix structure allows transportation of nutrients through circulation in channels, as well as regulation of the waste in and out the biofilm. Inside the biofilm, cells behave more as members of a collective living system rather than as individual cells (Davies *et al.* 1998, Karatan and Watnick 2009) with diverse gene expression in different regions.

Bacterial biofilms are widespread in many environments and almost all species can produce or be part of biofilms. Biofilm communities allow survival and growth of several species in hostile environments (Francolini, Donelli, *et al.* 2004, Dickschat 2010). Biofilms offer a preventive and secure environment for bacteria, providing higher tolerance against several extreme conditions like high or low temperature, salinity, pH and environmental agents or stresses in general (de Kievit and Iglewski 2000, Watnick and Kolter 2000). Inside the biofilms matrix the conditions are favourable for cell-to-cell interactions. For instance, it is known that sensibility of bacteria to antibiotic is altered within biofilms. In fact, bacterial biofilms are much less sensitive to antibiotics that when they are in 'free suspended cells' form (Costerton 1995, Miller and Bassler 2001).

In some cases, biofilms consist on a mixture of diverse bacterial populations, but often may consist of a single bacterial species (Stoodley *et al.* 2002, Annous *et al.* 2009).The essential steps of formation of biofilms (Figure 2-9) are:

attachment, maturation, aggregation and dispersal (Parsek and Greenberg 2005).

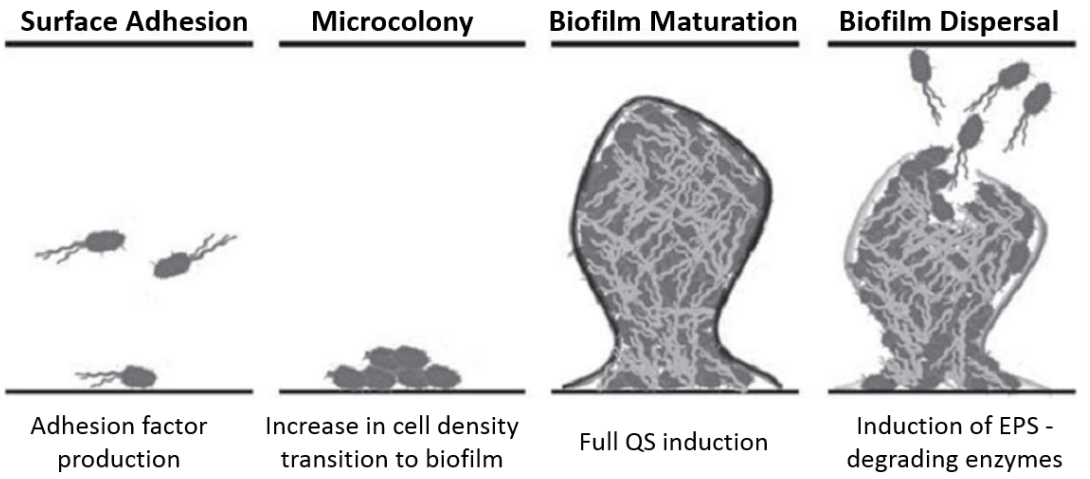

Figure 2-9 General scheme of biofilm formation (*adapted from* Landini *et al.* 2010)**.**

2.1.4.2.1 Attachment

Free and planktonic cells are randomly and reversibly attached to a solid surface or a substratum, through an exopolymeric material formation (Costerton 1995, Toole *et al.* 2000, Stoodley *et al.* 2002). The adhesion depends on the surface nature and on several microbial factors such as the bacterial structures (e.g. flagellum) (Parsek and Greenberg 2005, Karatan and Watnick 2009).

2.1.4.2.2 Maturation

The second step involves cell-to-cell aggregation, proliferation, growing and formation of microcolonies (Stoodley *et al.* 2002). During maturation, biofilms can assume different architectures from flat and homogenous to highly complex films. The type of architecture influences the antimicrobial tolerance of the bacteria present in the biofilm. The architecture can be affected by several factors such as motility or extracellular polymeric substances (EPS) production (Costerton 1995, Branda *et al.* 2005, Parsek and Greenberg 2005). Regardless

the type of architecture in the maturation step biofilms is formed in a 3-dimensional structure enclosing cells in packages with several channels between them. These channels allow water and nutrients transportation, which maintain the cells' survival (Davey and O'toole 2000, Stoodley *et al.* 2002, Annous *et al.* 2009).

2.1.4.2.3 Detachment and Dispersion

At the last step of biofilm formation, the detachment of cells from the biofilm, and their dispersion, occur. Once detached, these cells can attach to other biofilms or be dispersed as planktonic cells (nonadherent cells) (Stoodley *et al.* 2002, Karatan and Watnick 2009, Moons *et al.* 2009). Apparently the dispersed cells might facilitate colonisation of new surfaces, reinitiating the biofilm process at a new location (Parsek and Fuqua 2004, Parsek and Greenberg 2005) or inducing an infection process (Toole *et al.* 2000, Cámara *et al.* 2002, Asad and Opal 2008). The same pathogenic bacteria can use a biofilm as a negative regulation of their virulence factors. It is common for several non-virulent bacteria to grow inside a biofilm. When biofilm dispersion occurs, a high concentration of planktonic bacteria quickly becomes virulent and can be released at the same time (Smith and Iglewski 2003, Karatan and Watnick 2009). Quorum Sensing has been associated with the release of bacteria from the extracellular matrix of the biofilm (Spoering and Gilmore 2006, Nadell *et al.* 2008).

Several infections, such as chronic bacterial infections, are linked to biofilm formation and the usual therapy with antibiotics is generally insufficient for their elimination (Costerton *et al.* 1999, Irie and Parsek 2008). Biofilms represent a resistance mechanism in the sense that they make impossible for antibiotic agents to enter inside the bacterial matrix. Consequently, various medical treatments involving the use of regular antimicrobials fail in destroying biofilms and the bacterial infections (Costerton *et al.* 1999, Francolini, Norris, *et al.* 2004, Defoirdt *et al.* 2010). Biofilms are contributing to the development of antibiotic

resistance, becoming a significant key in the virulence of several pathogenic bacteria (Landini *et al.* 2010). Because of all these issue related with biofilms, it is important to find solutions to prevent biofilm formation and promote the eradication of those already formed. One possible approach, which has been already used for *P. aeruginosa*, is exploiting the relation between biofilms and QS (de Kievit and Iglewski 2000). It has been shown that when QS was blocked, bacterial pathogenicity declined (Francolini, Donelli, *et al.* 2004).

Growing within a biofilm gives advantages for bacterial cells. First, the cells are protected from environmental, chemical and physical stresses such as antimicrobial compounds. Second, the dehydration of bacterial cells is reduced because the polymeric matrix provides the liquid support. Third, the fact that bacterial cells are close to each-other makes easier the transport of nutrients necessary for bacterial maintenance (Costerton 1995, Davey and O'toole 2000, Nadell *et al.* 2008, Karatan and Watnick 2009).

2.1.4.3 Biofilms and Quorum Sensing

As previously described, QS is a complex regulatory process that is dependent on bacterial cell-density (Miller and Bassler 2001). QS is implicated on gene expression and regulation, and in maturation and maintenance of biofilm formation as a manager of available resources (Waters and Bassler 2005b, Jayaraman and Wood 2008).

Cell-to-cell communication is required for bacterial biofilm formation, so QS is inherently linked to the formation of bacterial biofilms (Asad and Opal 2008, Dickschat 2010). Inside a biofilm, the bacterial cell concentration is high; so it is not surprising that QS is responsible for the control and activation of several cell pathways including the induction of formation of mature and differentiated biofilms (de Kievit and Iglewski 2000, Irie and Parsek 2008). Therefore, QS might regulate virulence factors' production in Gram-negative and in Gram-positive bacteria within biofilms (Dickschat 2010, Landini *et al.* 2010). As it was mentioned above, *P. aeruginosa* has two different QS systems (LasR/LasI and

RhlR/RhlI) for cell-to-cell signalling. These systems were related to biofilm formation; also signal molecules are involved in biofilm differentiation (Davies *et al.* 1998). QS seems to be associated with all the steps on biofilm formation (Figure 2-9). Therefore, QS control could be a great approach to mediate biofilm formation , and in this way prevent the adherence of pathogenic microorganisms (Parsek and Greenberg 2005).

Several studies have confirmed that when cell density increases the probability of bacterial infections also increases. Most pathogens delay their production of virulence factors until a crucial population density is reached, which allows a successful infection process against the host (De Lamo Marin *et al.* 2007).

The characterisation and a better understanding of QS in biofilms might be useful to develop new strategies against several problems related to biofilms (Smith and Iglewski 2003). Also, a better understanding of the chemical nature of QS structures (autoinducers) may be useful to identify new compounds that can interfere with QS mechanisms, and slowing down some processes, such as biofilm formation and expression of virulence factors (Annous *et al.* 2009). Indeed the higher levels of resistance to antibiotics shown by bacteria in biofilms suggest the need for the development of new therapies focused in inhibition and dispersal of the biofilm structure may help to overcome this problem. These strategies do not aim to eliminate bacteria; they rather make bacteria/biofilm more susceptible to the action of conventional antibiotics or even disinfectants. Perhaps the future against biofilm-mediated infections could be a chemotherapeutic approach, combining conventional antibiotics with drugs possessing anti-biofilm activity (Paul *et al.* 2009, Landini *et al.* 2010).

2.1.5 Antibiotic Resistance

The ability of bacteria to evolve quickly and the heavy and sometimes unjustified use of antibiotics have contributed to the development of multi-drug resistant microorganisms (Beceiro *et al.* 2013). Antibiotics can be classified

according to their mechanism of action. Mechanisms include interference with cell wall synthesis, inhibition of protein synthesis, interference with nucleic acid synthesis, inhibition of a metabolic pathway, and disruption of bacterial membrane structure (Romero *et al.* 2011). Bacteria may be intrinsically resistant to one or more classes of antimicrobial agents, but more worryingly they may also acquire resistance by the acquisition of resistance genes from other organisms (Azevedo *et al.* 2013, Tacão *et al.* 2014). The resistance genes can work in many different ways such as enabling a cell to produce enzymes that destroy the antibacterial drug; they may be able to prevent the drug from reaching its intracellular target; they can modify the drug's target site, and they can promote an alternative metabolic pathway that bypasses the action of the drug (Tenover 2006). In addition to this, once bacteria have created a biofilm, not only the penetration of the antibiotic is more difficult, but also some mechanisms of resistance are more efficient, making the destruction of the bacterial biofilm nearly impossible (Landini *et al.* 2010).

Regardless of the mechanism of resistance developed by the microorganisms, the process is initiated by a survival reaction: bacteria have evolved to learn how to resist to antimicrobial drugs. As explained above, the new approaches to fight bacteria are focussing on the disruption of QS, without necessarily killing the microorganism. Control of QS would allow keeping the bacterial growth low and prevent the microorganisms from becoming virulent and form biofilms (Rutherford and Bassler 2012, Gowda and Marie 2014).

2.1.6 Inhibition of QS – Quorum Quenching

Bacterial infections are treated using antibacterial compounds that may be bactericidal or bacteriostatic; the first kill the bacteria and the second inhibit bacterial growth. The most common antibiotics usually target cellular processes such as bacterial DNA replication and repair, cell wall biosynthesis and/or the protein synthesis (Defoirdt *et al.* 2010). Nevertheless, after sometime bacteria are capable to acquire resistance to these antibacterial compounds. Different

strategies – that do not imply killing or inhibiting bacterial growth - have been investigated. In fact, by controlling the expression of virulence factors, bacterial virulence can be decreased without inducing any bacterial resistance (Defoirdt *et al.* 2010, Kirby *et al.* 2012). Controlling cell-to-cell communication (QS) has been explored as a virulence control strategy, since several bacterial species make use of QS as a mechanism to regulate virulence genes and toxins production (Antunes and Ferreira 2009, Tay and Yew 2013).

Swift and co-workers (1999) reported a significant decrease in expression of virulence factors and in the virulence characteristics of pathogens, when QS mechanism was inactivated. Each QS component can be used as a target in antimicrobial strategies (Finch *et al.* 1998, Williams 2002). Frequently, QS is the crossing point between bacterial populations and the host. The mechanism capable of interrupting cell-to-cell communication is described as Quorum Quenching (QQ) (Waters and Bassler 2005a). QS inhibitors must be highly specific since QS molecules are highly conserved in different bacteria. Furthermore, blocking of plant-associated bacteria QS can also be useful to manage a number of plants diseases and maybe even to increase their productivity (de Kievit and Iglewski 2000).

2.1.6.1 Mechanisms to block QS

QS inhibition has been explored as a measure to block the formation of biofilms, the attenuation of virulence and the adjustment of other mechanisms related to QS. Three strategies have been used (Figure 2-10): 1) blocking signal generator (Rasmussen and Givskov 2006), 2) enzymatic degradation of signal molecule and 3) blocking signal reception (Hentzer and Givskov 2003, Daniels *et al.* 2004).

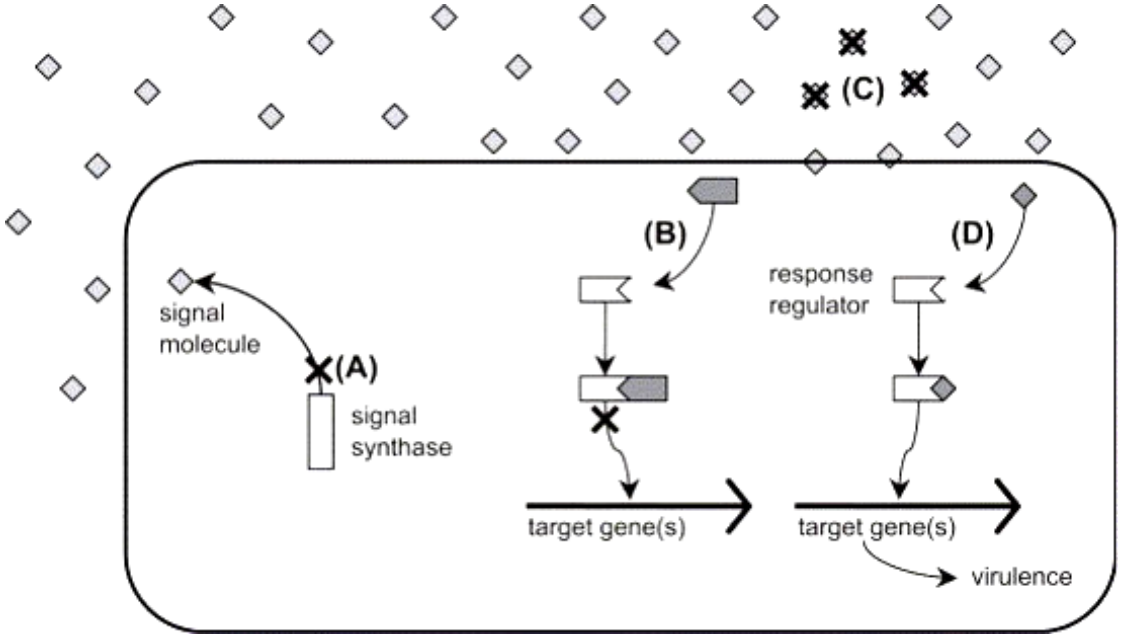

Figure 2-10 Schematic overview of different strategies that have been developed to inhibit bacterial QS. (A) Inhibition of signal molecule's biosynthesis by the application of substrate analogues; (B) Blocking signal transduction by the application of QS antagonists; (C) Chemical inactivation and biodegradation of signal molecules; (D) Application of QS agonists to evoke virulence factor expression at low population density (*adapted from* Defoirdt *et al.* 2004)**.**

2.1.6.1.1 Signal Generator

The use of compounds that interfere with the signal molecule is a strategy to disrupt QS (Figure 2-10 A). In most Gram-negative bacteria the synthesis of autoinducers (AHLs) is encoded by *luxI* or homologue genes (Defoirdt *et al.* 2004). The AHL signals precursors are acyl-ACP and SAM (S-adenosylmethionine), which are used as substrates (Whitehead *et al.* 2001) and the chemical reaction involving LuxI suggests that specific inhibitors for QS can be identified (Rasmussen and Givskov 2006). Parsek and co-workers (1999) reported that analogues of SAM inhibit 97% of the LuxI homologue (RhII) activity in *P. aeruginosa*. The reaction between AHL synthase and SAM has shown to be exclusive. This is important, as SAM is a frequent intermediate in prokaryotic and eukaryotic pathways, and the exclusivity of the reaction

improves the possibility of using SAM analogues as specific inhibitors of QS signal generator, without disturbing eukaryotic enzymes that use SAM as substrate (Hentzer and Givskov 2003).

2.1.6.1.2 Signal Molecule

Autoinducers have a high specificity to cognate receptors and for this reason a better understanding about their structure and composition is very important to synthesise specific analogues (Gray *et al.* 1994). The acyl side chain of autoinducers in Gram-negative bacteria has a high importance in the structure of the cognate receptor. The interaction between the autoinducer and LuxR-like proteins can be disconnected by differences in the length structure or even in substitutions in the acyl side chain groups, resulting in an inhibition of QS (Figure 2-10 B) (Parsek *et al.* 1999, Defoirdt *et al.* 2004). This specificity involving cognate receptors and the functional group of side chain of the signal molecule guarantees that only specific types of signals are formed (or disrupted) in different species (Jayaraman and Wood 2008).

Another approach capable of inhibiting QS involves promoting the degradation of signal molecules. Most Gram-negative bacteria seem to be able to degrade AHLs. Enzymes able to degrade AHLs have been described in several species. Two types of enzymes have been identified: AHL lactonases and AHL acylases (Defoirdt *et al.* 2004). The degradation of AHLs by lactonases – lactonolysis - can occur at alkaline conditions. Lactonase catalyses the hydrolysis of the ester bond in the lactone ring, opening the ring, leading to the production of N-acyl-homoserines (Yates *et al.* 2002). A small number of bacteria possess different enzyme, acylases, which catalyse the hydrolysis of the amide bond, connecting the lactone ring to the acyl chain, releasing a homoserine lactone and a fatty acid (Dong *et al*. 2001, Defoirdt *et al*. 2004, 2010).

2.1.6.1.3 Signal Receptor

Another strategy of QQ is blocking the signal receptor of the autoinducers. As well as the signal generator, the signal receptor is also highly specific for the signalling molecules (Figure 2-10 C). Alterations in receptor specificity can result in QS disruption (Paul *et al.* 2009). This specificity is especially important for pathogenic bacteria (Jayaraman and Wood 2008). Kock and colleagues (2005) have reported that a mutation in the LuxR protein resulted in insensitivity of the receptor.

Another strategy to disrupt QS is using small molecules that can compete with the AHLs to the cognate receptor. This can be achieved by the production of antagonists QS molecules that can bind and occupy the receptor (Defoirdt *et al.* 2004, Koch *et al.* 2005).

2.1.6.2 Applications of Quorum Quenching

As it was mentioned before, QS and expression of virulence factors are interconnected in several pathogenic bacteria (Bassler and Losick 2006). Therefore, techniques that can disrupt QS can be extremely useful to fight a wide range of bacterial infections (Camilli and Bassler 2006, Jayaraman and Wood 2008). If signal molecules are detected at early stages, the use of QS inhibitors might offer a new tool to fight the progress of bacterial infections (Boyen *et al.* 2009). This approach can be considered as an alternative to the use of antiobiotics. One of its advantages is the fact that, in principle, bacteria do not develop resistance, because this strategy should not influence the bacterial growth, but only their capability to become virulent (Defoirdt *et al.* 2010).

Compounds able to disrupt QS have been shown to increase the susceptibility of *P. aeruginosa* biofilms to classical treatments (Hentzer and Givskov 2003, Defoirdt *et al.* 2010, Dickschat 2010).

For instance, there is still not enough information about how QS and virulence are linked in aquatic pathogens. More research is necessary to be able to fight some of the infectious diseases that occur in aquaculture. However there is indication that many problems could be solved using QS disruption (Defoirdt *et al.* 2004, Gera and Srivastava 2006, Jiang and Su 2009).

2.2 *Vibrio fischeri* Characterisation

V. fischeri is a rod shape, Gram-negative bacterium found globally in marine environments. The bacterium produces bioluminescence and it is commonly found in symbiosis with marine animals like squids. In fact, organisms like squids have evolved organs to house such bacteria and use their bioluminescence during particular nocturnal behaviours (Miyashiro and Ruby 2012, Verma and Miyashiro 2013). *V. fischeri* bioluminescence is regulated by QS and this makes the bacterium one of the most used model organisms to study QS and its disruption.

2.2.1 *Vibrio fischeri* and QS

As mentioned above, *V. fischeri* produce bioluminescence as a phenotype resultant of QS intervention (Fuqua *et al.* 1994, Lupp *et al.* 2003). The QS mechanism of *V. fischeri* was one of the firsts to be discovered and studied. N-(3-oxohexanoyl)-L-homoserine lactone (3-oxo-C_6-AHL) is the signal molecule produced by *V. fischeri* and it was the first AHLs identified as an autoinducer (Engebrecht *et al.* 1983).

The QS mechanism of *V. fischeri* is the typical of Gram-negative bacteria and it is based on LuxR/LuxI, which are the two regulatory proteins essential in the mechanism. Such system was actually identified and described for the first time in *V. fischeri* and *V. harveyi* (Nealson *et al.* 1970, Bassler 1999, Miller and Bassler 2001). Briefly, the LuxI protein is responsible for synthesis of acyl-HSL;

and LuxR protein for binding autoinducer and promoting transcription of luciferase operon lux*CDABE* for production of light (Parsek *et al.* 1999, Atkinson and Williams 2009).

2.3 *Aeromonas hydrophila* Characterisation

The genus *Aeromonas* has a widespread distribution (Figure 2-11) in aquatic environments, such as rivers, estuarine and marine waters, and even wastewater and drinking water (Holmes and Nicolls 1995, EPA 2006).

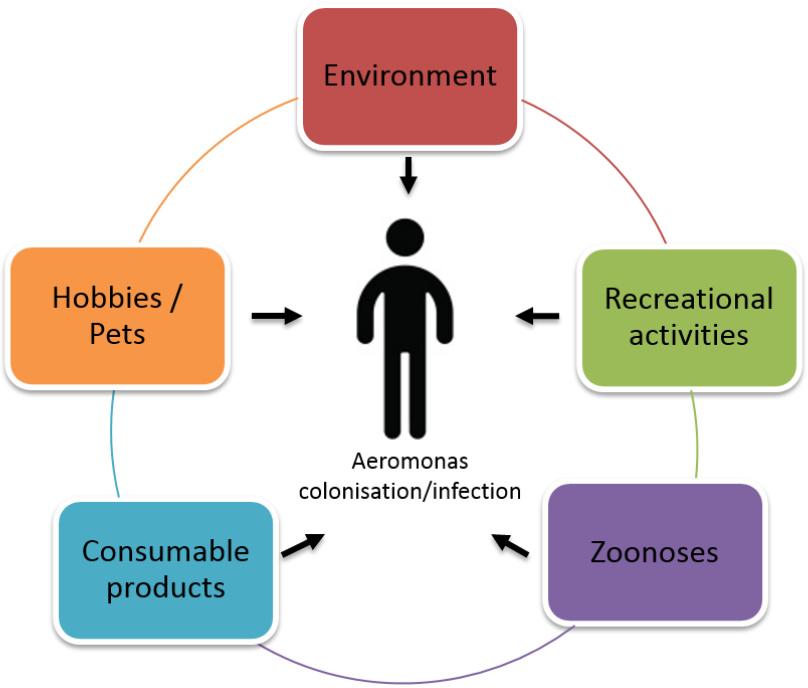

Figure 2-11 Environmental sources of *Aeromonas* species with potential for possible of human infection/colonisation (*adapted from* Janda and Abbott 2010)**.**

Aeromonas spp. are facultative anaerobic, oxidase positive and Gram-negative bacteria. They can grow between 0 ºC and 45 ºC but the optimal growth temperature is between 22 ºC and 32 ºC. *A. hydrophila* grows between 28 ºC

and 37 ºC (Martin-Carnahan and Joseph 2005, EPA 2006). Several *Aeromonas* have been linked to animal diseases, including humans. *A. hydrophila* and *A. salmonicida* are responsible for skin lesions, septicaemia and haemorrhagic diseases in fish, reptiles, birds, amphibians and mammals (Martin-Carnahan and Joseph 2005, Janda and Abbott 2010). *A. hydrophila* has also been linked to motile aeromonad septicaemia and intestinal and extra intestinal infections (Swift *et al.* 1999, Vila *et al.* 2003, Janda and Abbott 2010). In 1998, *A. hydrophila* was considered the first and second most important microorganism in the "Contaminant Candidate List" of potential waterborne pathogens (USEPA 1998, EPA 2006, Chopra 2008). The complete genome of *A. hydrophila* ATCC 7966 (Seshadri *et al.* 2006) was recently published.

The virulence of *Aeromonas* spp. is multifactorial and still not completely understood. Several factors contribute to the virulence, including proteases, toxins, lipases, adhesins (e.g. pili), haemolysins, the S-layer and a variety of hydrolytic enzymes (Galindo *et al.* 2006). All these virulence factors have an important role in *Aeromonas* pathogenicity. Bacterial infection and transmission of disease are mediated by virulence factors. The first step on the process of infection starts with the evasion of host defences (Chopra 2008, Janda and Abbott 2010). The regulation of virulence factors through the regulation of gene expression could be an advantageous method for the attenuation of infections (Fuqua *et al.* 1994). Quorum Sensing in *Aeromonas* spp. has been already described in the literature (Swift *et al.* 1997, 1999, Jangid *et al.* 2007, Garde *et al.* 2010) (see chapter 2.3.2).

2.3.1 *Aeromonas hydrophila* and Biofilms

As describe above, *Aeromonas* spp. are present in diverse aquatic environment, so they can colonise drinking water reservoirs and produce biofilms, that are able to resist disinfection (Bomo *et al.* 2004, Elhariry *et al.* 2012). When bacteria are aggregated in biofilms they express different genes,

becoming more resistant to stress conditions, host immune responses, disinfectants and antibiotics (Nadell *et al.* 2008, Webb and Kahler 2008).

Aeromonas spp. has been shown to form biofilms (Lynch *et al.* 2002, Rahman *et al.* 2007, Garde *et al.* 2010, Santos *et al.* 2011). As described above, a biofilm is a well-structured microbial community that can allow the survival of several bacterial species (Stoodley *et al.* 2002). Therefore, *Aeromonas* biofilms are less susceptible to environmental stresses. This is extremely relevant in drinking waters, where *Aeromonas* spp. are predominant (Bomo *et al.* 2004). Chung and co-workers have found biofilms of *Aeromonas* in microbial fuel cells circuits that affect the electric current. Lynch and co-workers (2002) have clearly demonstrated that biofilm production in *Aeromonas* is regulated by QS. *Aeromonas* pathogenicity is particularly relevant to the aquaculture industry and (EPA 2006, Janda and Abbott 2010). *A. hydrophila* causes haemorrhagic septicemia in fish.

Infectious diseases are one of the major limiting factors in aquaculture and the control of these diseases has become crucial for a successful fish farming management. *A. hydrophila* is one of the major responsible for economic losses in farm breeding fish (Carvalho-Castro *et al*. 2010).The control of several fish diseases in aquaculture is currently achieved using antibiotics and chemical compounds like vaccines (Gudding *et al.* 1999, Vivas *et al.* 2004). The increase of bacteria resistance to these compounds is a natural consequence of this type of treatment (Williams 2002, Chen *et al.* 2010). A few studies have reported the use of vaccines in aquaculture, as alternative to antibiotics, in the attempt to reduce diseases and economic losses (Defoirdt *et al.* 2004, Cole *et al.* 2009). However, only limited types of vaccines useful against a minority number of *A. hydrophila* serotypes are available. Alternative solutions, that avoid the use of antibiotics or improve their efficacy, are necessary.

2.3.2 *Aeromonas hydrophila* and QS

Swift and co-workers (1997) identified in *A. hydrophila* a LuxRI homologue and its associated signal molecules. *A. hydrophila* QS mechanism is similar to that observed in *V. fischeri.* The AhyI/AhyR are the QS proteins of *A. hydrophila* (Kirke *et al.* 2004). Recently, the LuxS protein, which is responsible for the formation of AI-2 was also found in *A. hydrophila* (Kozlova *et al.*, 2008). The N-butanoyl-L-homoserine lactone (C_4-HSL) is the most important AHL (signal molecule) produced by AhyI and AsaI (LuxI synthase); they also produce N-hexanoyl-L-homoserine lactone (C_6-HSL) as a second signal, but in smaller quantity (Swift *et al.* 1997). In *A. hydrophila* the recognition of C_4-HSL by AhyR (cognate receptor LuxR) protein is dependent on QS. The AhyR/C_4-HSL controls both extracellular protease production and biofilm formation; and target genes such as those encoding serine protease and metalloprotease production (Kozlova *et al.* 2011). The LuxR protein expression in *Aeromonas* seems to be responsible for control of virulence factors' production (Swift *et al.* 1999, Lynch *et al.* 2002).

Jangid and co-workers (2007) reported that LuxRI homologues are present in different species of *Aeromonas.* The genes responsible for QS system have been identified in *A. hydrophila* ATCC 7966 (Seshadri *et al.* 2006). LuxRI controls biofilm formation (Lynch *et al.* 2002), extracellular proteolytic activity, T6SS and also contributes to *A. hydrophila* virulence in fish and mice (Kirke *et al.* 2004, Kozlova *et al.* 2008). Nevertheless, LuxRI shows no effect on the swimming or swarming motility in *A. hydrophila.* On the contrary, LuxS, also regulated by QS, has shown to exhibit a negative regulation (reduction) of general *A. hydrophila* virulence (Daniels *et al.* 2004, Jangid *et al.* 2007, Khajanchi *et al.* 2009).

In conclusion, QS has an important role in biofilm formation by *Aeromonas*. The study of QS and its relationship with virulence factors can provide a better understanding of *Aeromonas* pathogenicity (Lynch *et al.* 2002, Khajanchi *et al.* 2009, Janda and Abbott 2010). The link between QS and biofilms formation

makes QS directly connected to *Aeromonas* pathogenicity (Galindo *et al.* 2006, Seshadri *et al.* 2006, Garde *et al.* 2010, Janda and Abbott 2010). As we know, several bacteria makes use of QS to control their colonisation and virulence factors, and therefore disruption of QS can be a good therapeutic strategy (Martin *et al.* 2008, Garde *et al.* 2010).

2.4 Molecular Modelling

Molecular modelling allows the creation and improvement of molecular geometry through computational design of bond lengths, bond angles and torsions and helping to find low energy conformations of molecules. The computational design allows to determine energy, electrostatic, spectroscopic and bulk properties (Allen and Tildesley 1987). Several types of software are commercially available: Quanta/Charmn/MCSS/HOOK (MSI, San Diego), InsightII/Ludi (MSI, San Diego, USA), Cerius 2 (MSI, San Diego, USA) and Sybyl (Tripos, San Diego, USA). The computational analysis was performed by Sybyl 7.3 (Tripos, San Diego, USA). The theoretical method that supports this computational design is the Molecular Mechanics (MM) frequently identified as Force Field method. This methodology can envisage the geometry of the molecules through several calculations. The molecules are considered as a collection of points (atoms) linked by strings (bonds) with different elasticities (force constant). The combination of these potential energy functions is the force field. Since structure and energy are intimately connected the MM involves both of them. MM is usually used to find the energy minimum (Tripos) of a given molecular structure.

$$E_{tot} = \Sigma E_{str} + \Sigma E_{bend} + \Sigma E_{oop} + \Sigma E_{tors} + \Sigma E_{vdw} \qquad a)$$

Figure 2-12 Equation (a) where are represented the parameters that contribute to the prediction of energies by Molecular Modelling

The Energy (E) of a molecule (Figure 2-12), in Tripos Force Field, is obtained by the calculation of all energy involved coming from all bonds, angles, torsion angles and non-bonded interactions (Clark *et al.* 1989). Based on the above equation, the total Energy (E_{tot}) is the sum of energies contributions, where:

E_{str} stretching energy from natural bong length

E_{bend} bending energy of bond angles from natural values

E_{oop} bending energy of planar atoms out of the plane

E_{tors} torsional energy from twisting bonds

E_{vdw} van der Waals' energy from non-bonded interactions

In Sybyl program, the MAXIMIN2 tool allows the energy calculations using the Tripos force field, and the optimisation of the molecule geometry (Labanowski *et al.* 1986). Using SIMPLEX technique, the internal strain is decreased until acceptable limits and then, though the conjugate gradient method, the atoms are optimised. Another tool that is also important in Sybyl program is the LEAPFROG algorithm. The evaluation of new active ligand molecules on the base of their score is allowed by LEAPFROG. This algorithm is calculated through the electrostatic/steric screening of applying different ligands, in different positions to the template. The LEAOPFROG binding energies of the ligands structures are saved in a Sybyl database. A rational selection of monomers allowing the interaction between monomers and targets (template) was evaluated and performed by computational simulation. The computational simulation was used in order to study interactions between a 22 functional monomers library and the targets. The virtual library contains functional monomers such as acrolein, acrylamide, acrylic acid, acrylonitrile, allylamine, EGDMA, itaconic acid, styrene among others (Piletsky *et al.* 2001). The residues of the functional monomers presents in the library, are suitable to interact with the targets by ionic and hydrogen bonds, van der Waal's and dipole-dipole interactions. The strength of the interaction ligand-target (referred in equation above) has determined the initial selection of the monomers.

Therefore Leapfrog was applied to identify the monomers with the strongest interactions for the target, as already done with microcystin-LR (Chianella *et al.* 2002), ephedrine, methadone, cocaine, morphine and deoxyephedrine (Piletsky *et al.* 2001, Piletsky *et al.* 2005). Simulated annealing or molecular dynamics are other essential steps in rational design of polymers. These tools are used to obtain low energies conformations of either a single molecule or more complex systems (multiple molecules). Before the polymerisation, the pre-arrangement of the functional monomer and the template in the monomer mixture was determinate by simulated annealing. In this way the most favourable monomers and ratio between monomers and template was calculated.

A previous study performed by Piletska and colleagues (2010, 2011) reported that the functional monomers MAA and IA were selected for polymers polymerisation, based on their interactions with the targets (AHLs). The keto-functional group of the target (AHLs) is suitable for binding to the acidic monomers (MAA or IA) (Weiss *et al.* 2003). The MAA is one of the most popular monomer and is often used as functional monomer in molecular imprinting. The methyl group present in MAA allows conformation changes and rotation and provides van der Waals interactions, when compared with others monomer, such as acrylic acid (Sellergren *et al.* 1988).

2.5 Linear Polymers

There are two different types of polymers: natural (polysaccharides, proteins) and synthetic (plastics, fibres). The word *polymer* originates from the Greek prefix *poly* (“many”) and *meros* (“part”). Polymers are the product from the accumulation of small and repeated monomers forming long chains. Polymerisation is the chemical reaction of monomers to originate polymeric molecules (Teegarden 2004). The number of repeat units (monomers) and the molecular weight of each monomer define the polymer size (Nicholson 1997). Homopolymers are polymers with only one type of monomer and copolymers have at least two different types of monomers. Different sequences and

arrangements result from the way the monomers are connected to the main chain (Teegarden 2004). A schematic representation of each type of polymer is represented in Figure 2-13.

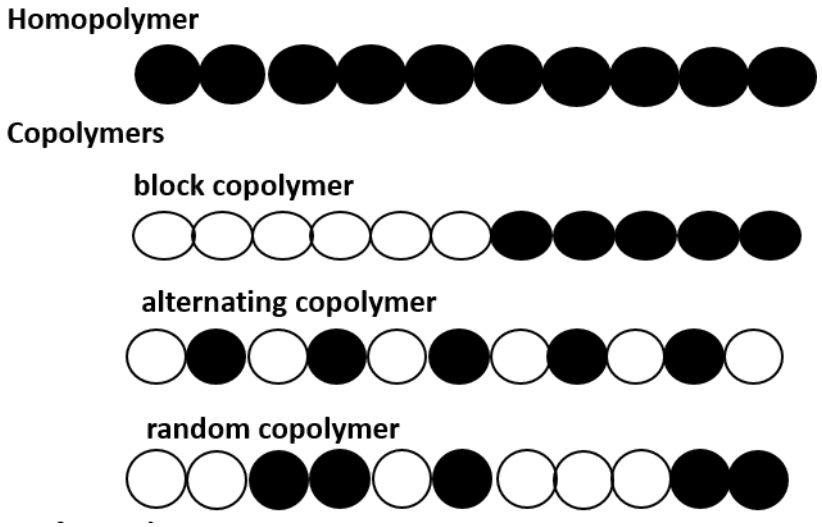

Figure 2-13 Illustration of distinct polymer chains types: black circle represent one type of monomer, white circle represents another (*adapted from* Teegarden 2004)**.**

Block copolymers have long sequences of both types of monomers along the backbone. The polymerisation occurs with low molar mass units ("block") of homopolymers (Nicholson 1997). Copolymers may have a random, alternating or a block sequence, depending on the purpose (Figure 2-13). Polymers may be linear or branched. Branching occurs when a monomer with more than one double bond, and therefore more than one point for polymerisation, is used. The monomer composition, the structure and the architecture of molecules in the polymer, provide different properties to the final polymer (Nicholson 1997; Teegarden 2004).

Copolymerisation is the polymerisation of a mixture of two (or more) types of monomers. The final polymer has the name of copolymer. A copolymer is a mix of two monomers integrated into each copolymer molecule. The monomers in the polymer chain can have block, statistical or alternating arrangement as

Figure 2-13 sows. Monomers chemistry and reactions conditions are responsible for these types of arrangements. Usually, the choice of one of the monomers is related with the thermal properties, while the second one is added to attain a better adhesion (Teegarden, 2004). From a technological point of view, copolymerisation is extremely important. Copolymerisation allows the production of polymers with tailor-made properties. Homopolymerisation is more limited, due to the reduced number of products (Odian, 2004).

Two types of classifications have been used for polymers so far. One classification is based on polymer structure (or composition) and classifies polymers into ***condensation*** and ***addition*** polymers; the other, based on the polymerisation mechanism, classifies them into ***step*** and ***chain*** polymers. Most of the times, these classifications are used mutually. 'Condensation' or 'step' represents the same type of polymerisation; and 'addition' or 'chain' corresponds to another polymerisation type (Odian 2004). Step-growth and chain-growth polymerisation have a large number of differences, such as different kinetics and different molecular weight of the resulting polymers (Davis 2004, Hosier *et al.* 2004).

2.5.1 Step Growth Polymerisation

Step-growth polymerisation is related to condensation polymerisation because during the polymer formation small molecules, such as water, are released. As the name suggests, on the step-growth polymerisation, the polymer-chain grows in a step-wise reaction of two functional monomers (Davis 2004, He *et al.* 2004). As a result, an intermediate molecule with a new functional group is formed. This new intermediate can react with another intermediate or with another monomer producing a larger intermediate (Teegarden 2004). In Figure 2-14 a general and simplified mechanism is represented.

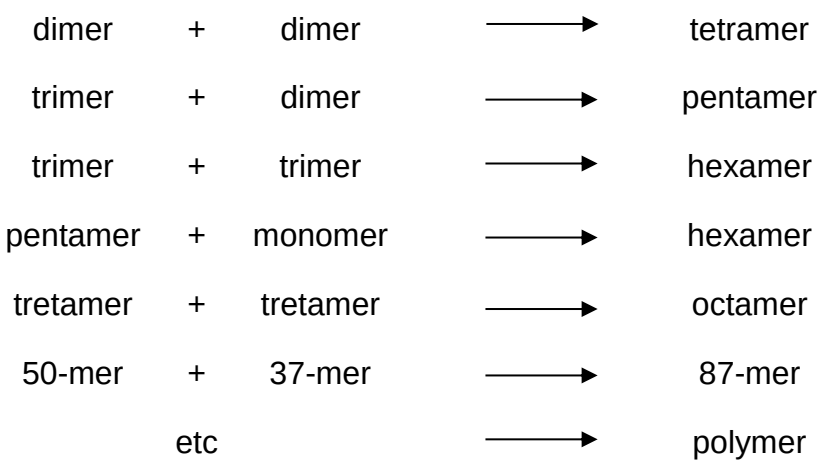

Figure 2-14 A general step growth polymerisation mechanism (Teegarden 2004)**.**

In step-growth polymerisations two distinct polymer groups can be formed based on the type of monomer. One group is related with the presence of two different bifunctional and/or polyfunctional monomers; the other group is associated with a monomer that contains both types of functional groups (Odian 2004)

a)

b)

Figure 2-15 Equations a) and b) represented general step growth polymerisation**.**

The two reaction groups (A and B) are represented in Figure 2-15 as different types of functional monomers. The features of these two polymerisation reactions are extremely similar. As described below, the synthesis of high

molecular weight polymers is achieved more easily through chain-growth polymerisation (Odian 2004).

An example of step growth polymerisation is the nylon-6,6. The nylon 6,6 is formed by the adipic acid (1,6-hexanedioic acid) reacting with hexamethylenedianime (1,6-diaminohexane), producing poly(hexamethylene adipamide) and water. This polymer is called nylon-6,6 because both the diacif monomer and the diamine monomer provide 6 carbons atoms in the polymer chain (Teergarden 2004).

2.5.2 Chain Growth Polymerisation

Chain-growth polymerisation involves monomers containing carbon-carbon double bonds (unsaturated compounds). The reactivity of these compounds is higher than that involved in a typical step-growth polymerisation. In the chain-grow polymerisation, intermediates between monomers and polymers do not exist and formation of high molar mass polymers is reached from the beginning of the reaction (Nicholson 1997).

In chain-growth polymerisation, the monomers are successively added to a growing chain. The classification of the polymerisation is defined according to the way of initiation and the nature of the propagating chain; this can be cationic, anionic or free radical. The most important route in terms of versatility is the free radical (Nicholson 1997, Aragrag *et al.* 2004). For chain-growth polymerisation, three basic processes are generally established: initiation, propagation and termination (Polowinski 1997). The initiator produces an initiating species with a reactive centre. The reactive centre can be an anion, a cation or a free radical, determining the way in which polymerisation occurs. Propagation, the second step, is dependent on the reactive centre by the addition of several monomers to the chain reaction. The production of the polymer is based on these successive additions of monomers. The polymerisation process is then stopped when one of several terminations

reactions destroys the reactive centre (Odian 2004). The step-growth polymerisation does not need an initiator to start the reaction; if monomers have appropriate functional groups, they are capable of initiating and continuing the reaction until the formation of large molecules. Chain-growth polymerisation needs an initiator to react with the monomers. For this crucial difference, the conversion of monomer into polymer is highest and faster in chain-growth polymerisation as shown in Figure 2-16.

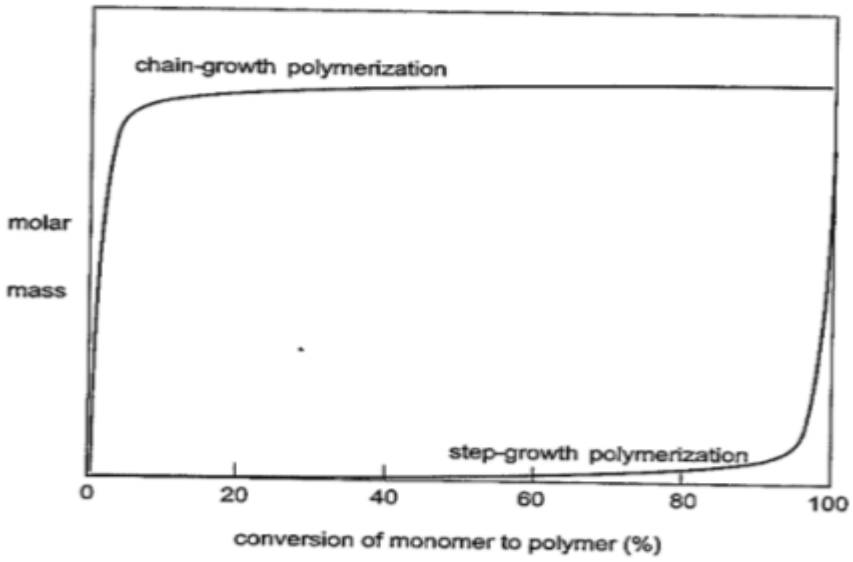

Figure 2-16 Polymer molar mass obtained in chain-growth *versus* step-growth polymerisation (*adapted from* Teegarden 2004)**.**

The most important differences between step-growth and chain-growth polymerisation are reported in Table 2-1.

Table 2-1 Comparison between step-growth and chain-growth polymerisation (*adapted from* Teegarden 2004*)*.

Step-Growth Polymerisation	Chain-Growth Polymerisation
Monomers have two reactive functional groups	Monomers have a carbon-carbon double bond
Polymer backbone contains carbon and others atoms (oxygen or nitrogen)	Polymer backbone contains only carbons
Functional groups react without initiator; reaction may be catalysed; reaction often gives off to small by products	Reaction usually begins with an initiator
Intermediates are compounds (e.g., oligomers) with the same two reactive functional groups as the monomer	Polymerisation proceeds by chain reaction through short-lived reactive intermediate (free radical, cation, anion); monomer reacts only with the reactive intermediate, not with other monomers
Polymer develops at slow rate; high polymer is formed only at the very end	High polymer is formed very rapidly
Reaction mixture contains monomers, oligomers, and polymer	Reaction mixture consists only of monomer and high polymer
The degree of polymerisation and the molar mass increase as the reaction proceeds	The molar mass of polymer formed early in the reaction is approximately the same as that formed later on; increasing time increases yield, not molar mass

2.5.2.1 Free Radical Polymerisation

Free radical polymerisation is probably the most well-known mechanism of polymerisation where successive addition of monomers to the radical chain is involved. Polymerisation with vinyl monomer is the one that represents this mechanism (Figure 2-17). Initiation begins with the formation of a free radical and at the same time a monomer is added to this radical.

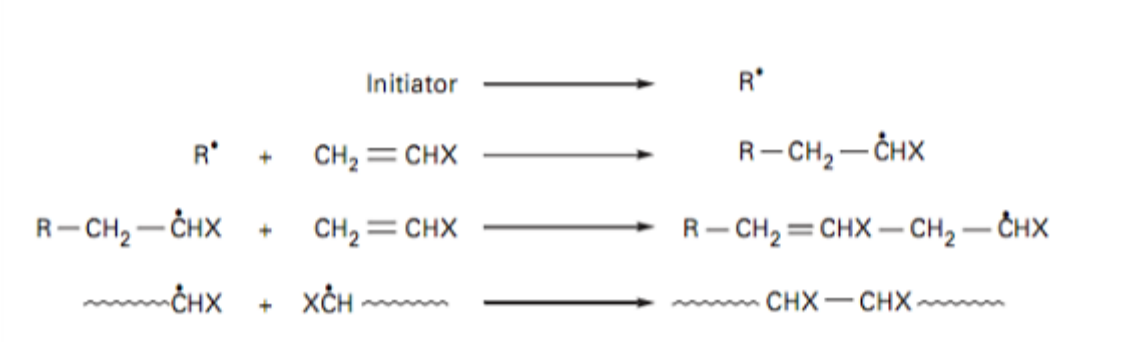

Figure 2-17 Mechanism of free radical polymerisation (*adapted from* Davis 2004)**.**

2,2'-azobis-(2-isobutyronitrile) (AIBN) has been used as a thermal free-radical initiator in several reactions (Figure 2-18). The propagation is the main step of the entire process. The molecular weight of the final polymer is dependent on the number of monomers that are added to each initiator molecule (Aragrag *et al.* 2004, Davis 2004, Odian 2004).

Figure 2-18 Thermal decomposition of AIBN initiator (*adapted from* Davis 2004).

As it was mentioned before, free radical polymerisation originates a high molar mass polymer quickly. Sometimes it is convenient to use a chain-transfer agent to control the molecular weight. Usually it is the solvent that exerts this function. The choice of the solvent, where polymers' synthesis occurs, should consider this characteristic (Aragrag *et al.*, 2004; Davis 2004). For the polymerisation reaction, the presence of water is not a concern; however, the presence of anionic species and oxygen might be an issue. Only solvents with highest purity should be used; monomers and solvents should be distilled to remove all

inhibitors that might be present; free radical polymerisations must occur under anaerobic conditions (Aragrag *et al.* 2004).

2.6 Molecular Imprinting

Molecular imprinting is a general method for the synthesis of specific polymers with properties of recognition. In comparison with natural receptors and antibodies, molecular imprinting polymers (MIPs) have higher selectivity and robustness. The concept of molecular imprinting was defined by Alexander and colleagues as: *"The construction of ligand selective recognition sites in synthetic polymers where a template (atom, ion, molecule, complex or a molecular, ionic or macromolecular assembly, including microorganisms) is employed in order to facilitate recognition site formation during the covalent assembly of the bulk phase by a polymerization or polycondensation process, with subsequent removal of some or all of the template being necessary for recognition to occur in the spaces vacated by the templating species"* (Alexander *et al.* 2006).

The principle of molecular imprinting makes use of an interaction between a molecular template (target analyte) and an arrangement of functional monomers chemically fixed by co-polymerisation using a cross-linking monomer. The result is a polymer matrix with a template implanted. The washing out of the template exposes specific recognition sites. A typical imprinting system must have a template molecule, at least one type of functional monomer, a cross-linker, and a porogenic solvent (Ye and Mosbach 2001). Molecular imprinting promotes the polymerisation of functional monomers in the presence of a template, leading to the creation of selective recognition sites in polymer matrix. After the imprinting process, synthetic polymeric materials with cavities with specific size, shape and moieties to the template, capable of molecular recognition are obtained (Pichon and Chapuis-Hugon 2008).

2.6.1 Synthesis of MIPs

The synthesis (Figure 2-19) of MIPs can be divided in three steps:

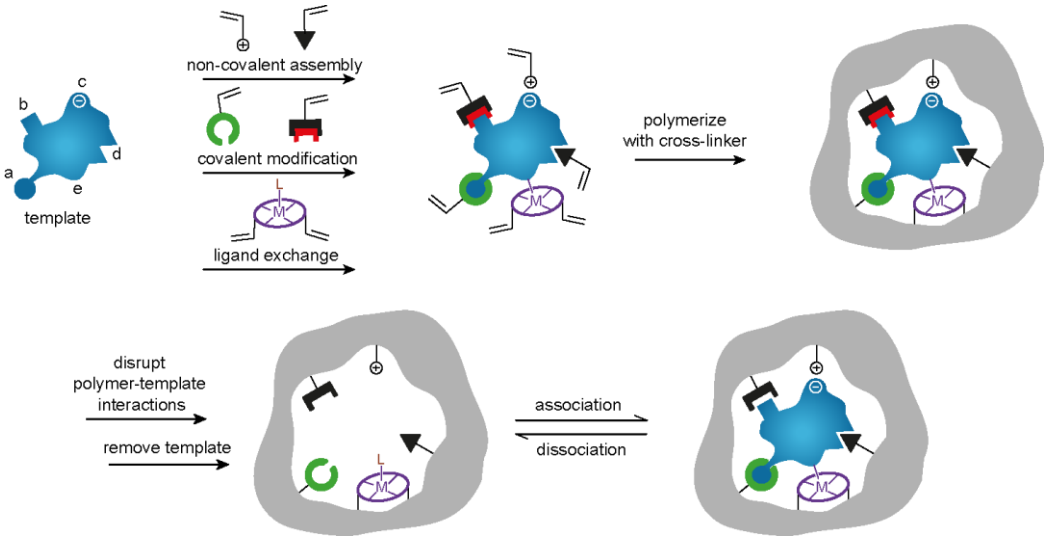

Figure 2-19 General scheme of molecular imprinting process.

The first step of MIPs synthesis involves the complexation in solution (with a porogenic solvent) of the template (print molecule) with the functional monomers, by specific and definable interactions. These intermolecular interactions can be non-covalent or reversible covalent (Pichon and Chapuis-Hugon 2008). A correct choice of the cross-linker is particularly important since a high degree of cross-linking (70-90%) is necessary for specificity. Ethylene glycol dimethacrylate (EGDMA), divinylbenzene and trimethylopropane trimethacrylate (TRIM) are the cross-linkers more commonly used. Among these, in many cases, EGDMA is the most appropriate cross-linker for the imprinting process due to its low price and purification easiness (Wulff 1995). The second step is the co-polymerisation of the monomers, interacting with the template, in the presence of an initiator and with the help of a high percentage of cross-linking. The polymerisation can be thermal, redox or photochemical (UV irradiation). In both cases, free radicals can be generated by the cleavage of the initiator. It is thanks to these radicals and to the cross-linker that a cross-linked polymer network is created, with the template molecules trapped inside

the network (Pichon and Chapuis-Hugon 2008). In the final step, after the polymerisation, several and extensive washing steps of the polymeric materials are carried out to remove the template molecules. Therefore, cavities, i.e. free binding sites, are left behind in the polymer and accessible for the template rebinding. These cavities have the right size, shape and composition necessary for the recognition of the template (Pichon and Chapuis-Hugon 2008).

2.6.2 Approaches to Prepare MIPs

There are two main approaches to preparing MIPs based on the link between the monomers and the template (Pichon and Chapuis-Hugon 2008):

a) The covalent approach, pioneered by Wulff and co-workers, where the monomers and the template are covalently bound. After the polymerisation, the template is cleaved by acidic hydrolysis. This disconnection leaves functionalities in the binding sites that are able to bind the target molecules by restoring the covalent bonds. This approach has the advantage that the moieties are only connected with the template site (Alexander *et al.* 2006). On the other hand, just a few compounds can be imprinted using this approach: alcohols (diols), ketones, amines, aldehydes and carboxylic/boronic acids (Whitcombe and Vulfson 2001).

b) The non-covalent approach, pioneered by Mosbach and co-workers, where heterogeneous binding sites are obtained as a result of reversible noncovalent ligations (Ye and Mosbach 2001). In the non-covalent approach, the interactions between template and monomers during polymerisation and between polymer and template after the polymerisation (during the re-binding) are the same, as long as the solvent used for polymerisation and rebinding is the same (Alexander *et al*. 2006). The interactions involved are hydrogen-bonding, dipolar association, dipole-dipole interactions, hydrophobic interactions and ion-pairing. This is a flexible and easy method to synthesise MIPs. Several of the functional monomers used in this approach are commercially available. In this

approach polymers that make use of a single functional monomer can also be produced (Whitcombe and Vulfson 2001, Mayes and Whitcombe 2005). For all these reasons, the non-covalent imprinting is one of the most used techniques in the imprinting technology (Chianella *et al.* 2003).

2.6.3 Selection of Reagents for MIPs

Several factors can influence the structure and the recognition properties of MIPs: the composition of the monomers, the reactivity of the monomer, the volume and nature of the solvent, the level of cross-linking, the synthesis temperature, the initiator and its concentration and the method of initiation (thermal, photochemical or redox) (Whitcombe and Vulfson 2001). The selection of the template molecule is critical, especially as most MIPs are synthesised for a specific analytical application. The binding site properties of the polymeric matrix are defined by the structure of the template molecule. Important factors to have in consideration when selecting a template, are the availability, the cost and the chemical adaptabilities to interact with the monomers. The imprinting is more efficient when the templates have low molecular weight (Ye and Mosbach 2001). Usually the template molecule is the target that needs to be retained in the polymer. In non-covalent approaches, because the interactions are weaker, the template must have multiple functional sites to promote the strength of template-monomers assemblies (Pichon and Chapuis-Hugon 2008).

In analytical applications, the synthesis of most MIPs is carried out by the non-covalent approach. In this approach, the porogen solvent is one of the more important reagents, which is responsible for an effective molecular recognition. The physical and chemical characteristics of the porogenic solvent should promote the interactions between the template and the monomer (Alexander *et al.* 2006). Frequently, MIP synthesis is developed using methacrylic acid (MAA) or 2- or 4-vinylpyridine (VP) as functional monomers, ethylene glycol dimethacrylate (EDMA) as cross-linker and toluene, dichloromethane,

chloroform or acetonitrile as porogenic solvents. These organic media, promote strong polar interactions like hydrogen bonds and electrostatic interactions for acid or basic templates. Imprinting in aqueous samples is more difficult as most of the polar interactions between the template and the monomers are much weaker (Pichon and Chapuis-Hugon 2008).

The selection of the cross-linker is also very important to produce imprinting binding sites because the degree of cross-linking increase the binding capacity and the selectivity of the resulting materials (Pichon and Haupt 2006). Some studies compared pentaerythritol triacylate (PETRA), ethylene glycol dimethylsulphoxide (EDMA) and divinylbenzene (DVB) and showed that polymers synthesised with PETRA have the highest selectivity for the template (Alexander *et al.* 2006).

To obtain MIPs with high affinity for the targets, an appropriate selection of monomers is also important. The functional monomers need to be chemically complementary to the template. Because of that, their stoichiometry is also important (Takeuchi and Matsui 1996). Selection of monomers can be rationally done by computational methods with a virtual library, which allows choosing the monomers capable of interacting strongly with the targets (Pichon and Chapuis-Hugon 2008). Piletsky and colleagues have developed an approach for the choice of the monomers based on “virtual imprinting” (Piletsky *et al.* 2001). A functional monomer library is screened against the template to assess the strength of monomer-template interactions. The results can be used to identify the best monomers and their molar ratios to prepare specific and selective imprinted polymer (Mayes and Whitcombe 2005). Guerreiro and co-workers have developed a library of 31 functional monomers as potential candidates to form a complex with nonylphenol. Using the screening process, they were able to reduce to five the number of monomers candidates suitable for production of MIPs specific to the target analyte (Guerreiro *et al.* 2008).

Methacrylic acid (MAA) is one the most used functional monomer in noncovalent approaches. This compound is an hydrogen bond donor and

acceptor, capable of establishing ionic interactions (Ye and Mosbach 2001). Other compounds that are used as functional monomers are acid monomers such as acrylic acid, basic monomers such as 4-vinylpyridine and N,N-diethylaminoethyl methacrylate, neutral monomers such as 2-hydroxyethyl methacrylate (HEMA) and acrylamide (Whitcombe and Vulfson 2001; Alexander *et al.* 2006). To achieve better MIP binding properties, mixtures of functional monomers have also been used. For example 2-vinylpyridine has been mixed with methacrylic acid (Ramström *et al.* 1998) and acrylamide with methacrylic acid (Meng *et al.* 1999).

The initiator is also relevant in the polymerisation reaction. The most commonly used are the azo-initiators, since their thermal decomposition provides a supply of free radicals (methyl) methacrylate-based MIPs. Azo-initiatiors can also be used to prepare MIPs at low temperature, with high effectiveness using UV irradiation due to their easy photochemical decomposition (Sellergren and Shea 1993).

The degree of specificity of the cavities designed for the target analytes is responsible for the selectivity and specificity of the resulting MIPs. The interactions between the template and the monomer in a porogen solvent are crucial. Several approaches have been investigated to evaluate these interactions during the polymerisation step. Usually in these studies a non-imprinted polymer (NIP), also named control polymer, is synthesised in parallel. This polymer is synthesised as the MIP but in absence of the template. The performance difference between the two polymers indicates the ‘strength of the imprinting’ (Pichon and Chapuis-Hugon 2008). Different methodologies (binding experiments and chromatography approaches) are used to assess the presence of the specific cavities in MIPs (Michailof *et al.* 2008).

MIPs can be synthesised in several formats. The most used and simplest method is preparing MIPs in a bulk format. To obtain particles with 25-150 µm, the bulk polymer monolith, produced at the end of the polymerisation step, needs to be crushed, ground and sieved. The sedimentation is the last action to

eliminate fine particles. After this, the particles with the correct dimensions can be packed into disposable cartridges for SPE or HPLC columns (Haginaka 2008). Other methods used for MIP synthesis are seed polymerisation, suspension polymerisation or dispersion/precipitation polymerisation, all producing either nano- or micro-particles and thin films for sensing applications (Haginaka 2008, Pichon and Chapuis-Hugon 2008).

2.6.4 Advantages and Disadvantages of MIPs

Molecularly imprinted polymers are attractive for several applications because of their advantages over other natural and synthetic receptors: MIPs can have affinity and selectivity as high as natural receptors; they have high stability, they are easy and inexpensive to prepare (as long as the template is cheap) and they can be easily adapted for different applications (Ye and Mosbach 2001, Alexander *et al.* 2006, Pichon and Chapuis-Hugon 2008). Nevertheless there are some limitations related to the development of MIPs: a lack of a common process for MIP preparation; difficulty in incorporating the MIPs with transducers; difficulty in changing the binding event into an electrical signal and reduced performance in aqueous solution (Piletsky *et al.* 2006). Several efforts have been done to resolve these problems. Approaches such as combinatorial and computational methods have allowed the development of MIPs with selectivity and affinity comparable to antibodies (Chianella *et al.* 2003).

MIPs are used in several areas as tailor-made materials for separation, as enzyme mimics in catalytic applications, as recognition elements in biosensors, as antibody and receptor binding mimics (Mosbach 1994, Wulff 1995, Andersson *et al.* 1996, Ye *et al.* 2000).

2.7 MIP Nanoparticles

As mentioned above, MIPs are frequently prepared as a bulk monolith, which is then ground and sieved to get randomly shaped particles of a suitable size for various applications. The method can cause loss of material and it is a time-consuming procedure, that becomes inappropriate for several applications, such as industrial application (Poma *et al.* 2010). In order to overcome these problems, several other methods have been developed to obtain structural formats able to enhance polymer properties: films, membranes, micro- and nanoparticles (Pérez-Moral and Mayes 2006).

MIP nanoparticles (MIP NPs) have higher surface-to-volume ratios than bulk polymers. Their imprinted cavities are more reachable by the template and the binding kinetics are enhanced (Tokonami *et al.* 2009). The MIP NPs format fits well with surface imprinting strategies, allowing a quick design and synthesis of this type of materials, and making the design of *in vitro* assays with enzyme-conjugated probes much easier. In addition MIP NPs are more easily kept in solution, an aspect which improves the performance and accuracy of the assays based on these products (Guerreiro *et al.* 2009, Poma *et al.* 2010). The degree of cross-linker and the request for a strong interaction between template-monomer determines the protocol to make MIP NPs, which can be a drawback for the synthesis of these particles (Pérez-Moral and Mayes 2006). MIP NPs can be prepared by different approaches: the precipitation polymerisation, the mini- and micro-emulsion polymerisation processes, the core–shell approaches, including the core-shell emulsion polymerisation, and the grafting procedures. All these procedures have advantages and disadvantages (Piletsky *et al.* 2005, Tokonami *et al.* 2009).

The first and most used approach to obtained MIP NPs is the precipitation polymerisation. The formation of imprinted nanoparticles is performed in an excess of solvent (2% V/V monomer concentration). The chains of the polymer do not coagulate during the growth, and precipitation just ends when their size makes the polymer insoluble in the reaction medium (Poma *et al.* 2010). This

technique gives reasonable yield, it is not too time consuming and it is easy to perform (Ye *et al.* 2000). Nevertheless, the concentration of cross-linker, template, alteration of temperature and amount of initiator can largely affect the polymer size and characteristics (Ye *et al.* 2000; Pérez-Moral and Mayes 2006; Poma *et al.* 2010).

Preparation of MIP NPs by macro- and mini-emulsion polymerisation requires an oil phase (organic solvent), where all the polymerisation components are dissolved, and an aqueous phase containing a surfactant to improve stability and homogeneity of the resulting nanoparticles. By high-shear homogenisation and/or ultrasonication the oil phase is dispersed in the water phase with the formation of droplets of micro or nano size. Polymerisation is then initiated and the droplets are polymerised producing nanoparticles (Vaihinger *et al.* 2002). Using this method, nanoparticles in a wide size range have been obtained (50-500 nm) (Van Herk and Monteiro 2003). This method offers the possibility to produce high yields of small nanoparticles. However, the need of using water and a surfactant, both interfering with the imprinting process, and the long and tedious purification steps are among the disadvantages (Poma *et al*. 2010).

Finally, the preparation of MIP NPs can be done by core-shell approaches. These consist in deposition of a MIP layer on preformed nanospheres composed of various materials such as silica, porous polymers (e.g. styrene) and magnetite (Pérez-Moral and Mayes 2002, Tan and Tang 2007). The MIP-shell can be prepared either by emulsion polymerisation, as explained above, in presence of water and a surfactant, or by grafting (Poma *et al.* 2010). Grafting can be grafting-from or grafting-to. In grafting-from a living initiator or iniferter, which can be activated and deactivated by switching on and off UV light, is attached to the core and then used to initiate the MIP polymerisation (Pérez - Moral and Mayes, 2007). In grafting-to the core is functionalised with a compound containing double bonds, which is the starting point for the formation of the MIP-shell (Gao *et al.* 2007). Between grafting-from and grafting-to the former allows better control of the formation of the MIP layer. Advantages of the core-shell approaches are suitability for surface imprinting and possibility of

using cores with specific properties (e.g. fluorescence and magnetism). Disadvantages are the possible presence of interfering compounds (water and surfactant), possible formation of aggregates and poor imprinting if the MIP shell is too thin (Poma *et al.* 2010).

2.7.1 MIP NPs Prepared by Solid-Phase Approach

In all the imprinting approaches mentioned above the template is solubilised in the polymerisation mixture and, subsequently, all the interactions between functional monomers and polymerisation compounds occur in the liquid phase. Nevertheless a different approach, where the synthesis of MIPs occurs with the template covalently immobilised on an appropriate support (e.g. glass beads), has also been reported (Poma *et al.* 2013). Such support, with the template immobilised, is then mixed with the polymerisation components in a specific porogen and the nanoparticles are formed by either heat or UV irradiation. Once produced, high affinity MIP nanoparticles are isolated by washing the solid – phase with a series of steps, which first remove the non-reacted reagents and the low affinity nanoparticles and only at the end allows the collection of a purified fraction of the high affinity nanoparticles (Guerreiro *et al.* 2009).

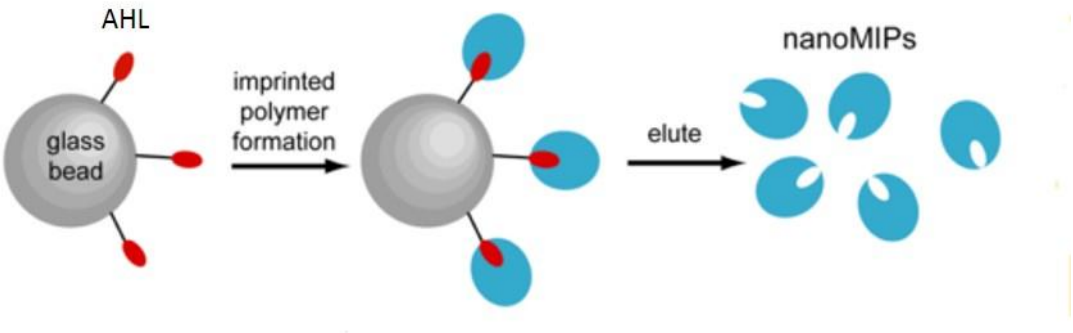

Figure 2-20 MIP NP general synthesis (*adapted from* Chianella *et al.* 2013).

This synthetic approach has interesting advantages such as the possibility to imprint substances not soluble in polymerisation mixtures and lack of requirement of a surfactant during the polymerisation to get homogenous particles. In addition, by using an immobilised template, the imprinting effect is enhanced and the heterogeneity of the binding sites is reduced due to the immobilisation step that forces the template to be oriented in a specific way.

2.7.2 Applications of MIP NPs

Molecularly imprinted polymers nanoparticles have shown to have several advantages in comparison with the larger size counterparts. For example, both the template removal and the rebinding kinetics are improved (Yilmaz *et al.* 2000), also, the low cost and robustness makes MIP NPs potentially very valuable. The applications of MIP NPs are definitely numerous, from artificial receptors in sensors, to drug delivery and to antibody substitutes (Chianella *et al.* 2003, Hoshino, Koide, *et al.* 2010, Piletska and Piletsky 2010, Shutov *et al.* 2014).

MIP nanoparticles synthesised through precipitation polymerisations have been applied to different situations. For applications in the industry and for sensing purposes, MIP NPs can be prepared with a UV fluorescent monomer. MIP NPs specific for melittin, a toxic peptide found in bee venom, prepared by precipitation polymerisation were tested *in vivo.* In this study, a reduced mortality (up to 50%) was seen in mice injected with both the venom and the MIP NPs as compared with mice injected only with the venom (Hoshino *et al.* 2010). This demonstrated that MIP NPs were able to sequestrate melittin from the animal bloodstream, making the peptide unable to perform its toxic activity. In another study, MIP NPs were prepared for human rhinovirus antibodies and were used to create a stamp on a sensor surface capable to recognise the virus itself. The results showed that nanoparticles stamps were more sensitive than the natural antibodies (Schirhagl *et al.* 2010). MIP NPs were also prepared by precipitation polymerisation for drug delivery of 5-fluorouracil (5-FU). Results,

obtained from *in vitro* studies showed that the material is a promising candidate for drug delivery systems (Rostamizadeh *et al.* 2013). MIP NPs, prepared with the solid approach, have been used as replacement of antibody in a pseudo-ELISA for vancomycin (Chianella *et al.* 2013), where a very low limit of detection was achieved (2.5 pM) also when measurements were performed in serum. The same MIP NPs were also successfully immobilised on an optical fibre to develop a novel sensor for vancomycin (Korposh *et al.* 2014). In another example, magnetic MIP NPs (MINA) specific for vancomycin were prepared using the solid-approach and the pseudo-HRP catalytic activity of the magnetic core was used to perform a pseudo-ELISA, without the use of any biomolecules (Shutov *et al.* 2014).

Although precipitation polymerisation seems to be a suitable approach to get MIP NPs with appropriate imprinting for different types of compounds (Poma *et al.* 2010), the need of working in high dilutions can have a negative impact on the interactions between the template and the monomer. Additionally, the composition mixture and the polymerisation conditions have to be strictly controlled in order to obtain a reproducible shape, size and imprinting properties (Hoshino, Haberaecker, *et al.* 2010, Poma *et al.* 2010). Such issues do not exist with the solid—phase approach where working in a high dilution system is not necessary and the polymer composition and polymerisation conditions are not as critical as in precipitation polymerisation. In addition, whereas removal of template from NPs produced by precipitation polymerisation requires long and tedious washing steps (e.g. dialysis), removal of template from the NPs prepared by solid approach is straightforward and done during the washing steps necessary to elute the high affinity nanoparticles. This is performed by packing the solid-phase in a column and passing volumes of warm solvents (e.g. 60 °C acetonitrile) capable of disrupting the interaction between the MIP NPs and the template attached to the solid phase. The high affinity particles are eluted and the template remains attached to the solid phase and can be potentially re-used for a subsequent synthesis (Poma *et al.* 2013).

Due to all these benefits, in this work MIP NPs with affinity for AHLs (QS signal molecules) were synthesised using the solid approach, with the purpose of using them to sequestrate the autoinducers, with consequent attenuation of QS and hopefully also reduction of bacterial virulence. MIP NPs were synthesised using glass beads as the non-degradable support, to which an analogue of the target analyte was attached. As the following chapters will show, after characterisation by dynamic light scattering (DLS), transmission electron microscopy (TEM) and surface plasmon resonance (SPR, BIAcore), the resulting high affinity MIP NPs were tested for attenuation of QS by reducing the bioluminescence in *V. fischeri* and biofilms' formation in *A. hydrophila.*

Chapter 3

Linear Polymers

3 Linear polymers effect on *V. fischeri* and *A. hydrophila* QS

This chapter describes the development and application of linear polymers based on itaconic acid, methacrylic acid and methyl methacrylate. The information is reported in a 'manuscript format' to have it ready, after minor alterations, for submission.

3.1 Introduction

Quorum sensing (QS) is a refined system of communication, mediated by small diffusible molecules called autoinducers (Fuqua *et al.* 1994, Bassler 1999, Miller and Bassler 2001). Autoinducers (AIs) allow the chemical communication between bacteria in a cell-density-dependent manner (Bassler and Losick 2006, Antunes *et al.* 2010). These molecules are produced inside the cell at low levels and diffuse outside, crossing cell membranes. Whenever in the extracellular medium the concentration of signal molecules reaches a critical value, these molecules re-enter inside the bacterial cells affecting their behaviour (Fuqua *et al.* 1994, Antunes *et al.* 2010, Decho *et al.* 2010) - autoinducers regulate gene expression as a function of cell population density (Bassler and Losick 2006, Williams 2007a). Quorum Sensing is highly specific due to the specificity of the interactions between the signal molecules and their receptors. N-acylhomoserine lactones (AHLs) are the most commonly produced autoinducers of Gram-negative bacteria (Fuqua *et al.* 2001). The first AHL identified as an autoinducer was N-(3-oxohexanoyl)-L-homoserine lactone (3-oxo-C_6-AHL) expressed by *V. fischeri* (Engebrecht *et al.* 1983). Quorum Sensing is related to several bacterial phenotypes: bioluminescence (Nealson 1978, Defoirdt *et al.* 2008), conjugation (Zhang *et al.* 1993), expression of several virulence factors such as toxins (Winzer & Williams 2001; Whitehead et al., 2001), and this cell-to-cell communication also plays an important role in the development of mature antibiotic resistant biofilms (Waters and Bassler 2005,

Defoirdt *et al.* 2010). This has special relevance for bacterial pathogens (Kievit *et al.* 2001, Dickschat 2010, Rutherford and Bassler 2012).

Bacterial infections are routinely treated using antibacterial compounds that may be bactericidal or bacteriostatic. The most common antibiotics target cellular processes such as bacterial DNA replication and repair, cell wall biosynthesis and/or the protein synthesis (Defoirdt *et al.,* 2010). Nevertheless, bacteria can acquire resistance to these molecules, a phenomenon increasingly reported both in the clinical and natural environments (Kollef *et al.,* 2011, Tacão *et al.,* 2014). Consequently, new strains of resistant microorganisms and even of superbugs have emerged with serious consequences for human health (Muniesa *et al.,* 2012). A strategy based on the control of the expression of virulence factors should lead to the decrease of bacterial virulence without inducing bacterial resistance phenotypes (Defoirdt *et al.,* 2010). Since bacteria make use of QS to regulate virulence genes and toxins' production (Antunes and Ferreira 2009), quorum quenching (QQ) may be considered as a potential therapeutic strategy. In fact, most pathogens delay the production of virulence factors until a crucial population density is attained, ensuring a successful infection of the host (De Lamo Marin *et al.* 2007). Swift and co-workers (1999) reported a significant decrease in virulence factors expression and virulence of pathogens, when the QS mechanism was inactivated.

Quorum Quenching has been explored as a strategy to attenuate virulence, to block the formation of biofilms, and in the adjustment of other QS-mediated mechanisms. If signal molecules can be controlled at early stages of the bacterial infections, the use of QS inhibitors offer a new tool to fight bacterial diseases (Boyen *et al.,* 2009). An important advantage is that the QS inhibition does not impose selective pressure for the development of bacterial resistance, as with antibiotics.

Synthetic linear polymers based on methacrylates (e.g.PMMA) were already used to delay bacterial attachment of *P. aeruginosa* (Gottenbos *et al.* 2001). In

this work, we describe the development of biocompatible non-cytotoxic polymers able to sequester AHLs and interfere with QS of *V. fischeri* and *A. hydrophila*. A set of copolymers of itaconic-acid with methyl methacrylate (IA-MMA), and methacrylic acid with methyl methacrylate (MAA-MMA) were synthesised by free radical polymerisation (FRP). *V. fischeri* and *A. hydrophila,* an emergent human pathogen (Swift *et al.* 1999), were utilised as model system to test copolymers. The study also includes the evaluation of biocompatibility and cytotoxicity of the developed polymers by *in vitro* cytotoxicity tests.

3.2 Material and Methods

3.2.1 Materials

Itaconic acid (IA, 99 %), methacrylic acid (MAA 99 %, containing 250 ppm monomethyl ether hydroquinone as inhibitor), methyl methacrylate (MMA 99 %, containing ≤ 30 ppm monomethyl ether hydroquinone as inhibitor), ethylene glycol dimethacrylate (EGDMA), acetonitrile, ethyl acetate 2-butanone, 2-methoxyethanol N,N-dimethylformamide (DMF), 2,2'-azobis-(2-isobutyronitrile) (AIBN), N-(β-ketocapryloyl)-DL-homoserine lactone (3-oxo-C_6-AHL), N-hexanoyl-DL-homoserine lactone (C_6-HSL), N-butyryl-DL-homoserine lactone (C_4-HSL), and anti-bumping granules were purchased from Sigma (Sigma-Aldrich, UK). Nutrient Broth Nº 2 (NB), Luria-broth (LB) and Agar Bacteriological (Agar Nº 1), were purchased from Oxoid (Basingstoke, UK).

3.2.2 General Procedure for Copolymers Synthesis

A 3:1 monomer ratio was used to synthesised copolymer (or linear polymers) by free radical polymerisation: 3:1 (MMA: IA/MAA) as described in Table 3-1. The polymerisation solvent used was a mixture of 2-butanone and 2-methoxyethanol (1:1; v:v). MAA and MMA were distilled under vacuum. Purified monomers were kept at 4ºC and used without further purification. The 2,2'-azobis-(2-

isobutyronitrile) (AIBN) was purified by fractional crystallization from ethanol (m. p. = 104 ºC). Other reagents (extra-pure grade) were used without purification.

Table 3-1 Composition of copolymers synthesis

Copolymer	Functional Monomers			Initiator
	IA	MAA	MMA	AIBN
pIA_{25}-co-$pMMA_{75}$	3.02 g; 0.023 mol	—	6.98 g; 0.069 mol	0.313 g
$pMAA_{25}$-co-$pMMA_{75}$	—	2.23 g; 0.026 mol	7.77 g; 0.078 mol	0.313 g

Polymerisation reactions were prepared as described (Table 3-1). The monomers were poured into a 250 ml three-necked round-bottom flask. The solvent mixture was added to the round-bottom flask and a condenser and a thermometer were connected. The flask was placed on a magnetic stirrer/heater, immersed into an oil bath and degassed with nitrogen. At 60 ºC conventional radical copolymerisation started by the addition of the initiator 1,1'-azobis (cyclohexane-carbonitrile), and carried out for 20 h. The linear polymers were precipitated, drop by drop, in ultra-pure water. The precipitate was recovered by vacuum filtration (Whatman filter paper nº 1). The copolymers were re-dissolved in DMF (~20-30 ml). Afterwards, a new precipitation was carried out, followed by filtration and solubilisation in DMF. This procedure was performed three times. The copolymers were dried under vacuum in a desiccator at room temperature for 4 days and kept at room temperature until use.

3.2.3 Linear Polymers Characterisation

3.2.3.1 Optical Microscopy

The polymers were characterised by optical microscopy using an Axioskop2 microscope with an Achroplan 10X objective and an Axiocam CCD camera (Carl Zeiss Ltd, UK). A small portion of dry particles was spread on a slide glass and then covered with a coverslip. The image was acquired using AxioVision 3.1 software (Carl Zeiss Ltd, UK).

3.2.3.2 Nuclear Magnetic Resonance (NMR) Spectroscopy

The NMR spectra were obtained using a JEOL ECX-400 NMR spectrometer (Jeol, Welwyn Garden City, UK). The NMR solvents, $CDCl_3$ and CD_3OD, were obtained from Cambridge Isotopes Limited (UK). Twenty mg of copolymer were solubilised in NMR solvent. Itaconic acid polymers were solubilised in methanol-D4 (CD_3OD) and methacrylic acid polymers were solubilised in chloroform-D ($CDCl_3$). All the polymers were analysed by ^1H NMR (400MHz). The resulting NMR spectra were analysed with JOEL Delta^{TM} data processing software.

3.2.3.3 Gel Permeation Chromatography (GPC)

Gel permeation chromatography (GPC) was performed on a Polymer Labs GPC 50 Plus system fitted with a differential refractive index detector. Separations were performed on a pair of PLgel Mixed-D columns (300 × 7.8 mm, 5 µm bead size, Polymer Labs UK) fitted with a matching guard column (50 × 7.8 mm). The mobile phase was DMF with 0.1 % LiBr (w/v) at a flow rate of 1 mL/min. Column calibration was achieved using narrow poly[methyl methacrylate] standards (1.96 – 790 kDa, Polymer Labs, UK). Samples were prepared at 1–5 mg/mL in the mobile phase and injected (100 µL) onto the column. Molecular weight and polydispersity index were calculated using Polymer Labs Cirrus 3.0 Software.

The poly[methyl methacrylate] standards allowed the determination of molar masses. Most polymers are polydisperse, containing polymer molecules of different molecular weights. The polydispersity of a polymer is quantified using the PDI (Polydispersity Index) which is defined by the Mw/Mn, where the Mw is the weight average molar mass and the Mn is the number average molar mass of a polymer. Mw and Mn are calculated by averaging the number or the weight of polymer chains with a defined molar mass, respectively. By definition, Mw ≥ Mn, so the minimum PDI of any polymer sample is PDI = 1. Mn and Mw are associated to macroscopic polymer properties and relevant parameters, for example in the polymer kinetics (Young and Lovell, 2011).

3.2.3.4 Binding Capacity Determination Studies

Polymer binding capacity towards the lactones 3-oxo-C_6-AHL, C_4-HSL and C_6-HSL was evaluated by HLPC-MS, as described previously (Piletska *et al.* 2011) with slight modifications. A stock solution of each AHL (1 mg/ml) was prepared in acetonitrile. Several dilutions were prepared in water: 0.1, 0.5, 1.0, 2.5, 5, 10, 20, 50, and 100 µg/ml, in order to build an HPLC-MS calibration curve. Ten mg of each copolymer were suspended in 1 ml of each AHL (25 µg/ml) and incubated overnight (200 rpm, at room temperature). After incubation, samples were centrifuged at 10,000 rpm for 20 minutes, and the supernatant were collected and filtered through 0.45 µm pore nylon filter. A Waters 2975 HPLC system equipped with a Luna C18 (2) column (150 x 3 mm, 3 µm, Phenomenex) was used. Elution was achieved by a gradient of methanol (0–70 %, v/v) acidified with formic acid (0.1 %) at a flow rate of 0.2 ml/min. A fragment of AHL with m/z of 102 was detected by mass-spectrophotometer Micromass Quatro Micro (Waters, UK) equipped with an ESI interface in positive ion mode (Morin *et al.*, 2003). Mass Spectrometry parameters were: desolvation gas - 850 L/h, cone gas- 50 L/h, capillary- 4.5 kV, cone-25 V, CE- 20, source temperature- +120 ºC, desolvation temperature- +350 ºC, collision energy- 25 V, multiplier-

650 V (Piletska *et al.* 2011). The concentration of free AHL was determined and the amount of AHL adsorbed was calculated by subtraction.

3.2.4 Immobilisation of Copolymers

Linear polymers *pMAA$_{25}$-co-pMMA$_{75}$* and *pIA$_{25}$-co-pMMA$_{75}$* were solubilised in dry methanol (1 mg/ml). One hundred ml of solubilised copolymers were dispensed in flat-bottom, polystyrene 12-well microplate. The solvent was allowed to evaporate overnight at room temperature (Chianella *et al.* 2013).

3.2.5 Bacterial Strains Growth Conditions with Copolymers

The wild strain *V. fischeri* ATCC 7744 and an environmental strain of *A. hydrophila* were used as model organisms. *V. fischeri* and *A. hydrophila* were grown overnight at 180 rpm, at 25 ºC and 30 ºC, in Luria-broth (LB) and in Nutrient Broth nº 2 supplemented with 2 % NaCl, respectively. Copolymers were added to 250 ml Erlenmeyer flasks (10mg/ml), and sterilised by irradiation with UV light for 20 minutes. Fifty ml of culture medium and an aliquot of overnight grown bacteria culture (500 µl) was added to the culture. All cultures were incubated at the bacteria optimum growth temperature with agitation (180 rpm). Copolymer-free cultures and media supplemented with the respective copolymer were used as negative controls. At selected intervals, the optical density at 600 nm (OD_{600nm}) was measured using a UV mini-1240 UV-VIS Spectrophotometer (Shimadzu). At the same time, an aliquot was collected and diluted in PBS (10^{-1}-10^{-9}). The diluted aliquots were plated in Marine Broth Agar (MA) or Luria Broth Agar (LA), for *V. fischeri* or *A. hydrophila* and incubated at adequate temperature for 24 h, and the number of colonies forming units (CFU) was determined. All samples were analysed, at least by three independent experiments performed in triplicate.

3.2.6 Effect of Copolymers in *V. fischeri* bioluminescence

To evaluate the effect of copolymers on *Vibrio fischeri* ATCC 7744 bioluminescence, the culture was grown as described previously (3.2.5). *Vibrio fischeri* luminescence was measured on a luminometer (TD-20/20 Luminometer, Turner Designs, INC., USA).

3.2.7 Biofilm Formation in *A. hydrophila*

Biofilm formation was analysed in a 12-well microplate coated with 0.1 mg/ml of solubilised polymers (Merritt *et al.* 2011). Microplates were firstly sterilised for 20 minutes under UV light radiation. The microplate method is an indirect method commonly used to determine biofilm (Djordjevic *et al.* 2002). Each well was inoculated with 1 ml of 1:100-diluted *A. hydrophila* culture (~0.9 $O.D_{600nm}$); microplates were incubated at 30º C, for 27 hours without agitation. Afterwards, the supernatant (planktonic cells) was collected and transferred to another 12-well sterilised microplate. Each well was gently rinsed three times with PBS. After adding 500 µl of 5 % sterile resazurin solution (v:v) was added to each well and the microplates were incubated at cell's optimal growth temperature, according to Pettit *et al.* 2005, Mariscal *et al.* 2009. Resazurin was solubilised in PBS and sterilised by filtration (0.22 µm). Briefly, after rinsing three times with PBS, 500 µl of 5 % resazurin solution (v:v) was added to each well and the microplates were incubated at a suitable temperature. After 1 hour for planktonic cells and 2 hours for biofilm cells, well contents were removed and transferred to another microplate. The absorbance of both, planktonic and sessile cells, were measured at 570 nm and 600 nm using a microplate reader (Multiskan Spectrum Microplate spectrophotometer, Thermo Scientific). All the assays were performed in triplicate. *A. hydrophila* biofilm was determined by the ratio between planktonic (free cells) and biofilm (sessile) cells.

3.2.8 Cytotoxicity

The Vero cell line (ECACC 88020401, African Green Monkey Kidney cells, GMK clone) was grown and maintained according to Ammerman *et al.* 2008. 12-well microplates coated with copolymers (0.1 mg/ml) were sterilised by UV radiation for 20 minutes. Cytotoxicity evaluation was performed by the resazurin metabolism assay (Pina *et al.* 2010). Linear polymers were solubilised and coated onto a 12-well microplate at a 0.1 mg/ml, prior to 20 minutes UV sterilisation. Vero cells were seeded into 12 well plates at a density of $1x10^5$ cells/well, and incubated for 24 h and 48 h at 37 ºC with 5 % CO_2. After each time of incubation, the growth medium was aspirated and replaced with fresh medium supplemented with 10 % of 0.1 mg/ml resazurin, for 2:30 h at 37 ºC. The cell viability was measured through metabolic activity by resazurin reduction. Viable cells are able to metabolically reduce resazurin to resorufin. This is a reaction where the starting reagents are blue and non-fluorescent detectable at 570 nm (resazurin) and the products are pink with a fluorescent signal detectable at 600 nm (resorufin) as Figure 3-1 describes (O'Brien *et al*. 2000). Afterwards, the well content was removed and transferred to another microplate and the absorbance at 570 nm and 600 nm was measured in a microplate reader (Multiskan Spectrum Microplate spectrophotometer, Thermo Scientific). All the experiments were made in triplicate. Percentage of cytotoxicity for each copolymer was calculated as: (OD_{570}/OD_{600} sample - OD_{570}/OD_{600} medium) / (OD_{570}/OD_{600} control - OD_{570}/OD_{600} medium) x 100 (Cruz *et al.* 2013). Vero cell morphology in the presence of copolymers was evaluated by inverted light microscopy. Images were acquired using a CKX41 Olympus inverse microscope with a digital colour camera Olympus CAM-SC30 and a 20X objective. The image acquisition was obtained by the AnalySIS getIT software (Soft Imaging System, Munster, Germany).

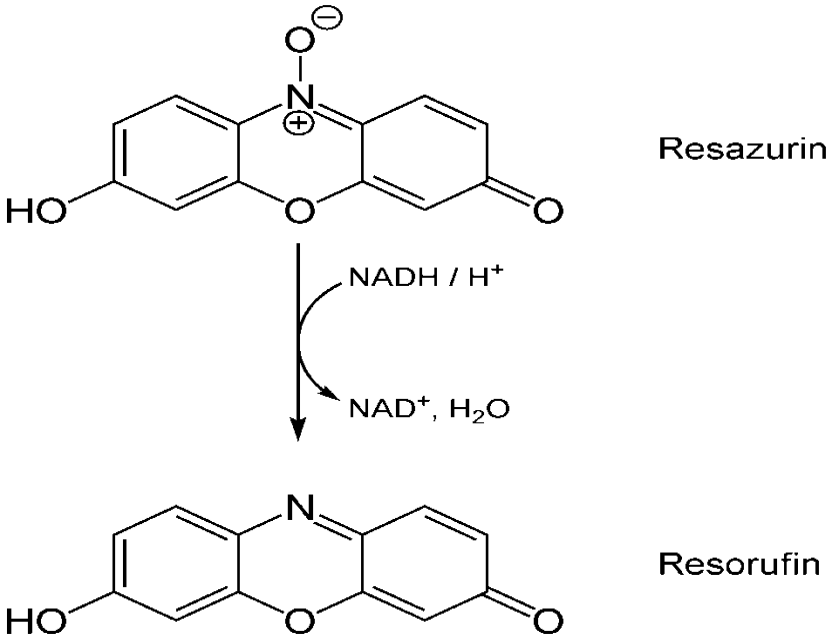

Figure 3-1 Reduction of resazurin to resorufin by viable cells.

3.2.9 Statistical Analysis

Statistical analyses were performed using GraphPad Prism v.5 software (GraphPad Software Inc.). For cell viability one-way ANOVA followed by Bonferroni's Multiple test with a statistical confidence coefficient of 0.95 was used; consequently p values <0.05 were considered significant.

3.3 Results and Discussion

3.3.1 Copolymerisation Synthesis

Based on a previous study of molecular modelling performed by Piletska and colleagues (2010), itaconic acid and methacrylic acid were selected as best monomers due to their strong interactions with 3-oxo-C_6-HSL, C_4-HSL and C_6-HSL (Piletska *et al.* 2010). The monomers' selection was performed using a library containing 20 of the most commonly used commercial monomers (Piletsky, Karim, *et al.* 2001). The linear polymers synthesised in this work were

produced using methyl methacrylate (MMA) as inert monomer to build the backbone of the materials. The mixture of copolymers (IA/MMA and MAA/MMA) was synthesised by free radical polymerisation in a solvent mixture of 2-butanone: 2-methoxyethanol (1:1; v:v) with 0.313 g of the initiator AIBN. General procedure of each copolymer is summarised in Figure 3-2 and Figure 3-3. The performance of these polymers is related with a balance between hydrophobic and hydrophilic interactions with the target analyte (Girod *et al.* 2013).

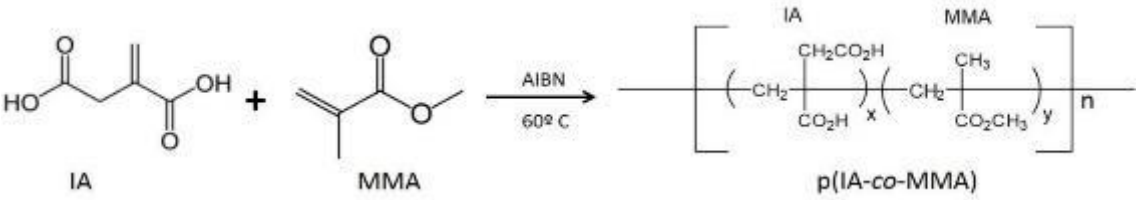

Figure 3-2 Scheme of polymerisation of itaconic acid (IA) with methyl methacrylate (MMA).

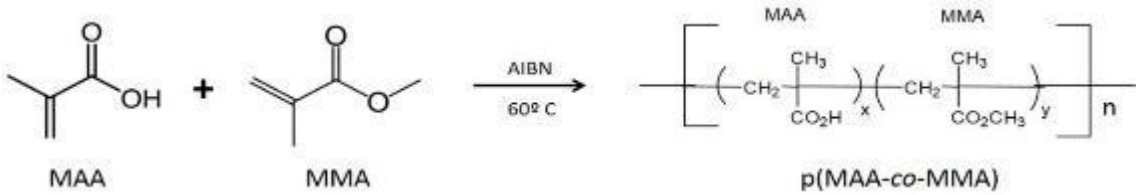

Figure 3-3 Scheme of polymerisation of methacrylic acid (MAA) with methyl methacrylate (MMA).

The mechanism of the free radical polymerisation was divided in 3 steps: initiation, propagation and termination (Figure 2-17). Initiation has involved a creation of a free-radical active centre through two steps. The initiator (AIBN) formed free radicals, and one of those free radicals was added to the functional monomer (IA/MAA or MMA). The thermal decomposition of the AIBN has occurred at 60ºC. The propagation step, the core of the process, has included the growth of the polymer chain by rapid sequential addition of monomer to the carbon-based free active centre. Basically, the number of monomer units was added to each initiator molecule, and this has determined the molecular weight

of the final material. In the termination step the active centre was irreversibly destroyed and the propagation ceased (Young and Lovell, 2011). The size and morphology of polymer synthesised were evaluated by optical microscopy (Figure 3-4). In a dry state the copolymers' particles presented many different shapes, resulting in an asymmetrial powder. In *pMAA$_{25}$-co-pMMA$_{75}$* polymer the particle size ranges from 3.91 µm to 17.67 µm (Figure 3-4 B) whereas in *pIA$_{25}$-co-pMMA$_{75}$* particles are smaller, 2.47 µm to 12.28 µm (Figure 3-4 A). Many polymers present irregular morphology (as bulk polymers) and that is mainly due to the drying process. Although polymers morphology is irregular, this did not interfere with the capacity of action of the material, as shown by the binding capacity studies. The linear polymers prepared by free radical polymerisation have several advantages compared to other polymerisation methods (e.g. ionic chain polymerisation): a relative insensitivity to monomer and media impurities (decreasing synthesis costs) and the possibility of using a broad range of monomers (Hong *et al.* 2002).

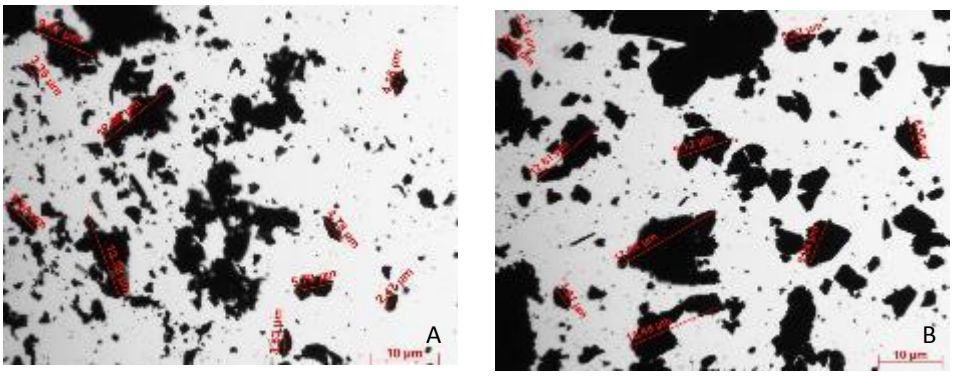

Figure 3-4 Optical microscopy of copolymers dry powders; A) *pIA$_{25}$-co-pMMA$_{75}$* copolymer, B) *pMAA$_{25}$-co-pMMA$_{75}$* copolymer (40X magnification). Scale bar represents 10 µm.

3.3.2 ^{1}H-NMR spectroscopy, GPC and Binding Capacity Studies

The monomer composition was determined from the integral intensities of ^{1}H NMR signal of methyl peak (3.6 ppm) of methyl methacrylate (Table 3-2 and Appendix A1). The monomer ratio of each polymer was calculated based on integration of methyl peak from MMA (***c*** in Appendix A1) in comparison with the functional monomer (IA or MAA). The methyl peak is on its own significant to calculate the ratio of monomers in the polymer. The integrals of the peaks are proportional to the number of hydrogen atoms giving the signal. According to this it is possible to have two simultaneous equations for each polymers (Figure 3-5; A) for *pMAA$_{25}$-co-pMMA$_{75}$* and B) for *pIA$_{25}$-co-pMMA$_{75}$*).

$$3\,Y = 3$$

$$5\,X + 5\,Y = \text{value of integration peak} \qquad \text{A)}$$

$$3\,Y = 3$$

$$4\,X + 5\,Y = \text{value of integration peak} \qquad \text{B)}$$

After solving both equations and finding the X and Y values, the percentage of functional monomer (MAA or IA) is given by the following equation:

$$\%\ \text{monomer} = [\,X / (Y+X)\,] \times 100. \qquad \text{C)}$$

Figure 3-5 Equations A) B) and C) used for ^{1}H NMR calculations

Table 3-2 Free-radical polymerisation of MAA/IA (M1) and MMA (M2). Characterisation of copolymers determined by NMR and GPC.

	Monomer feed (mol %)		^{1}H NMR (mol %)		GPC		
	M1	**M2**	**M1**	**M2**	**M_n (g/mol)**	**M_w (g/mol)**	**PDI**
$pMAA_{25}$-co-$pMMA_{75}$	25	75	28.28±4.75	71.72±4.78	11288.00	29634.50	2.63
pIA_{25}-co-$pMMA_{75}$	25	75	20.80±8.03	79.20±8.03	23729.00	42273.50	1.78

For both copolymers, the functional monomer content was slightly different from the predicted one. However, considering the standard deviation obtained for different polymer batches, the difference is not significant. The characterisation of polymers is given in Table 3-2; the theoretical monomer feed for each polymer is presented by 25 % for the functional monomer (M1) of each polymer; and 75 % for backbone monomer (M2). The real composition of each polymer obtained by ^{1}H NMR was calculated using the equations above. The results showed that *$pMAA_{25}$-co-$pMMA_{75}$* has around 28 % of MAA, and the *pIA_{25}-co-$pMMA_{75}$* has 21 % of IA. The percentage of the backbone MMA was determined by subtraction, 72 % for *$pMAA_{25}$-co-$pMMA_{75}$* and 79 % for *pIA_{25}-co-$pMMA_{75}$.*

The polymer production was properly controlled and reproducible. The dispersity of the size of the particles is used to characterise any type of polymer. Polydispersity index is determined by the mass-average molar mass (Mw) and the number-average molar mass (Mn). The Mw is more sensitive to molecules of high molecular mass whereas Mn is more sensitive to molecules of low molecular mass. The PDI is basically a measure of the distribution of molecular mass in the polymer. The dispersity varies according the type of mechanism of polymerisation and can be affected by a variety of reaction conditions.

The size of the particles was analysed by gel permeation chromatography (GPC). The GPC analysis determined the Mw, Mn and the distribution of molecular weights for each polymer. The GPC calibration was performed using PMMA standards. For both polymers the GPC results show higher Mw compared with the Mn. Between the two polymers the *pIA$_{25}$-co-pMMA$_{75}$* showed a higher Mw than *pMAA$_{25}$-co-pMMA$_{75}$*.

The PDI of *pMAA$_{25}$-co-pMMA$_{75}$* was higher (2.63) than that of *pIA$_{25}$-co-pMMA$_{75}$* (1.78) validating the data obtained by microscopy (Table 3-2). The copolymers were solubilised in dry methanol. The process of complete dissolution of the polymers particles lasted for several hours. Nevertheless, and although time consuming, solubilisation of this type of polymers is still possible because they are linear and not cross-linked.

Table 3-3 Binding capacity of copolymers towards 3-oxo-C_6-HSL, C_6-HSL and C_4-HSL

	3-oxo-C_6-HSL (mg per g of polymer)	**C_6-HSL** (mg per g of polymer)	**C_4-HSL** (mg per g of polymer)
pMAA$_{25}$-co-pMMA$_{75}$	0.95 ± 0.11	0.71 ± 0.11	0.66 ± 0.11
pIA$_{25}$-co-pMMA$_{75}$	0.28 ± 0.06	0.24 ± 0.12	0.13 ± 0.03

The average binding capacity of each polymer against AHLs is shown in Table 3-3. Binding capacity studies were performed in water. The polymers were incubated with several concentrations of AHLs for a period of 24 hours. During the incubation time, the AHLs were bound by each polymer. With the use of HPLC-MS to quantify the amount of AHLs left in the solutions after incubation, the binding of each AHLs (3-oxo-C_6-HSL, C_6-HSL and C_4-HSL) by the polymer *pMAA$_{25}$-co-pMMA$_{75}$* and *pIA$_{25}$-co-pMMA$_{75}$.*, was calculated. The *pMAA$_{25}$-co-pMMA$_{75}$* polymer has a higher binding capacity towards all the AHLs assayed when compared with *pIA$_{25}$-co-pMMA$_{75}$* copolymer. The polymers' binding to

AHLs is probably governed by electrostatic and van der Waals interactions, between the carboxylic groups of polymer and the lactone ring of AHL. The copolymers binding capacity for 3-oxo-C_6-HSL observed here is comparable to that seen for a cross-linked polymers prepared with 5% of IA, developed by Piletska and colleagues, which was adsorbing 0.27 µg of lactone for g of polymer (Piletska *et al.* 2010). Nevertheless, the solubility of our linear polymers in organic solvents makes the integration of this type of material easier (e.g. mixing them with paints) and suitable for specific applications.

3.3.3 Effect of Copolymers on QS Regulated Phenotypes: Bioluminescence of *V. fischeri*

V. fischeri bioluminescence is a QS-regulated phenotype (Engebrecht *et al.* 1983, Fuqua *et al.* 1994). *Vibrio fischeri* has been used as a model microorganism to assess the efficiency of the polymers to disrupt QS: if the polymers are able to adsorb AHLs, then *Vibrio* bioluminescence should be reduced. The growth of *V. fischeri*, in the presence of copolymers, was evaluated by determination of CFU (Figure 3-6). Usually this evaluation is performed by a simple measurement of absorbance (OD_{600} nm). However, the tests were performed incubating the polymer suspension with a culture of *V. fischeri*, and the polymer particles interfered with the measurement reading (Appendix A-2). For this reason, the effect on growing of *V. fischeri* was performed using CFU as methodology. The results showed the *V. fischeri* was not affected by the presence of linear polymers. In the graphic of Figure 3-6 the results of CFU for *V. fischeri* when incubated with polymers (*$pMAA_{25}$-co-$pMMA_{75}$* and *pIA_{25}-co-$pMMA_{75}$)* show to be very similar to the control (just *V. fischer*i) despite some points are not exactly related. This can be justified by the fact that the number of *V. fischeri* cells can be variable in a certain range. When an extra dose of AHL was added to the control and also to the culture with the polymer, no relative differences were noticed.

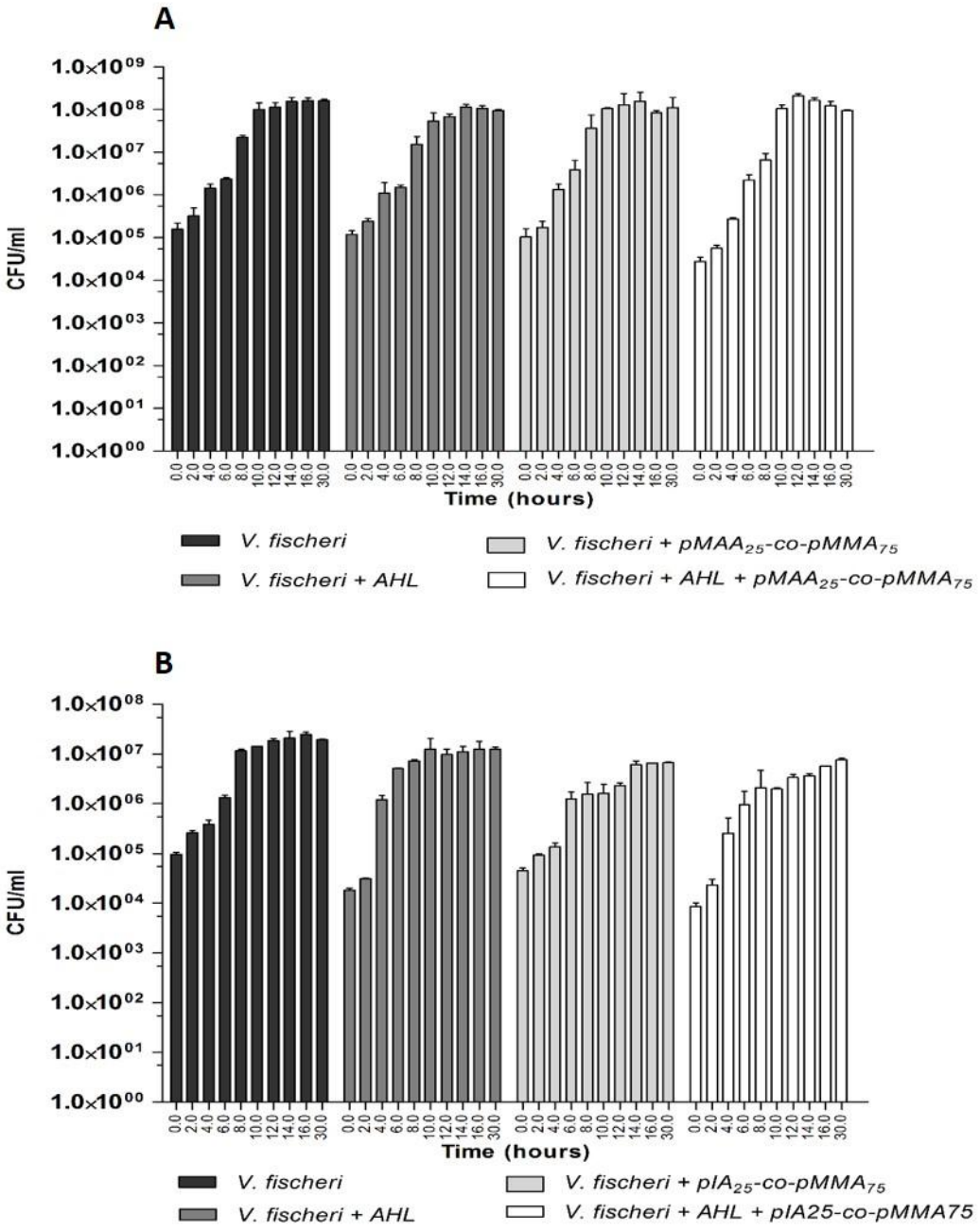

Figure 3-6 Bacterial growth (CFU/ml) of *V. fischeri* (A and B) in the presence of *pMAA$_{25}$-co-pMMA$_{75}$* and *pIA$_{25}$-co-pMMA$_{75}$* copolymers. The culture was supplemented with 100 µM of AHL for each copolymer.

As mentioned before, the *V. fischeri* bioluminescence is a QS-phenotype dependent. The bioluminescence was measured in the presence of both

polymers. Any effect on bioluminescence would represent an evidence that QS signal molecules are affected. When the AHLs are not available, the bacterial cell does not recognise the others cells, and the bioluminescence is not produced. If bioluminescence has interferences (delays intensity) means that the polymer is removing AHLs from the environment, and in this way is interfering with Quorum Sensing. Regarding the effect on *V. fischeri*, the presence of *pIA$_{25}$-co-pMMA$_{75}$* reduced bioluminescence at the exponential phase by one log unit at 4 hours (black squares, Figure 3-7 B). Interestingly, this linear polymer showed a lower binding capacity for AHLs than the *pMAA$_{25}$-co-pMMA$_{75}$* polymer (Table 3-3), demonstrating that testing conditions may influence the polymer performance. The capability of reducing luminescence in *V. fischeri* by a highly cross-linked polymer based on IA, was also reported by Piletska and co-workers (2010).

At this point, it should be stressed that the effect of these polymers on the reduction of *V.* bioluminescence is not due to a toxic effect on cells or cell growth. As seen in Figure 3-6, the addition of *pMAA$_{25}$-co-pMMA$_{75}$* or *pIA$_{25}$-co-pMMA$_{75}$* has no effect on cell growth, suggesting that in fact, these polymers are able to interfere with QS by sequestration of lactones. To further demonstrate that bioluminescence reduction was due to AHL sequestration by the polymer, *V. V. fischeri* lactone (3-oxo-C$_6$-HSL) was added in the culture. As expected, an increase in bioluminescence (open circles, Figure 3-7 B) was seen. Nevertheless, even after the addition of exogenous 3-oxo-C$_6$-HSL, the *pIA$_{25}$-co-pMMA$_{75}$* was still

able to reduce *V. fischeri* bioluminescence (open squares,

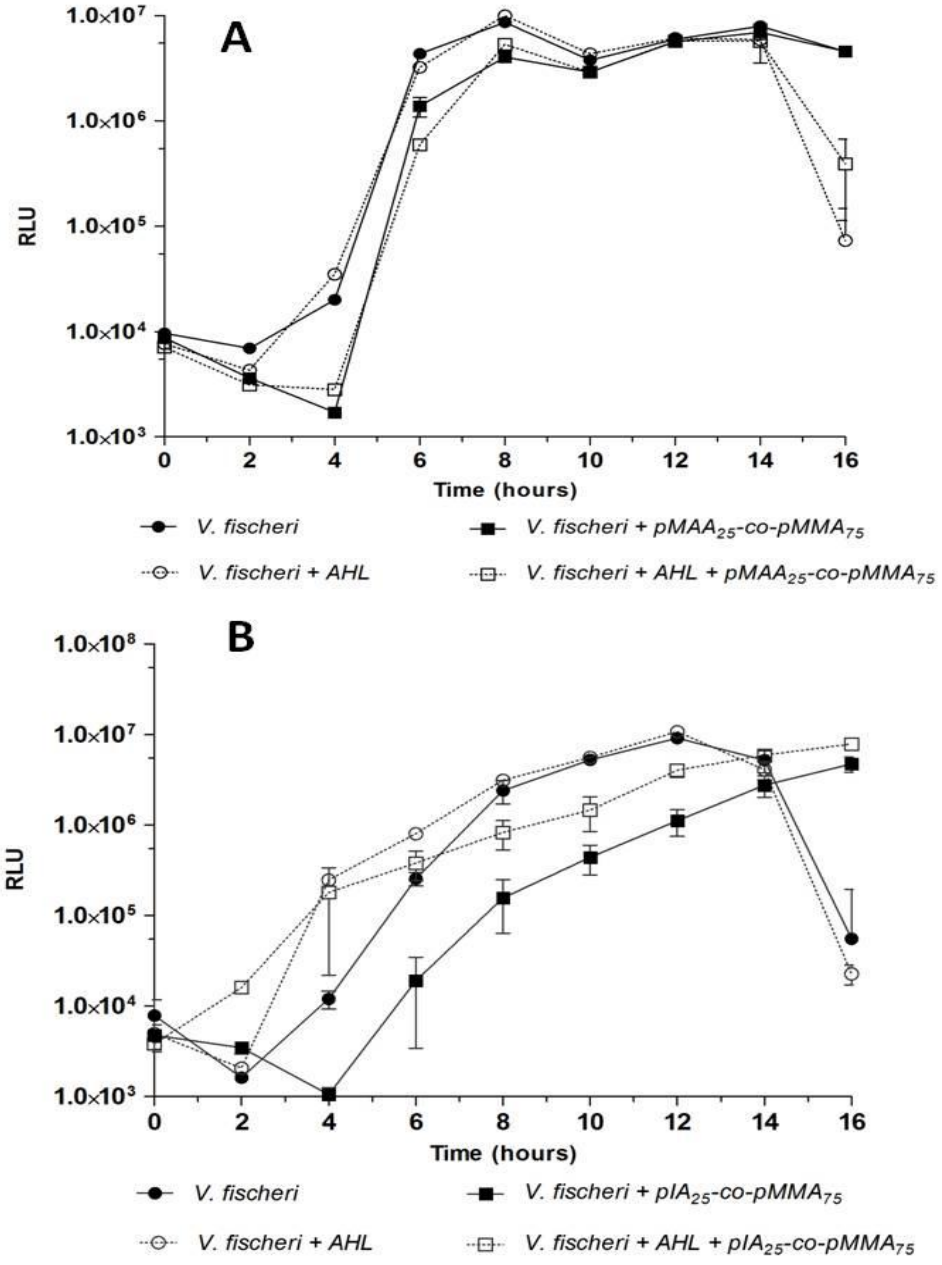

Figure 3-7 B).

The *pMAA$_{25}$-co-pMMA$_{75}$* polymer also caused a decrease in bioluminescence (black squares,

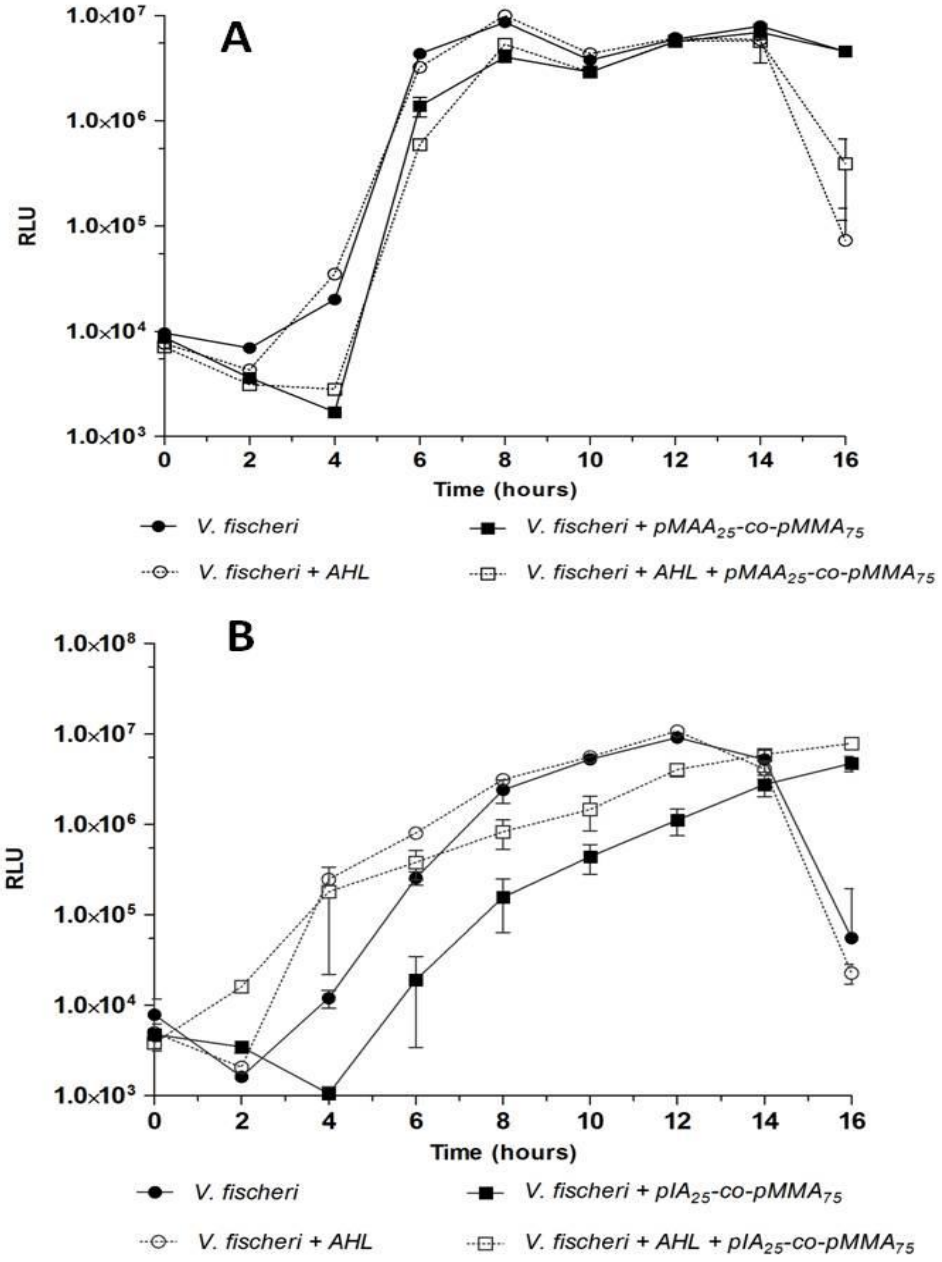

Figure 3-7 A). The reduction effect on bioluminescence of *V. fischeri* by this polymer was not as high as *pIA$_{25}$-co-pMMA$_{75}$,* but still significant. After the addition of AHLs, a similar trend to that obtained with *pIA$_{25}$-co-pMMA$_{75}$* was observed (open squares, Figure 3-7 A).

In conclusion, both polymers were capable to reduce *Vibrio* bioluminescence, when compared to the control. As mentioned before, Piletska and colleagues (Piletska *et al.* 2010) have described cross-linked polymers based on the same monomers, able to decrease *V. fischeri* bioluminescence in the early hours of growth. The effect of Piletska's cross-linked polymer and the linear polymers synthesised by us on bioluminescence may be related to strong interactions established between monomers and AHLs, studied previously by *in silico* computational molecular modelling (Piletska *et al.* 2010). Nevertheless, despite the cross-linked polymers also appear to have capacity for AHLs and decrease bioluminescence, our linear polymers can be considered better candidates as QS inhibitors; due to their solubility in organic solvents, which allows a simpler integration for real applications (e.g. inclusions in paints or even in membranes).

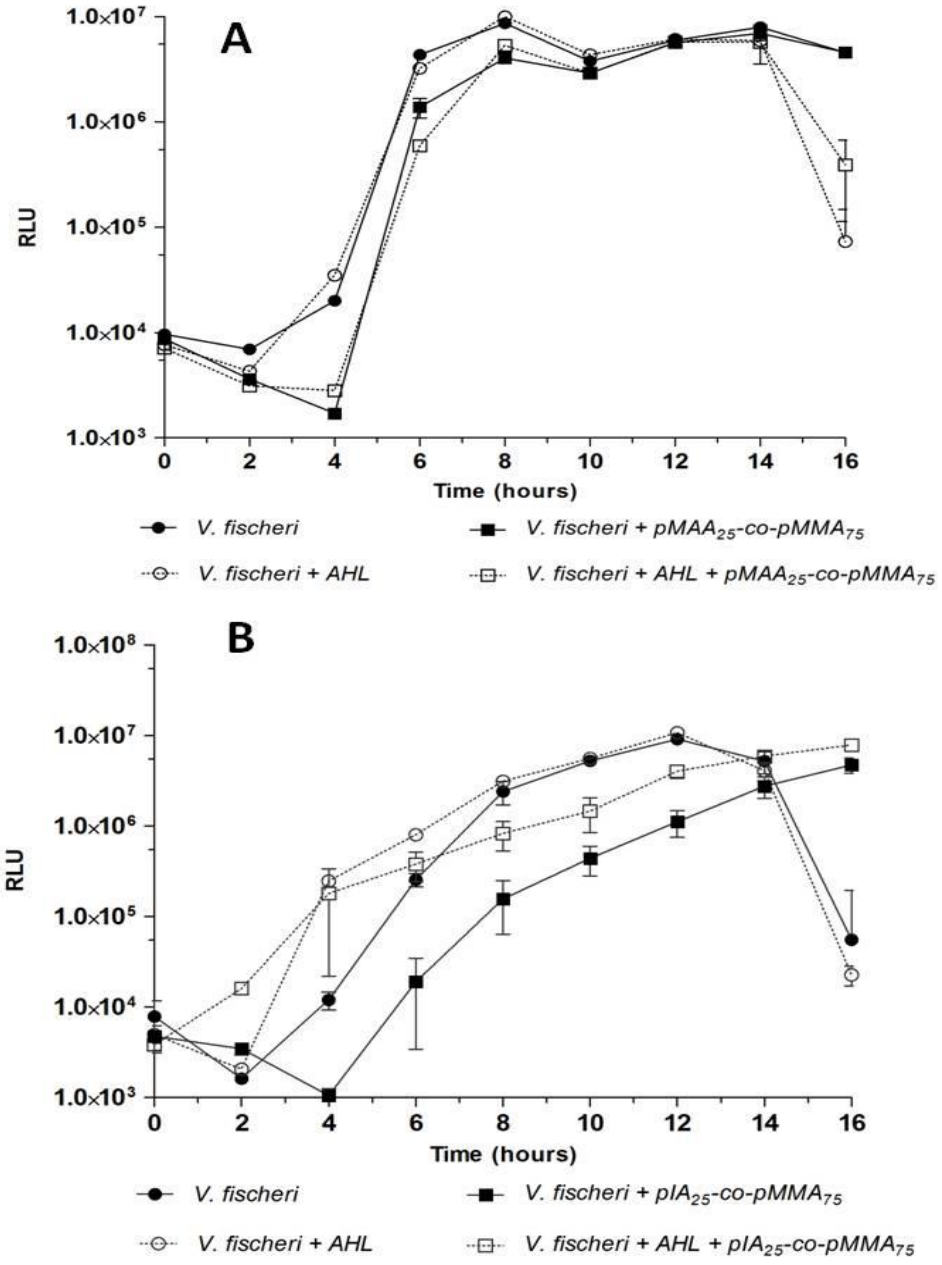

Figure 3-7 Bioluminescence (RLU) signal of *V. fischeri* in presence of $pMAA_{25}$-co-$pMMA_{75}$ (A) and pIA_{25}-co-$pMMA_{75}$ (B) copolymers. A supplement of 100 µM of AHL (3-oxo-C_6-HSL) was added to each copolymer experiment. The data represent means (standard deviations) of three independent experiments performed in triplicate.

3.3.4 Effect of Copolymers on QS Regulated Phenotypes: Biofilm Formation of *A. hydrophila*

It is known that bacterial biofilm formation is linked to QS via AHLs production. Formation of biofilm strongly increases the survival and growth of the bacteria in hostile environments (Miller and Bassler 2001; Nadell *et al.* 2008). Biofilms contribute to the development of antibiotic resistance. As previous described for *V. fischeri,* this study the effect on *A. hydrophila* growth was evaluated. The effect of the linear polymers on *A. hydrophila* was assessed by CFU determination, rather than measuring the absorbance (OD_{600} nm), for the same reason reported above. Similarly to *V. fischeri*, the presence of the polymers has little effect on *A. hydrophila* growth (Figure 3-8).

The effect of linear polymers on *A. hydrophila* was evaluated using the strain IR-13, with the polymer immobilised on wells of microplates as explained before. It is known that biofilm formation in *A. hydrophila* is controlled by QS mediated through AHLs (Lynch *et al.* 2002).

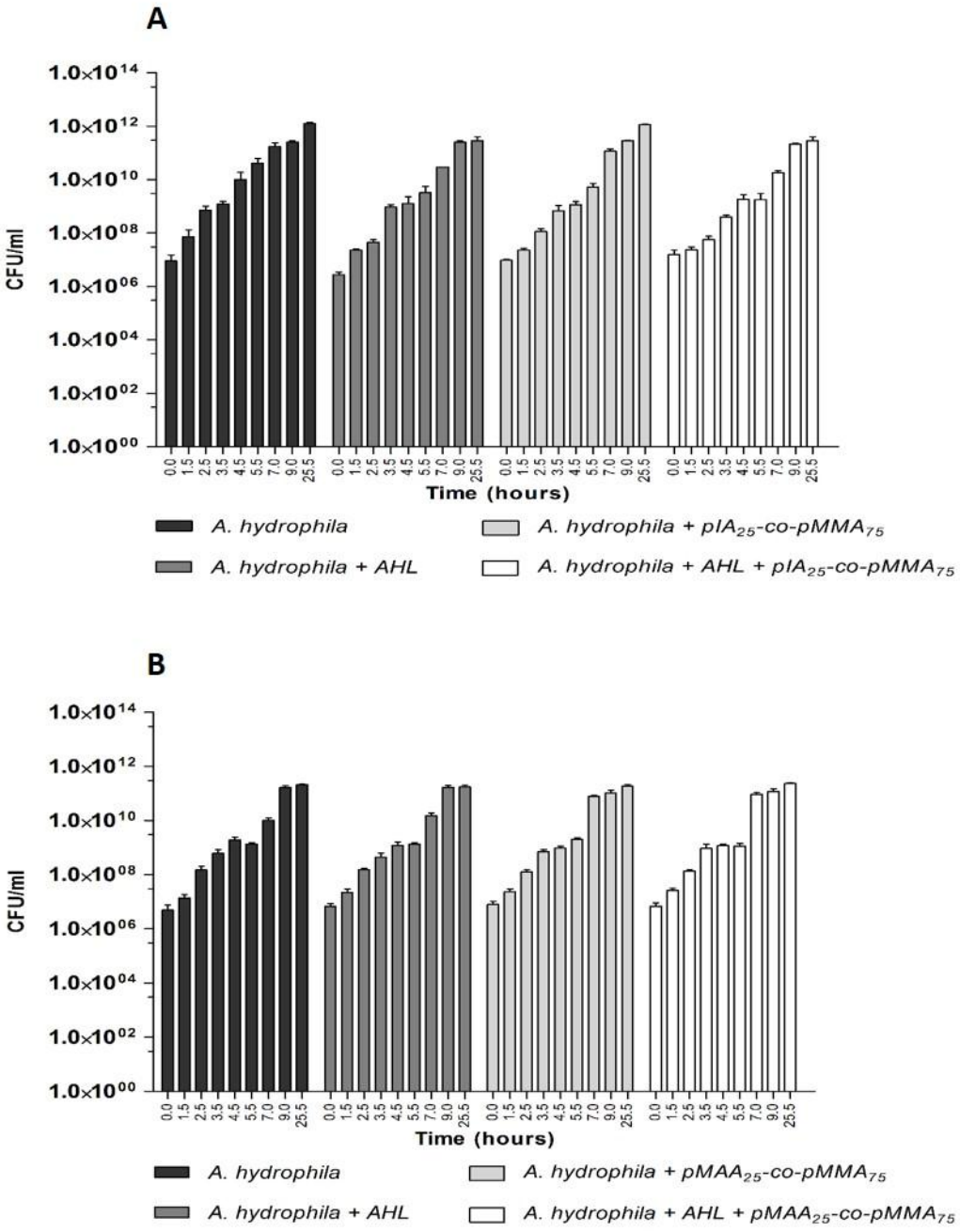

Figure 3-8 Bacterial growth (CFU/ml) of *A. hydrophila* in the presence of pIA_{25}-co-$pMMA_{75}$ (A) and $pMAA_{25}$-co-$pMMA_{75}$ (B) copolymer. The culture was supplemented with 100 µM of AHL for each copolymer**.**

The biofilm formation in *A. hydrophila* was assessed by resazurin methodology. Using this methodology it is possible to quantify living cells within a biofilm. The resazurin assay gives a better assessment of biofilm formation rather than the crystal violet assay. Basically, resazurin is metabolised by viable cells and it is reduced to resorufin. This methodology was also chosen having in mind that the presence of the polymers could affect cells by damaging bacterial cells and resazurin assay would highlight this. The crystal violet is a good tool to indicate quantify of biomass in a biofilm but not cell viability into the biofilm. Using resazurin it was possible to determine the viable cells in suspension during the biofilm formation (planktonic cells) and the cells attached/adsorbed to the surface forming the biofilm (sessile cells). The calculations were performed in terms of ratio between the sessile cells and planktonic cells; having in mind that if the ratio is above 1, it means that sessile cells are in a higher number compared with the planktonic cells, meaning that a significant amount of biofilm is present. The production of biofilm by *A. hydrophila* biofilm was significantly ($p<0.001$) reduced by both polymers (Figure 3-9). AHL-mediated QS in *A. hydrophila* regulates biofilm formation (Lynch *et al.* 2002). To confirm that biofilm reduction resulted from sequestration of AHLs by the linear polymers, we supplemented the cultures with 100 µM of C_4-HSL (the signal molecule). The cultures with exogenous AHL recovered their ability to form biofilm, probably due to the fact that the amount of copolymers present in the experiments was not enough to fully adsorb the exogenous AHL. These results demonstrated the interference of polymeric materials in biofilm formation, interfering with QS through sequestration of AHL, leading to reduced bacterial adhesion (McCoy *et al.* 2012). The reduction of the effect upon AHL administration was probably due to inability of the limited amount of copolymers attached to the wells to fully adsorb both, the endogenous and exogenous AHL.

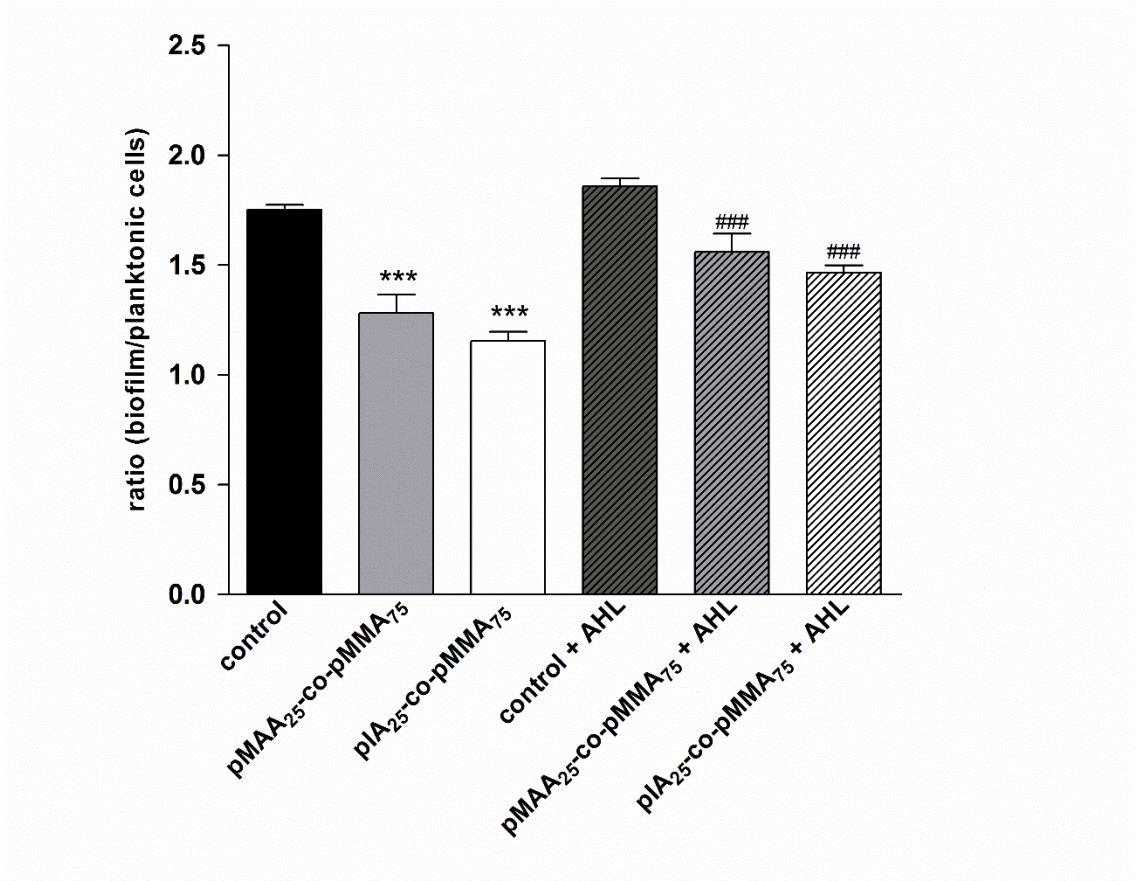

Figure 3-9 Linear polymers effect on biofilm formation by *A. hydrophila* and *A. hydrophila* supplemented with 100 µM of AHL. One-way ANOVA, followed by a Bonferroni's multiple comparison test, was performed to determine statistical significance of copolymers against the control (*** $p<0.001$) and the control supplemented with AHL ($^{###}$ $p<0.001$). Vertical bars represent standard deviation**.**

3.3.5 Cytotoxicity Evaluation

Polymers capable of disrupting QS must be also bio-safe, in order to be readily applied. It is important to ensure that polymers capable to disrupting QS aer not toxic. Therefore, the cytotoxicity of linear polymers was evaluated with Vero cell line (epithelial cells from African green monkey kidney). The cellular metabolic activity was assessed by resazurin assay during 48 hours (Figure 3-9).

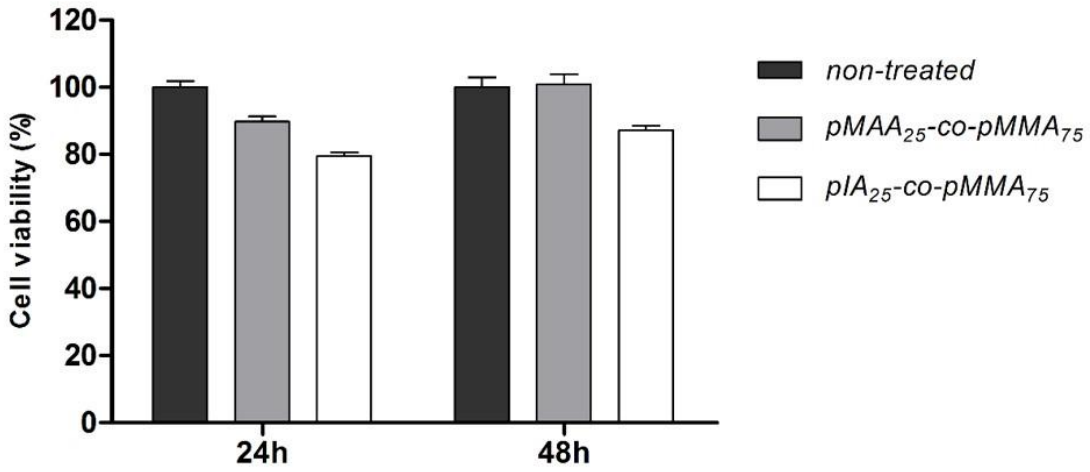

Figure 3-10 Cytotoxic effect of linear polymers evaluated by the viability of Vero cells, along 48 hours, determined by resazurin. One-way ANOVA was performed followed by a Bonferroni's multiple test ($p<0.05$). Data represents three independent experiments performed in triplicate.

Resazurin is a metabolic assay used in cellular viability, to quantify the cell viability all over time. It shows the efficiency that cells have to metabolise resazurin in resorufin. The great advantage of using resazurin, rather than other common methods used for the same purpose, is that resazurin is not toxic for the cells. The quantification of viability is assessed exactly in the same exposed cells, first after 24 hours and then after 48 hours incubation.

In the first 24 hours (Figure 3-10), cell viability was slightly affected ($p<0.05$) by both polymers. Whereas in the presence of *pMAA$_{25}$-co-pMMA$_{75}$*, cell viability was approximately 90%, in the presence of *pIA$_{25}$-co-pMMA$_{75}$*, cell viability was reduced to 80 %. Nevertheless, after 48 hours of contact with the polymers, Vero cells recovered nearly all their viability. In the presence of *pMAA$_{25}$-co-pMMA$_{75}$*, the viability was around 100%, and with *pIA$_{25}$-co-pMMA$_{75}$* was around 90% (Figure 3-10). These results were confirmed by inverted microscopy (Figure 3-11). In the first 24 hours the image obtained in presence of *pIA$_{25}$-co-pMMA$_{75}$* shows some "holes" between cells, when compared with the control

(non treated Vero cells) meaning that cells are adapting to the environment. However, after 48 hours for the same polymer, the confluence of cells is observed, where no more space between cells exists meaning that the cells have recovered. In the presence of *pMAA$_{25}$-co-pMMA$_{75}$* both after 24 hours and 48 hours the cell morphology is very similar to the control (non treated Vero cells). Despite the fact that *pIA$_{25}$-co-pMMA$_{75}$* had a more pronounced effect on cell viability in the early 24 hours, after 48h hours Vero cells recovered. The effect on the first 24 hours of incubation was probably due to the fact that the two polymers are acidic (with *pIA$_{25}$-co-pMMA$_{75}$* more acidic than *pMAA$_{25}$-co-pMMA$_{75}$*) and at the beginning of the experiments this might have lower the pH, slightly affecting the cell. As the system matures, the pH is restored and the cell recovered. In conclusion this study has demonstrated that the linear polymers are not cytotoxic in conditions selected for the experiments.

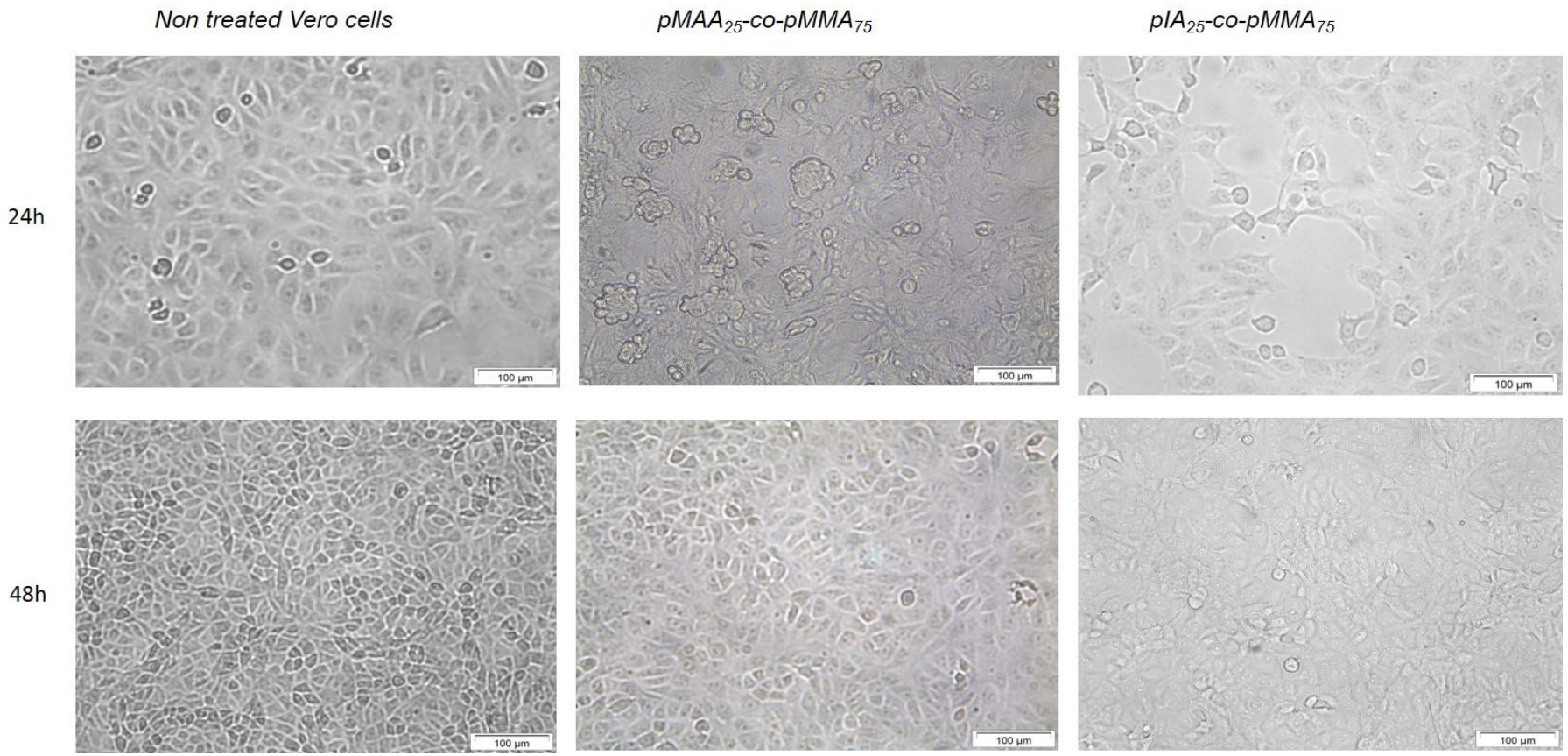

Figure 3-11 Inverted microscopy of Vero cells exposed to copolymers after 24 and 48 hours. Images were taken under 200X magnification. Scale bar 100 µm.

3.4 Conclusions

In this study, two non-toxic copolymers - *pMAA$_{25}$-co-pMMA$_{75}$* and *pIA$_{25}$-co-pMMA$_{75}$* - were synthesised by free radical polymerisation. Their interference with QS-regulated phenotypes, such as the decrease of bioluminescence in *V. fischeri*, and the reduction of biofilms produced by *A. hydrophila*, confirmed the ability of the polymers to disrupt bacterial QS.

Bacterial diseases and bacterial resistance are regulated by QS. Therefore, the use of harmless synthetic materials capable to interfere with QS is an exciting alternative to more toxic solutions to control bacterial diseases. Linear polymers are new compounds capable to overcoming bacterial related problems (such as biofilms and antibiotic resistance). In this study, the linear polymers did not show cytotoxicity in the conditions tested, demonstrating to be useful candidates as materials to decrease bacterial virulence. Their solubility in organic solvents, make them excellent candidates for integration in filters (e.g. for water filtration) or in paints to be used both in environmental and medical settings. The filters and the painted surfaces containing the polymers would be capable to adsorb QS signal molecules delaying bacterial virulence, reducing bacterial resistance and enhancing the effect of commonly used antibacterial agents.

Chapter 4

Molecularly Imprinted Polymer Nanoparticles

4 Molecularly Imprinted Polymer Nanoparticles on *V. fischeri* and *A. hydrophila*

This chapter describes the development and application of molecularly imprinted nanoparticles specific for AHL and capable to affect bacterial QS. The information is reported in a manuscript format to have it ready, after minor alterations, for submission.

4.1 Introduction

Bacterial virulence and pathogenicity are coordinated by gene expression which is regulated by a mechanism called Quorum Sensing (QS) (Kalia and Purohit 2011). Through QS, a cell-to-cell communication mechanism, bacteria are able to control a diversity of processes (Miller and Bassler 2001, Raina *et al.* 2009).

Bacterial pathogenicity includes the expression of virulence factors, production of toxins, antibiotic resistance (Raina *et al.*, 2009) and biofilm formation (Beceiro *et al.*, 2013). Since QS controls pathologically important phenotypes such as biofilm formation and bacterial virulence expression (Miller *et al.,* 2001), the use of QS inhibitors could be a potential approach to be utilised with/or in alternative of antibiotic therapy (McLean *et al.,* 1997). Nowadays, this is especially important because of the constantly increasing bacterial resistance to the antibiotics and antimicrobial drugs currently known and used.

Microbial biofilms have been described in several environments, with adhesion of bacteria to several surfaces. The survival of bacteria, in adverse conditions, can be dependent on the formation of biofilms. Bacteria are more protected in a than biofilm community rather in their planktonic state (Radzig *et al.,* 2013). In a biofilm community bacteria make use of QS mechanism to coordinate their behaviour (Ponnusamy *et al.,* 2013). Biofilms are associated with severe economic losses in industrial sectors, such as water purifications systems (Ponnusamy *et al.,* 2013), food and clinical environments. Several different

approaches have been investigated to reduce or inhibit biofilm formation (Simões *et al.,* 2010).

The interference of cell-to-cell communication (QS) is an excellent strategy to combat bacterial infections (Kalia *et al*. 2011). Over the last years the quenching of QS has been attempted using both natural and synthetic compounds (Hirakawa *et al..* 2013**)** One of the mechanisms used for the disruption of QS consists in the degradation or inactivation of QS signal molecules (Kalia *et al,* 2013, Tay *et al.,* 2013 Defoirdt *et al.,* 2004). A drawback of the use of natural compounds to do this is the small concentrations in which they are usually produced. The use of synthetic material with high specificity and affinity to the targets overcomes this problem. A great advantage of this type of strategy is that bacteria are not under a selective pressure, as they are when in presence of antibiotics (Bjarnsholt *et al.,* 2010). So they do not have tendency to produce resistance to these types of antivirulence compounds (Rasko and Sperandio, 2010; Maeda *et al.,* 2012; Glinel *et al.,* 2012). Examples have been reported in literature where antimicrobial compounds and polymeric materials have been investigated for the prevention of bacterial biofilms and QS inhibition.

For example, some enzymes have been used as antibacterial agents against free-living and biofilm-associated infections in *Escherichia coli* and *Pseudomonas aeruginosa*, (Boackstael *et al.,* 2009). Silver nanoparticles have also shown ability to inhibit growth and biofilm formation in Gram-negative bacteria such as *E. coli* and *P. aeruginosa*, without promotion of antibiotic resistance (Radzig *et al.,* 2013*).* Another example has shown that nanotubes of lithium were able to hamper *P. aeruginosa* growth and biofilm formation, when applied at the early stages of growing of *P. aeruginosa* (Diggikar *et al.,* 2013).

In another study, cyclic oligosaccharides (cyclodextrins) have shown to have a significant effect on virulence expression, mediated by AHLs in *Serratia marcescens,* a Gram-negative bacterium (Morohoshi *et al.,* 2013). The cyclodextrins were capable to trap the signal molecule, AHL, involved in the QS

mechanisms, reducing the production of the red pigment prodigiosin - a second metabolite dependent on QS (Morohoshi *et al.,* 2013). The adsorption and removal of AHLs from the environment stopped the bacteria from recognising their increase in number, preventing them from becoming virulent.

Komnatnyy and co-workers synthesised PEG polymeric nanoparticles with the purpose of controlling bacterial density and modulating QS by the release of proactive molecules. This technique appears to work, although bacteria were killed (Komnatnyy *et al.* 2014).

Other two types of polymeric materials, namely rationally designed polymers and molecularly imprinted polymers (MIPs) were also developed to attenuate QS-phenotypes in *Vibrio fischeri* (Piletska *et al*., 2010) and *P. aeruginosa* (Piletska *et al*., 2011*)*. Rationally designed polymers are computationally optimised materials containing a high percentage of functional monomers able to interact strongly with the target analyte (autoinducers) (Piletska *et al.,* 2008; Piletska *et al.,* 2010). MIPs are polymers with recognition capabilities achieved by synthesising the material in presence of the target analyte (signal molecule), which, at the end of the process, is washed out to leave behind specific cavities (Ye and Mosbach, 2001). When used to attenuate QS, both materials showed high affinity and specificity for the signal molecules (AHLs). In fact, through adsorption of the signal molecules, the rationally designed polymers were capable of reducing bioluminescence in *V. fischeri* and MIPs were able to reduce biofilm formation in *P. aeruginosa.*

However, both polymers have some drawbacks such as difficult large-scale production and also, due to the fact that they are produced in a bulk format (powder), awkward integration in the systems in which they need to be utilised (Poma *et al.,* 2010). Furthermore, MIPs have an additional drawback, namely traces of un-washed template can leach out of the material, promoting QS instead of attenuating it. This is due to the difficulty of achieving a total removal of the template at the washing stage, after the synthesis, especially from the inner sites of the material.

Most of these shortcomings can be resolved with the production of molecularly imprinted polymer nanoparticles, MIP NPs, prepared with a solid-approach (Poma *et al.,* 2013). Examples of protocols for production of MIP nanoparticles have been reported by several research groups (Pérez -Moral and Mayes 2007, Gao *et al.,* 2007; Ma *et al.,* 2012, Guerreiro *et al.,* 2009. Poma *et al.,* 2013). Nevertheless, the solid-phase approach pioneered by Piletsky and colleagues seems the most promising as it can be automated, allowing mass production of material. The approach consists in synthesising MIP NPs in presence of a solid support (e.g. glass beads) with the target analyte or template covalently attached to it. Once the nanoparticles are formed around the template, a sequence of washings is performed on the solid-phase to elute a purified fraction of high affinity NPs, completely free of template, which remains attached to the support (Poma *et al.,* 2013). The MIP NPs produced can be solubilised/dispersed in water and organic solvents to provide versatile materials for integration, which could be achieved for example by coating surfaces or membranes.

As with bulk MIPs, MIP NPs, prepared by the solid approach, can be used to adsorb the autoinducers. In this way they can interfere with QS and therefore with cell-to-cell communication of bacteria, hopefully without affecting bacterial growth and therefore without promoting resistance.

Therefore, in this work, to investigate whether MIP NPs can affect QS, *V. fischeri* was initially chosen as a model bacterium. In fact, *V. fischeri* is a Gram-negative bacterium, whose QS, mediated by AHLs, controls bioluminescence, a parameter that can be easily monitored. If MIP NPs were able to sequestrate AHLs, the autoinducers level in the environment would decrease and a suppression or decrease in bioluminescence should be noticed.

A. hydrophila, another Gram-negative bacteria*,* was also studied due to its widespread presence in water environments and to the fact that it is considered an emergent pathogen to humans and animals, especially to fish. This bacterium is associated with several fish diseases that are the cause of severe

economic losses in aquaculture. Pathogenesis of *A. hydrophila* is mediated by QS, where biofilm formation plays a crucial role (Swith *et al.,* 1999, Lynch *et al.,* 2002) and in this work, the ability of MIP NPs to inhibit biofilms was investigated. An effective reduction of cell communication by MIP NPs will provide basis for the development of novel mitigation strategies against biofilms and bacterial infection. Finally the cytotoxicity of the nanoparticles to a fibroblast cell-line and the effect on bacterial growth were also monitored to assess that the material is not toxic and does not decrease QS-phenotypes by eliminating the microorganisms.

4.2 Material and Methods

4.2.1 Materials

Methacrylic acid (MAA), ethylene glycol dimethacrylate (EGDMA), phosphate buffered saline (PBS), pentaerythritol-tetrakis-(3-mercaptopropionate) (CTA), 3-aminopropyltrimethyloxysilane (APTMS), trimethylolpropane trimethacrylate (TRIM), dimethylformamide (DMF), acid dodecanedioic, (S)-(−)-α-Amino-γ-butyrolactone hydrobromide, sodium carbonate (Na_2CO_3), sodium chloride (NaCl), N-hydroxysuccinimide (NHS), 2-[morpholino]ethanesulfonic acid (MES); N-(3-Dimethylaminopropyl)-N′-ethylcarbodiimide hydrochloride (EDC), methanol, acetone, toluene were purchased from Sigma Aldrich, UK. Sodium hydroxide, ethanol and dry acetonitrile (ACN) were purchased from Fisher Scientific (UK). The MES buffer was obtained from Thermo Scientific (UK). The N,N′-diethyldithiocarbamic acid benzyl ester (INIFERTER) was obtained from TCI Europe (Belgium). Glass beads (Spheriglass® 2429, 53 µm < diameter < 106 µm) were purchased from Blagden Chemicals, UK. Ultrapure water (Millipore) was used in all the analysis.

4.2.2 Preparation of Derivatised Glass Beads as Solid-Phase Media

Glass beads were prepared following the method described by Moczko and colleagues (Moczko *et al.* 2013) with slight modifications. The glass beads (75 µm) were stripped out of their surface coating by vibration with ceramic beads on a Retsch Vibratory Sieve Shaker AS 200 basic (Retsch, Germany) with 70% amplitude for 5 hours. The glass beads were then activated by boiling them for 10 minutes (80-100º) in a 1 litre round flask containing 1 M NaOH. This was followed by several washing steps: firstly with ultrapure water and secondly with acetone. Then the glass beads were dried at 80ºC overnight. In order to introduce amino groups on surface, dry glass beads were incubated overnight with 2 % v/v solution of 3-aminopropyltrimethyloxysilane (APTMS)/toluene, in a 250 ml bottle. After incubation, the glass beads were rinsed with acetone and dried using compressed air.

The EDC/NHS chemistry to crosslink carboxylic groups with primary amines was carried out according to the Thermo Scientific protocol. Briefly, a volume of 100 ml of activation buffer was prepared by mixing 2.172 g of MES (0.1 M) with 2.922 g of NaCl (0.5 M) in ultrapure water and adjusting the pH to 6.0. An activation mixture was then prepared in a 50 ml bottle as follows: 125 mg of dodecanedioic acid (5.43×10^{-4} mol) was added to 20 ml of DMF and solubilised. Then 2 g of EDC (0.01 mol), and 0.420 g of NHS (3.651×10^{-3} mol) were dissolved into 10 ml of fresh activation buffer and this was added to the dodecanedioic acid solution and mixed well. The glass beads, functionalised with APTMS, were incubated for 15 minutes in this solution. Then the beads were washed with 50% DMF in water, activation buffer and acetone. The template immobilisation on the surface of the beads was performed by incubating the glass beads functionalised with the activated dodecanedioic acid, in an aqueous solution (50 ml) containing 79.08 mg of (S)-(−)-α-Amino-γ-butyrolactone hydrobromide (4.344×10^{-4} mol) and 46.02 mg of sodium carbonate (4.344×10^{-4} mol). The immobilisation was carried out for 2 hours. The glass beads were washed with 50 % DMF in ultrapure water followed by

ultrapure water alone. Finally, the glass beads were dried under vacuum and stored at 4 ºC until used.

4.2.3 Polymerisation of MIP NPs

The protocol for the polymerisation was adapted from (Guerreiro *et al.* 2009). The polymerisation mixture was prepared in a 20 ml vial with 0.3 g CTA, 1.255 g INIFERTER, 4.8 g MAA, 5.4 g EGDMA, 5.4 g TRIM and 17.55 g. of ACN. The solution was mixed well and filtered through a 0.45 µm teflon filter into a new vial covered with aluminium foil. The derivatised glass beads were divided in two small beakers sealed with a lid. The beakers were then placed for 10 minutes in a vacuum oven to remove the oxygen. The polymerisation mixture was equally divided and added to both beakers and these were irradiated, sandwiched between two UV light sources (Philips model HB/171/A, each fitted with 4x15 W lamps) for 2 minutes and 30 seconds. Each solution (glass beads and polymerisation mixture) was poured into an extraction column fitted with a polyethylene frit (20 µm porosity), in order to separate glass beads (with the nanoparticles attached) from the other components. Two distinct washing steps were performed: 1) eight times with cold ACN (every 8 minutes) to remove the material with no affinity or with low affinity; and 2) six times with hot (60ºC) ACN to detach high affinity nanoparticles. The final total volume of the high affinity MIP NPs was about 250 ml. The solution of MIP NPs was kept at – 20 ºC.

4.2.4 Dynamic Light Scattering Analysis

The size of MIP NP was evaluated using DLS. For the analysis, an aliquot (1 ml) of the high affinity fraction of MIP NPs was concentrated and acetonitrile changed with ultrapure water using centrifugal filter units (Amicon Centriplus®, 30 kDa MWCO, Millipore, UK) followed by ultra-sonication for 20 minutes. An aliquot of MIP NPs was analysed in disposable polystyrene cuvettes at 25 ºC using a Zetasizer Nano (Nano-S) from Malvern Instruments LTD (Malverm, UK). The measurements were performed in triplicate.

4.2.5 Transmission Electron Microscopy Analysis

The MIP NP were also characterised by TEM. For the analysis, an aliquot (1 ml) of MIP NP solution was ultra-sonicated for 10 minutes and concentrated to 100 µl by evaporating the solvent (ACN) with nitrogen purging . A dilution to 1 ml with ultra-pure water was then performed. A drop of MIP NP solution was placed on a carbon coated copper grid and dried in air. The TEM analysis was carried out and TEM images were obtained on a Philips CM20 transmission electron microscope.

4.2.6 Treatment of BIAcore Gold Chips and Surface Immobilisation

Au-coated chips (SIA Kit Au, BIAcore) were cleaned with a mixture of tetrahydrofuran (THF) and methanol to remove all the glue. Then chips were cleaned by immersion for 5 minutes, in Piranha solution (H_2SO_4/H_2O_2, 3:1 v/v). The chips were then carefully rinsed with ultrapure water and kept in ethanol until the template immobilisation. For the immobilisation of the template, the chips were submerged in a solution of ethanol with 0.5 mg/ml of 11-mercaptoundecanoic acid 95% (Sigma, UK) for 24 hours at 4ºC. Afterwards chips were washed with ethanol and PBS and were incubated in a solution of 0.4 M of EDC with 0.1 M of NHS and 5 mg/ml of the template butyrolactone hydrobromide for 2h; and then washed with PBS pH 7.4. After immobilisation, chips were assembled on their holders and stored under Argon at 4 °C until used. Chips with melamine, immobilised for comparison, were also prepared with the same procedure (Poma *et al.* 2013).

4.2.7 Surface Plasmon Resonance Analysis

Affinity analysis was performed using a BIAcore 3000 SPR system (BIAcore, GE Healthcare, UK). The Au-chips with template immobilised on their surfaces

were used for the experiments. Solutions of high affinity MIP NPs were prepared in ultra-pure water as explained for DLS analysis, sonicated for 30 minutes and used as stocks to prepare 9 further dilutions from 1:10 to $1:10^9$. All the affinity experiments were performed using PBS as mobile phase at a flow rate of 35 µl/min and a temperature of 25 °C. For the tests 100 µl of each dilution was injected in the BIAcore and the sensor response was recorded for 2 minutes after every injection. Specificity of the MIP nanoparticles was performed by testing them against a control chip, on which melamine instead of the lactone was immobilised. Kinetic data were fitted using BIAEvaluation Software v4.1 (BIAcore, Sweden).

4.2.8 Cover Slips Coating with MIP NPs

Cover slips (Menzel-Glaser, Thermo Scientific) were clean with 70% ethanol. The MIP NPs stock in ultrapure water was filtered through a 0.45 µm acetate cellulose filter. The cover slips were coated by incubation with either 100 µl or 200 µl of MIP NP solution, and the water left to evaporate. After this, the coated cover slips were placed into 12 multiwell plates. Prior each assay, the microplates were sterilised by irradiation with UV light for 30 minutes.

4.2.9 Contact Angle Measurements

Cover slips were coated with MIP NP as described above and the contact angles were measured by depositing a drop of water on the coated cover slip using a CAM 100 optical Angle Meter (KSV Instruments Ltd, Finland) with the software provided. The measurements were repeated at least three times in different points of the cover slip and the mean values were calculated.

4.2.10 Cell Culture: Resazurin Assay and Microscopy

The Vero cell line (ECACC 88020401, African Green Monkey Kidney cells, GMK clone) was grown and maintained according to Ammerman *et al.* 2008. MIP NPs cover slips, coated with 100 µl and 200 µl of MIP NPs, were added to a 12-well microplate, and sterilised by UV radiation for 30 minutes. Wells with uncoated cover slips were used as negative control. Cytotoxicity evaluation was performed by resazurin metabolism assay (Pina *et al.* 2010). Vero cells were seeded into 12 well plates at a density of $1x10^5$ cells/well, and incubated for 24 h and 48 h at 37 ºC with 5 % CO_2. After each incubation time, the growth medium was aspirated and replaced with fresh medium supplemented with 10 % of 0.1 mg/ml resazurin, and incubated at 37 ºC until reduction of resazurin. The well content was removed and transferred to another microplate and the absorbance was measured at 570 nm and 600 nm by a microplate reader (Multiskan Spectrum Microplate spectrophotometer, Thermo Scientific). All the experiments were performed in triplicate. Percentage of cytotoxicity for MIP NPs was calculated as: (OD_{570}/OD_{600} sample - OD_{570}/OD_{600} medium) / (OD_{570}/OD_{600} control - OD_{570}/OD_{600} medium) x 100 (Cruz *et al.* 2013). Vero cell morphology, in the presence or not of MIP NPs, was evaluated by inverted light microscopy of the cover slips. Images were acquired using a CKX41 Olympus inverse microscope with a digital colour camera Olympus CAM-SC30 and a 10X objective. The image acquisition was obtained by the AnalySIS getIT software (Soft Imaging System, Munster, Germany).

4.2.11 Bacterial Culture Strains with MIP NPs

Bacterial strains (*A. hydrophila* and *V. fischeri*) were grown overnight at 180 rpm, at 30 ºC and 25 ºC, in Luria-broth (LB) and in Nutrient Broth nº 2 supplemented with 2 % NaCl, respectively. The MIP NPs stock solution (in water) was filtered through a 0.45 µm acetate filter and 5 ml volume was added to Erlenmeyer flasks. Fifty ml of media was weighed into each 250 ml Erlenmeyer flask. An aliquot of overnight bacteria strain cell culture (500 µl) was

added into the media of each sample. All the cultures were incubated at the respective temperature (25 ºC or 30ºC) with shaking at 180 rpm. MIP NPs free cultures and media supplemented with MIP NPs were used as negative controls. At selected intervals aliquots of each sample were collected and the optical density (O.D. 600 nm) was assessed using a UV mini-1240 UV-VIS Spectrophotometer (Shimadzu). All samples were tested at least in three independent experiments performed in triplicate.

4.2.12 Effect of MIP NPs in *V. fischeri* Bioluminescence

To evaluate bioluminescence of *Vibrio fischeri* ATCC 7744 in presence of MIP NPs, the culture was grown as described previously (4.2.11). Luminescence (RLU) and optical density (OD_{600}) of bacterial cultures were measured every 2 hours for 16 hours on a luminometer (TD-20/20 Luminometer, Turner Designs, INC., USA) and on UV mini-1240 UV-VIS Spectrophotometer, respectively.

4.2.13 Effect of MIP NPs in *A. hydrophila* Biofilm Formation

Biofilm experiments were performed by placing the MIP NPs coated cover slips inside 12-well microplate. Every microplate was sterilised for 30 minutes under UV light radiation prior to use. The microplate method is an indirect method commonly used to determine biofilm (Djordjevic *et al.* 2002). Each well was inoculated with 1 ml of 1:100-diluted of *A. hydrophila* culture (~0.9 O.D at 600 nm); when required 100 µM of AHL (C_4-HSL) was added to the cell culture. Microplates were incubated at 30º C for 27 hours. After the incubation time, the supernatant (planktonic cells) was collected and transferred to another 12-well microplate. Each well still containing the cover slips was gently rinsed three times with PBS. The metabolic activity of both planktonic and biofilm cells was measured through the resazurin method (Pettit *et al.* 2005, Mariscal *et al.* 2009). Bacterial cells can metabolically reduce resazurin to resorufin. This is a reaction where the starting reagents are blue and non-fluorescent and the

products are pink with a fluorescent signal detectable between 570 and 600 nm (O'Brien *et al.* 2000, Pettit *et al.* 2005). Resazurin is a non-toxic, stable and easy to handle stain useful to quantify viable cells in biofilms (Peeters *et al.* 2008, Van den Driessche *et al.* 2014). Resazurin was solubilised in PBS and sterilised by filtration (0.22 µm). Briefly, 500 µl of 5 % resazurin solution (v:v) was added to each well and the microplates were incubated at 30 ºC for 1 hour for planktonic cells and for 2 hours for sessile cells. After incubation the solutions were removed and transferred to another microplate. The absorbance of both, planktonic and adherent cells samples, was measured at 570 nm and 600 nm using a microplate reader (Multiskan Spectrum Microplate spectrophotometer, Thermo Scientific). All the assays were performed in triplicate. The biofilm amount was determined by the ratio between planktonic (free cells) and biofilm (sessile) cells. Cover slips were then removed, carefully rinsed in distilled water and used to assess the morphology of biofilms by optical microscopy.

4.2.14 Statistical Analysis

Statistical analyses were performed using GraphPad Prism v.5 software (GraphPad Software Inc.). For cell viability one-way ANOVA was used followed by Bonferroni's Multiple test with a statistical confidence coefficient of 0.95; consequently p values <0.05 were considered significant.

4.3 Results and Discussion

4.3.1 Synthesis and Characterisation of MIP NPs

The protocol used for the synthesis of MIP NPs was adapted from Hoshino *et al.* 2008. (S)-(−)-α-Amino-γ-butyrolactone hydrobromide, an analogue of the target analyte suitable to be used within this protocol, was utilised as template. The main difference between Hoshino and co-worker's protocol and this

presented here, is the use of a solid-phase (glass beads) to facilitate the synthesis of high affinity nanoparticles. In fact, following attachment of a silane with amino groups to the hydroxyl groups of the silica, standard coupling chemistry (e.g. EDC/NHS), Figure 4-1, was used to link the template to the glass beads.

Before the EDC/NHS coupling, the glass beads were activated by refluxing in a concentrated NaOH solution, which increased the amount of reactive silanol groups (-Si-OH) on their surface (Figure 4-2).

The chemistry reaction of a standard protocol of EDC/NHS is present in Figure 4-1. The NHS was used to prepare amine-reactive esters of carboxylate groups for the chemical immobilization to the glass beads. The carboxylate group (-COOH) (dodecanedioic acid) has reacted to NHS in the present of EDC (a carbodiimide), resulting an unstable NHS ester. This unstable ester has reacted with the primary amide (-NH2) (S)-(−)-α-Amino-γ-butyrolactone hydrobromide) forming a crosslink amide to link to a solid-phase such as glass beads. The Figure 4-2 represents the reaction between dodocanedioic acid and the S)-(−)-α-Amino-γ-butyrolactone hydrobromide *via* EDC/NHS; representing the template for functionalisation reaction of glass beads.

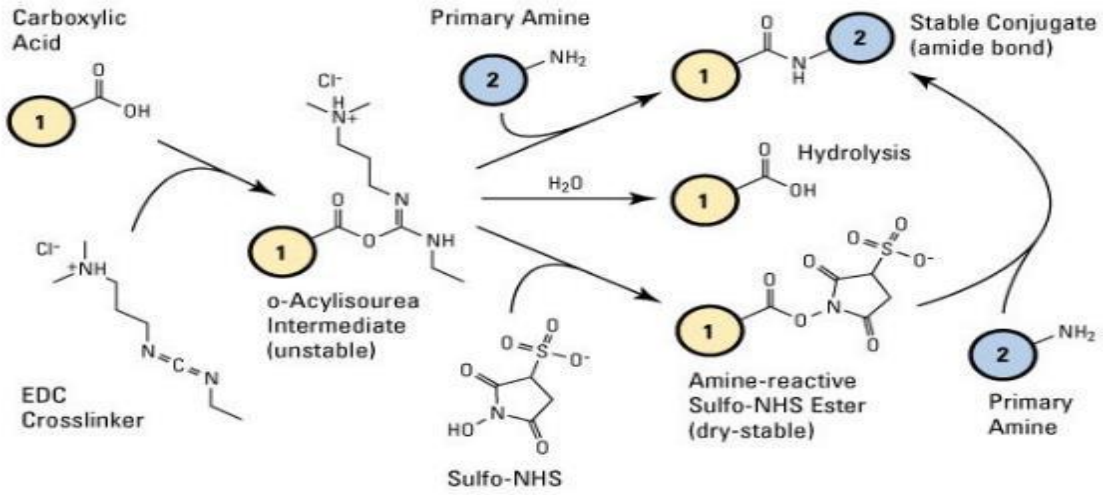

Figure 4-1 Schematic representation of the reaction of carboxylic groups and amino groups by EDC/NHS chemistry.

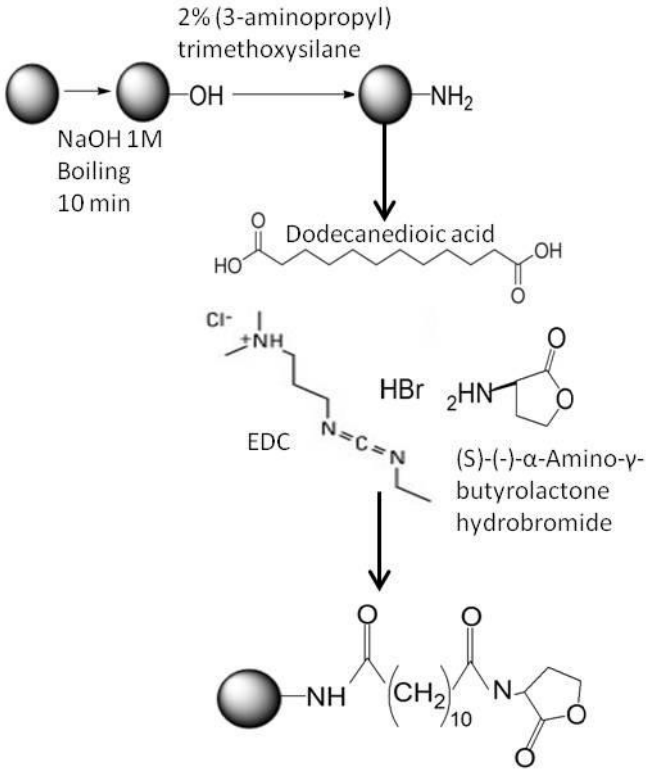

Figure 4-2 Schematic representation of immobilisation the (S)-(−)-α-Amino-γ-butyrolactone hydrobromide on the glass bead.

A previous study performed by Piletska and colleagues (2010), evidenced the strong interactions between the functional monomer MMA and C_4-HSL, C_6-HSL and 3-oxo-C_6-HSL. Therefore MMA was also used here as a functional monomer for the preparation of the nanoparticles. The template immobilised onto the glass beads in ACN was incubated with the polymerisation mixture and the polymerisation reaction was carried out by UV-irradiation (Figure 4-3).

The nanoparticles were formed; some of them around the template attached to the beads (high affinity), others either partially attached to the template (low affinity) or formed in solution (no affinity). After polymerisation, nanoparticles were packed in an empty column and washed with cold ACN to remove non reacted reagents and material with both low and no affinity for the template.

After this, to isolate the high affinity MIP NP, after polymerisation, the glass beads eluted by warm ACN according to Guerreiro *et al.* 2009.. During the cold washes the high affinity nanoparticles remain attached to the target so a high temperature is required, warm acetonitrile (60° C) to disrupt the non-covalent interactions between the nanoparticles and the template attached to the beads. A full scheme of the synthesis is reported in Figure 4-3.

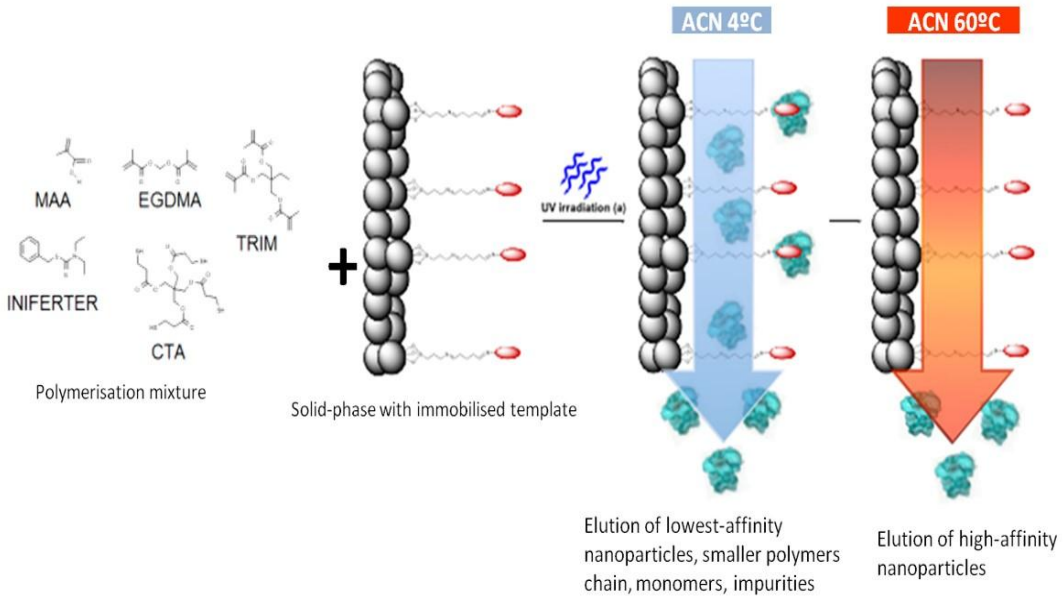

Figure 4-3 Schematic representation of solid-phase synthesis of MIP NPs.

The acetonitrile in the high affinity MIP NPs fraction was changed to ultra-pure water using centrifugal filter cartridges, for particles characterisation and testing. Four batches of MIP NP were synthesised and characterised. Before the DLS measurements, the water solution of the MIP NPs was ultra-sonicated for 15 minutes. The diameter of MIP NPs dispersed in water was measured by DLS. The ultrasonic bath was used before the measurements to disrupt possible nanoparticles aggregates, which would affect the measurements. The DLS results reported on Figure 4-4 shows monodisperse particles for all the

synthesised batches of MIP NPs; with the diameter ranging between 100 - 200 nm (see **Error! Reference source not found.**).

Table 4-1 Dynamic light scattering (DLS) diameter of four batches (A-D) of lactone MIP NPs.

MIP NPs batches	DLS (diam. nm)
A	152.6 ± 5.7
B	154.1 ± 5.5
C	147.3 ± 5.1
D	193.6 ± 2.2

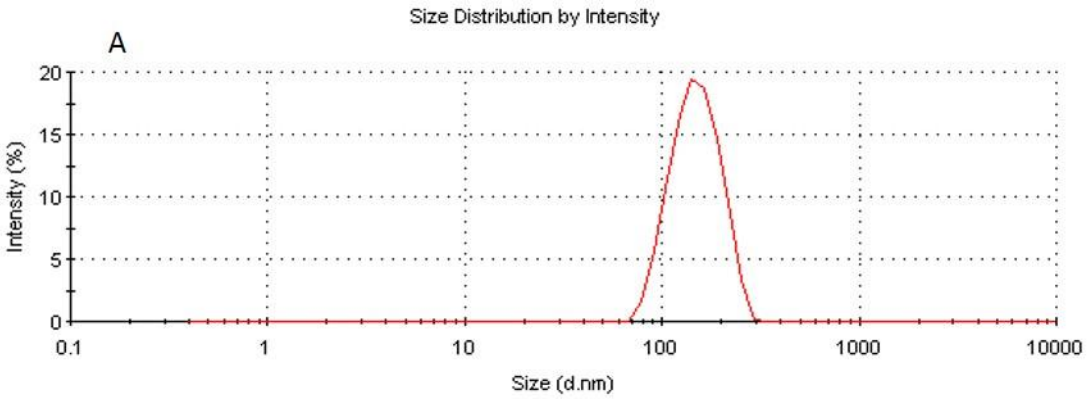

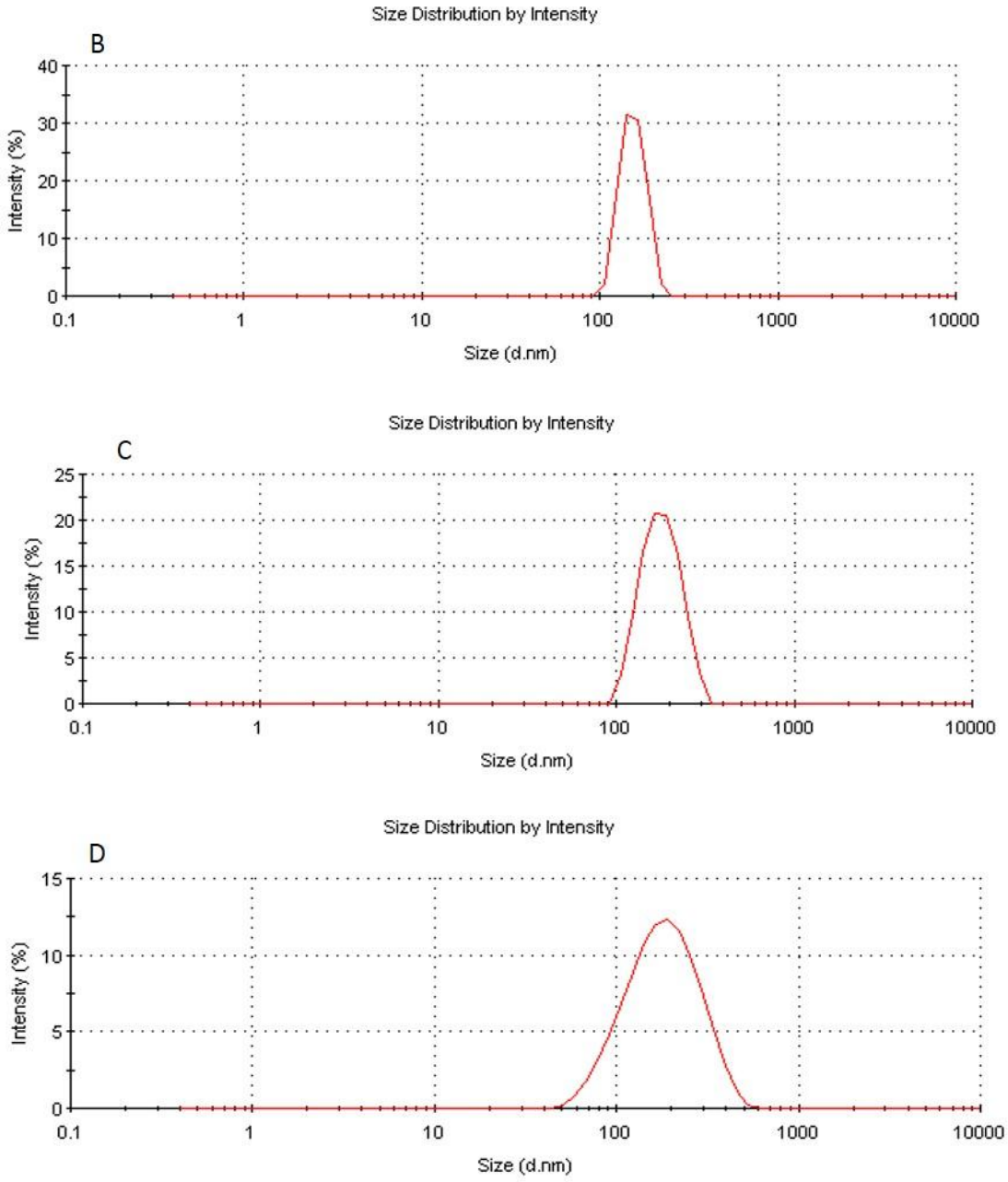

Figure 4-4 Dynamic light scattering (DL) size distribution of four batches (A-D) of MIP NPs.

It is common for DLS results to be different from the ones obtained by TEM. In fact, whereas DLS measures the hydrodynamic diameter of nanoparticles in a solvent (e.g. water), TEM is performed with dry particles. TEM analysis carried

out in this work on samples of high affinity MIP NPs showed nanoparticles with a diameter between 50 - 100 nm (Figure 4-5).

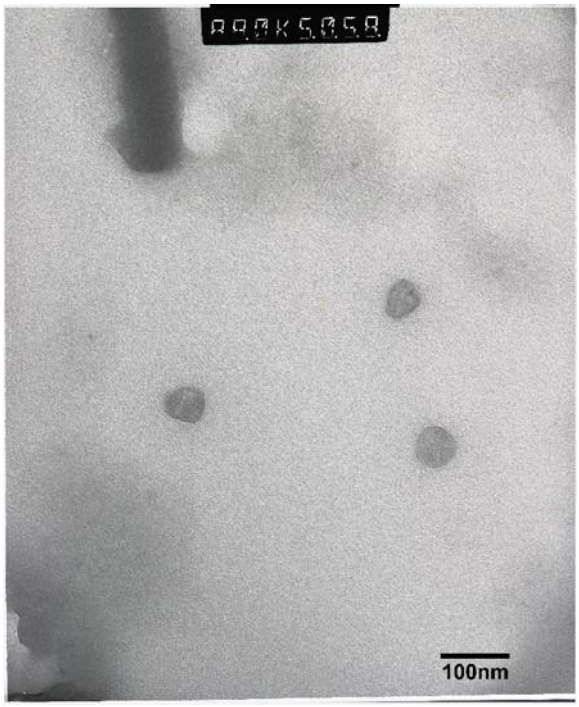

Figure 4-5 TEM image of dry MIP nanoparticle.

The average diameter from DLS measurements was then used in combination with the absorbance value, measured for the solution at 200 nm, to calculate the MIP NPs concentration in water (after exchange from acetonitrile). To do this, a calibration curve was performed by measuring DLS polystyrene standards with different molecular weights and diameters. The molecular weight of MIP NPs was determined by fitting the average diameter in the polystyrene curve. Then the absorbance value at 200 nm was used to determine the concentration of the NP in mg/m and using the molecular weight derived from the polystyrene curve, a concentration value of 20 nM was finally obtained.

The affinity and selectivity of MIP NPs were tested by Surface Plasmon Resonance (SPR) on a BIAcore 3000 system, using chips with immobilised

lactone as specific surface and sensor with immobilised melamine as non-specific surface or control. Several dilutions of MIP NPs were sequentially injected (from the lowest to the highest concentration) on each chip bearing the templates and their binding behaviour was recorded. For an assessment of the MIP NPs specificity, the same dilutions of different MIP nanoparticles were also injected on a melamine chip using the same testing conditions and the results were compared (Figure 4-6). A significant binding of the MIP NP can be observed in both surfaces, but whereas the dissociation curves from the non-specific surface is fast (steep curves) the dissociation from the specific surface seems slower, demonstrating higher affinity.

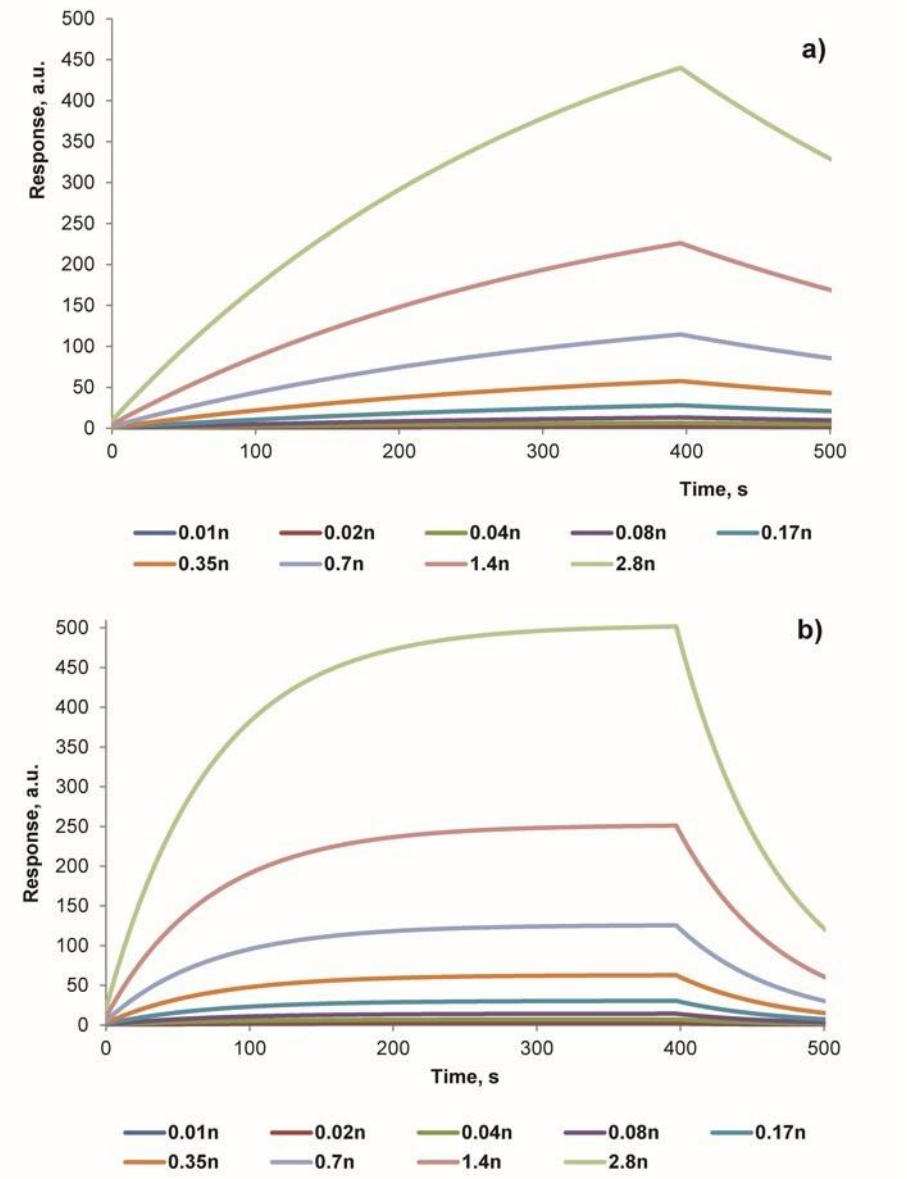

Figure 4-6 SPR sensorgram analysis of several concentrations of MIP NPs (0.01nM, 0.02nM, 0.04nM, 0.08nM, 0.17nM, 0.35nM, 0.7nM, 1.4nM and 2.8nM) on a specific lactone surface (a) and on a non-specific melamine surface (b).

This was confirmed by the apparent dissociation constants (K_D) for the lactone-specific MIP-NPs on the specific (lactone) surface and for the MIP NPs on the non-specific (melamine) surfaces.

This apparent dissociation constants (K_D) was calculated with BiaEvaluation software v 4.1 using a 1:1 binding model with drifting baseline fitting. This model has a basic interaction between the analyte (A) and the ligand (B). It is equivalent to the Langmuir isotherm used for adsorption to the surface (Figure 4-7).

$$A + B \underset{k_d}{\overset{k_a}{\rightleftharpoons}} AB \qquad A)$$

Figure 4-7 Equation A) for calculation of K_D

Since we considered a simple 1:1 binding, the affinity constant is equal to the ratio of the rate constants (equilibrium association $K_A = k_a/k_d$ and $K_D = k_d/k_a$). Where k_a is the association rate constant and k_d is the dissociation rate constant. Using known concentrations of analyte it was possible to determine the apparent equilibrium concentration (K_D).

In fact, the results show that the best K_D was demonstrated by MIP NPs on the specific lactone surface (20-30 nM), which was lower than the K_D of the NPs on the non-specific surface NPs (2-3 µM). Therefore, it is possible to conclude that the MIP NPs prepared here possess at least 100 times stronger affinity towards the specific surface in comparison with their binding to a non-specific surface.

Glass cover slips were coated with 100 µl of MIP NPs solution. The efficacy of coating was evaluated by measuring the contact angle, by dropping ultrapure water onto the surface of the cover slips. Figure 4-8 shows the contact angle values obtained for cover slips coated with four MIP NPs batches (from A to D) and uncoated cover slips was used as control.

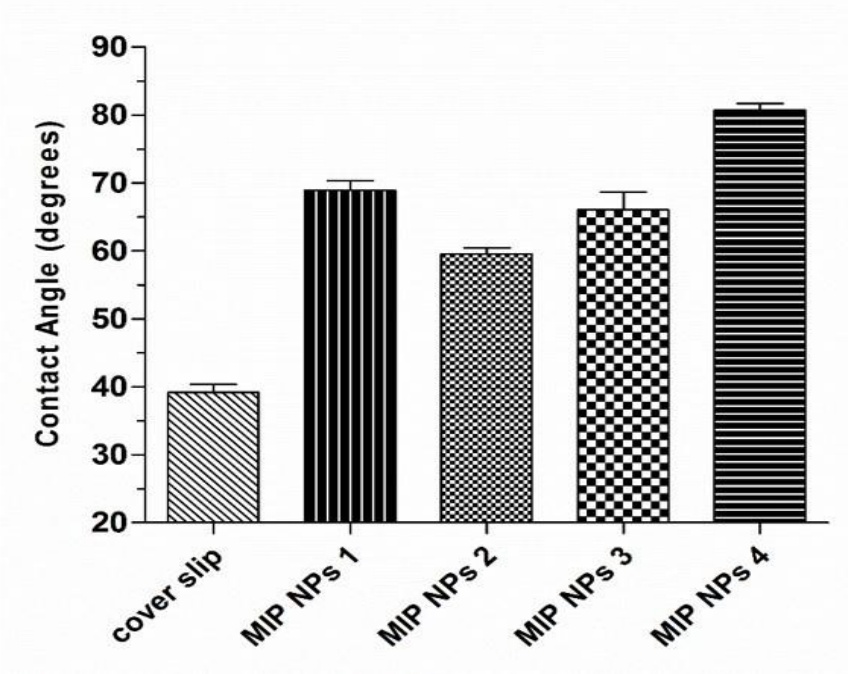

Figure 4-8 Static water contact angle measurements for the four batches of MIP NPs. All the measurements were performed in triplicate; error bars represent ±standard deviation.

All the contact angle values for MIP NPs batches are higher (above 60 degrees) then the control without MIP NPs (around 40 degrees). This means that the surface of the cover slips coated with MIP NPs is more hydrophobic when compared with the cover slip alone. However all the coated MIP NPs surfaces can be still considered hydrophilic as the contact angle is below 90 degrees. In fact, surfaces are usually regarded hydrophobic when contact angle values are higher than 90 degrees. The difference in values between the uncoated and coated slips demonstrates that the immobilisation of the MIP NPs was successfully achieved. Since batch 4 showed the greatest difference with the uncoated cover slip, probably due to a better coverage of the surface, this MIP NP batch was chosen for the subsequent biological assays.

4.3.2 Cytotoxicity Evaluation

The cytotoxicity of MIP NPs was evaluated by incubating Vero cells (fibroblasts - like kidney cells) with coated cover slips with 100 µl (A) and 200 µl (B) of 20 nM MIP NPs solution, for 48 hours. The metabolic activity was evaluated by the nontoxic resazurin assay (Figure 4-9) and the cells morphology was analysed by phase contrast microscopy (Figure 4-10). Resazurin is a nontoxic stain allowing the use of the same cells during the duration of the entire experiment.

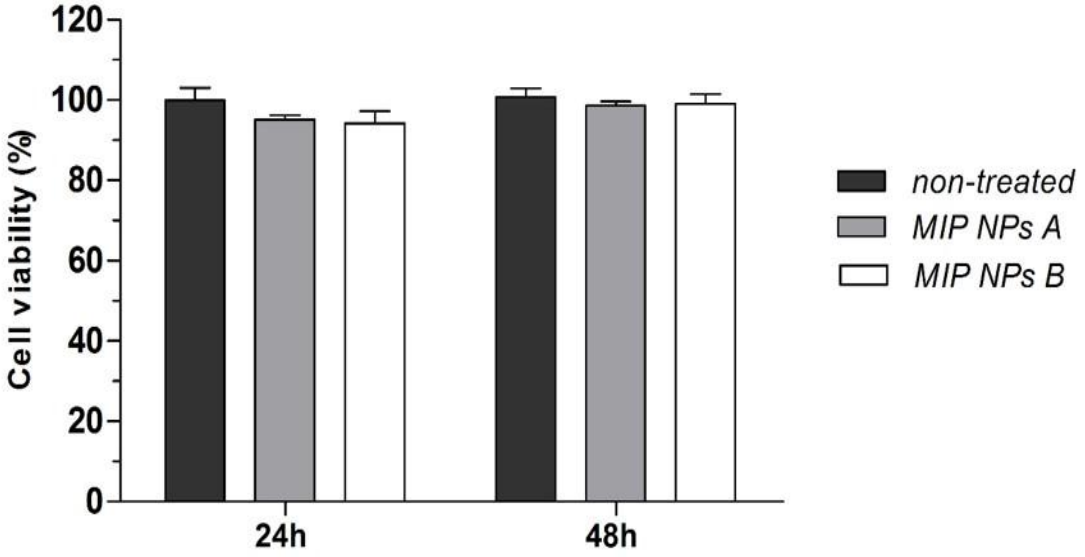

Figure 4-9 Cytotoxicity effect of MIP NPs on Vero cells, determined by resazurin method. MIP NPs A correspond to 100µl and MIP NPs B correspond to 200 µl of solution coated with the cover slips. One-way ANOVA was performed followed by a Bonferroni's multiple test ($p < 0.05$). Data represents three independent experiments performed in triplicate.

In the presence of both concentrations of MIP NPs (A and B, Figure 4-9), Vero cells retained the ability to reduced resazurin to resorufin, as compared to untreated cells ($p<0.05$), whether after 24 hours or 48 hours. These results show that, in the tested conditions, MIP NPs are not toxic for Vero cells, a

fibroblast-like cell line. The morphology of Vero cells did not exhibit alterations when exposed to coated MIP NPs cover slips (Figure 4-10), validating the previous metabolic resazurin assay. Microscopic images, after 24 hours and 48 hours, of Vero cells incubated in the presence of nanoparticles, showed to be very similar to the control (non treated Vero cells). Therefore it can be concluded that in the tested conditions, MIP NPs are not toxic for fibroblasts cells. A previous study tested methyl methacrylate copolymer nanoparticles in Vero cells and other two cell lines by MTT assay. The results obtained demonstrated a higher cell viability for Vero cells when in contact with these nanoparticles (Hoffmann *et al.* 1997).

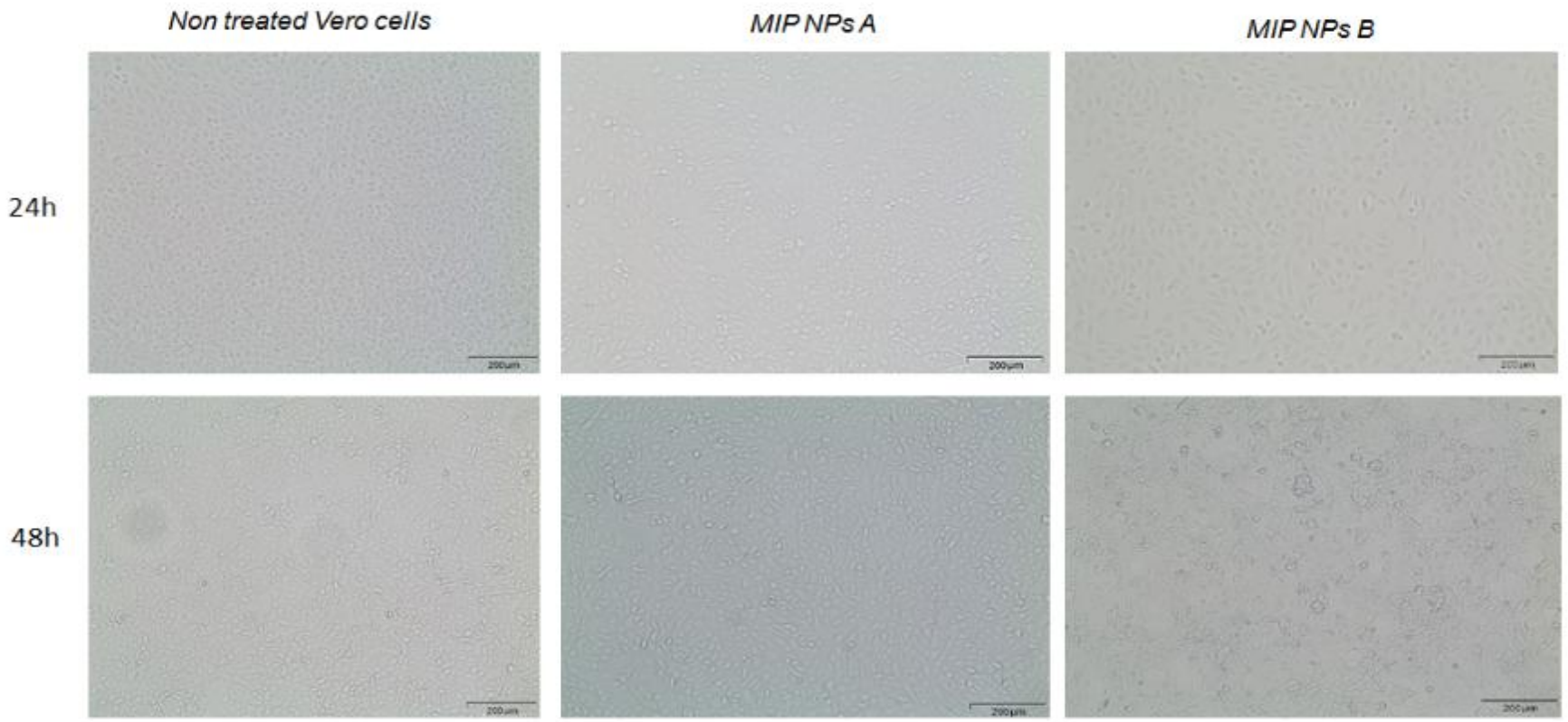

Figure 4-10 Inverted microscopy images of Vero cells monolayers morphology in cover slips, incubated with MIP NPs A (100 µl) and of MIP NPs B (200 µl) for 24 hours and for 48 hours respectively. Magnification 100X, scale bar 200 µm.

4.3.3 MIP NP Reduces Bioluminescence of *V. fischeri*

Bioluminescence of *V. fischeri* is a phenotype regulated by QS. *V. fischeri* was chosen as a model bacterium to assess the effect of the nanoparticles on QS-regulated phenotypes (Dunlap 1999), because of the simplicity of measuring bioluminescence. The MIP NPs were tested with *V. fischeri* to evaluate their efficiency to reduce bioluminescence by sequestrating the AHLs. A volume of 5 ml of MIP NPs (20 nM) was incorporated with *V. fischeri* cultures and the growth (OD_{600nm}) and the luminescence (RLU) were monitored. A culture without addition of MIP NPs was used as control. The bacterial growth curve was performed by measuring the optical density of several points over the growing culture (Figure 4-11). The determination of colony forming units (CFU) was also carried out (Figure 4-12). The data suggests that MIP NPs do not affect the bacterial growth of *V. fischeri*. Even with an extra addition of AHLs (100 µM) to the culture media, the growing rate was similar to the control (Figure 4-11; Figure 4-12).

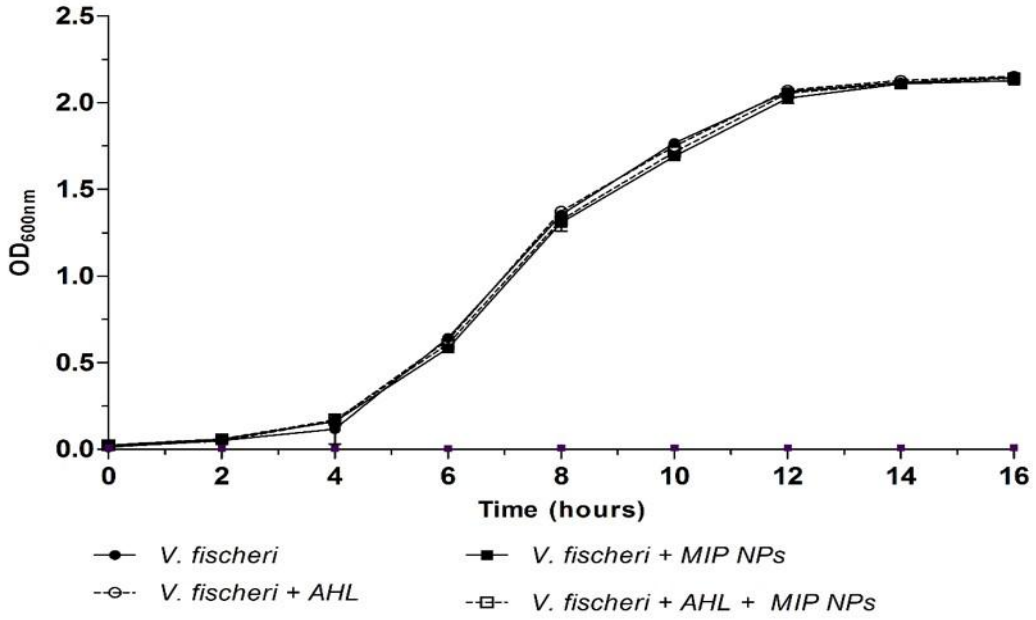

Figure 4-11 Bacterial growth (OD_{600} nm) of *V. fischeri* in the presence of MIP NPs. A supplementation of 100 µM of AHL (3-oxo-C_6-HSL) was added. The data represent means (standard deviations) of three independent experiments performed in triplicate**.**

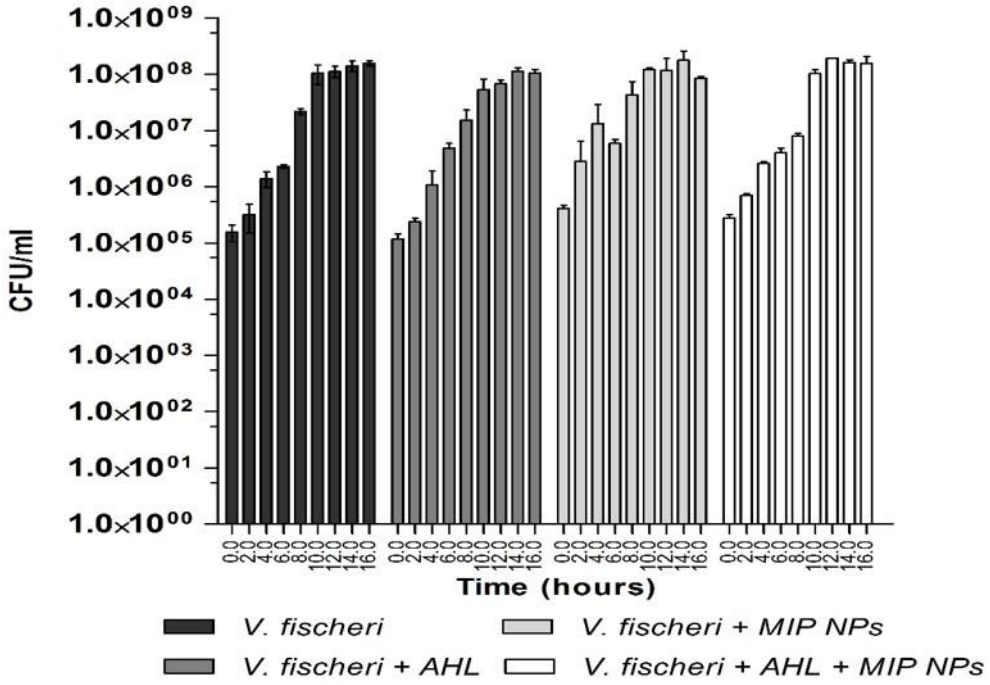

Figure 4-12 Bacterial growth (CFU/ml) of *V. fischeri* in the presence of MIP NPs. Each bacterial strain was supplemented with 100 μM of AHL. The data represent means (standard deviations) of three independent experiments performed in triplicate.

The monitoring of the bioluminescence is reported in Figure 4-13. The figure shows that in presence of MIP NPs (black squares) the bioluminescence of *V. fischeri* is reduced of around one log unit, starting from the lag phase (2 hours) to stationary phase (12 hours), as compared with the control containing *V. fischeri* alone (black circles).

To demonstrate that bioluminescence reduction was due to sequestration of AHLs by the MIP NPs, the culture was supplemented with 3-oxo-C_6-HSL (100 μM final concentration) (open circle, Figure 4-13). With the addition of this exogenous AHLs, a slightly increase in bioluminescence of *V. fischeri* was observed between 2 and 6 hours as compared with the control. In the presence of MIP NPs, after the addition of exogenous AHL the bioluminescence also had a slightly increase between 2 and 8 hours (open squares, Figure 4-13), as

compared with the culture with MIP NPs without additional AHL (black squares, Figure 4-13). The slight increase between 2 and 8 hours can be explained by the nanoparticles adsorption kinetic. It seems that MIP NPs cannot fully adsorb the large amount of lactone present initially in the environment and a full adsorption of both the endogenous and exogenous AHLs is achieved only after 8 hours of incubation. Nevertheless, these results show that the effect of the bioluminescence is indeed due the sequestration of AHLs from MIP NPs, demonstrating therefore their ability to interfere with *V. fischeri* QS.

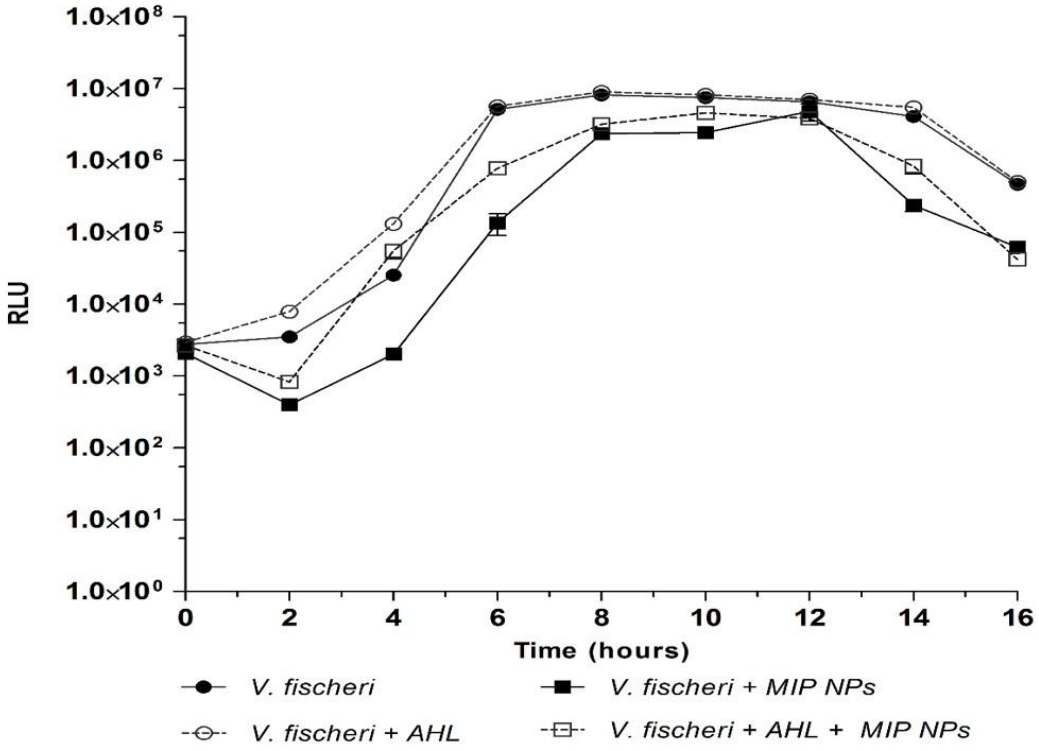

Figure 4-13 Bioluminescence (RLU) signal of *V. fischeri* in presence of MIP NPs . A supplement of 100 µM of AHL (3-oxo-C_6-AHL) was added. The data represent means (standard deviations) of three independent experiments performed in triplicate.

4.3.4 MIP NP Reduces Biofilm of *A. hydrophila*

Biofilm formation of *A. hydrophila* is a phenotype regulated by QS. The effect of MIP NPs on *A. hydrophila* QS was therefore evaluated. For the experiments the MIP NPs were incorporated in *A. hydrophila* cultures as described previously for *V. fischeri*. The bacterial growth curve was performed by measuring the optical density (OD_{600nm}) (Figure 4-14) and by the determination of colony forming units (CFU) of several points over time (Figure 4-15). The two figures show that as for *V. fischeri*, no effect of MIP NPs on *A. hydrophila* growth was detected.

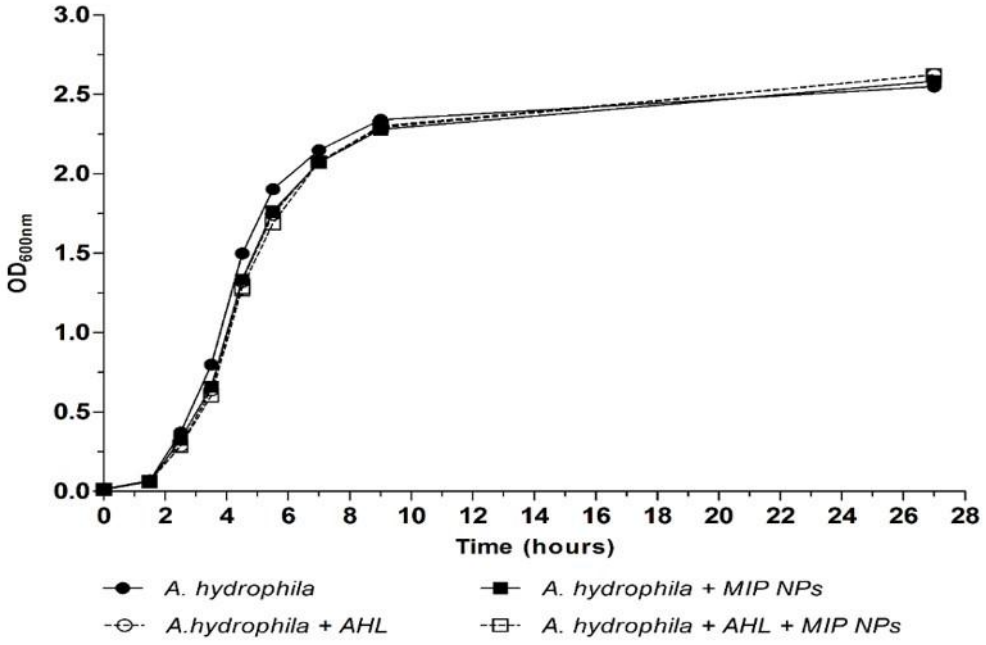

Figure 4-14 Bacterial growth (OD at 600 nm) of *A. hydrophila* in the presence of MIP NPs. A supplementation of 100 µM of AHL (C_4-HSL) was added. The data represent means (standard deviations) of three independent experiments performed in triplicate**.**

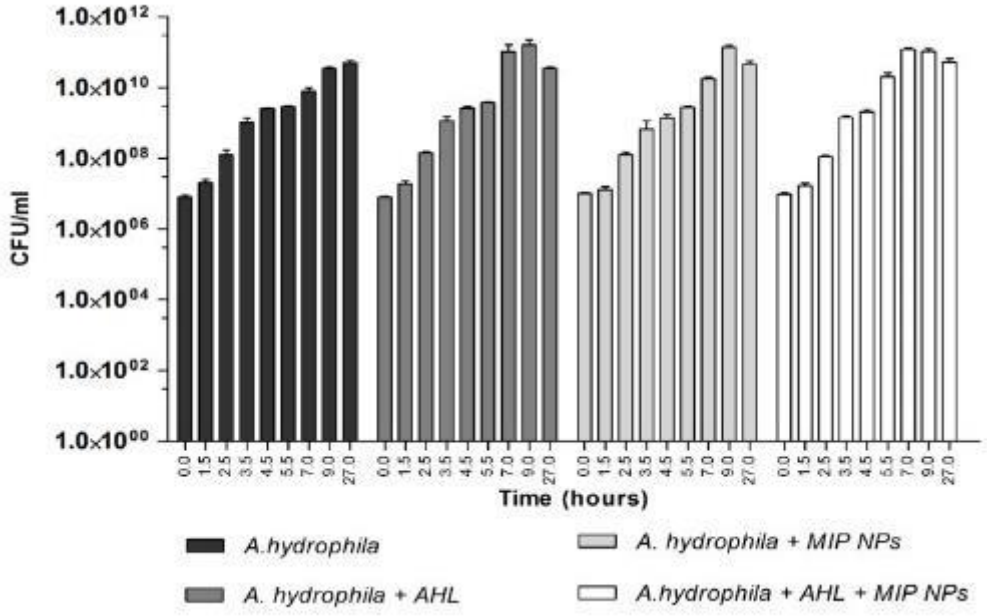

Figure 4-15 Bacterial growth (CFU/ml) of *A. hydrophila* in the presence of MIP NPs. Each bacterial strain was supplemented with 100 µM of AHL. The data represent means (standard deviations) of three independent experiments performed in triplicate

The effect of MIP NPs on biofilm production, which is a phenotype related with QS of *A. hydrophila* (Lynch 2002) was also assessed. For the experiments, a microplate containing cover slips coated (or uncoated) with MIP NPs was used to perform the assay. Uncoated cover slips were used as control, and the results showed that *A. hydrophila* preserve the ability to develop a normal biofilm on such controls (Figure 4-16). On the other hand, the production of biofilm by *A. hydrophila* on MIP NPs coated cover slips was significantly reduced ($p<0.05$) (Figure 4-16).

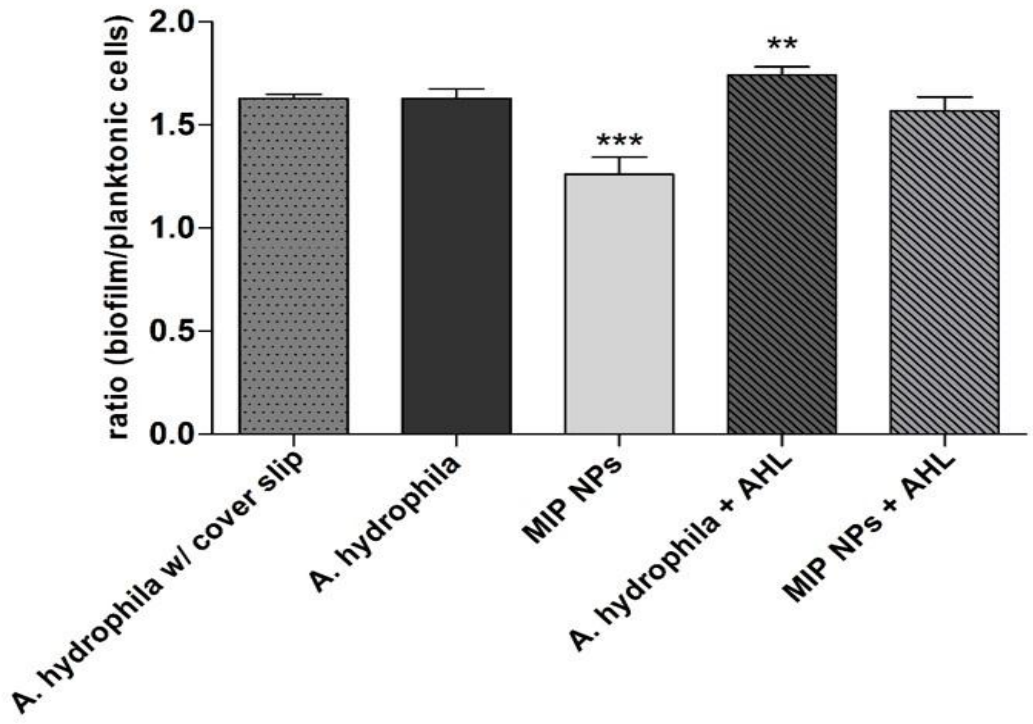

Figure 4-16 MIP NPs effect in biofilm formation of *A. hydrophila* and *A. hydrophila* supplemented with 100 µM of AHL and a control performed with only the cover slip. One-way ANOVA, followed by a Bonferroni's multiple comparison test, was performed to determine statistical significance of MIP NPs against the *A. hydrophila* biofilm (*** $p<0.05$). Vertical bars represent standard deviation**.**

An addition of 100 µM C_4-HSL (AHL of *A. hydrophila*) to *A. hydrophila* cultures with MIP NPs, resulted in a similar production of biofilm ratio similar to the control (Figure 4-16). Most likely, in this case the small amount of nanoparticles, attached to the cover slip, was saturated and unable to fully adsorb the exogenous AHL, producing a reverse effect with production of biofilm. Most probably, MIP NPs attached to a cover slip have lower binding capacity than MIP NPs freely dispersed in solution. In fact, since the immobilisation of the nanoparticles on the cover slip was random, some of their specific binding sites might not be available to adsorb the target analyte. Nevertheless, this is a

further confirmation that the inhibition of biofilm formation is really due to the adsorption of the QS signal molecule by the MIP NPs. The results reported in Figure 4-16 were also corroborated by microscopy analysis (Figure 4-17), which clearly shows that *A. hydrophila* barely forms biofilm in the presence of MIP NPs (Figure 4-17 B).

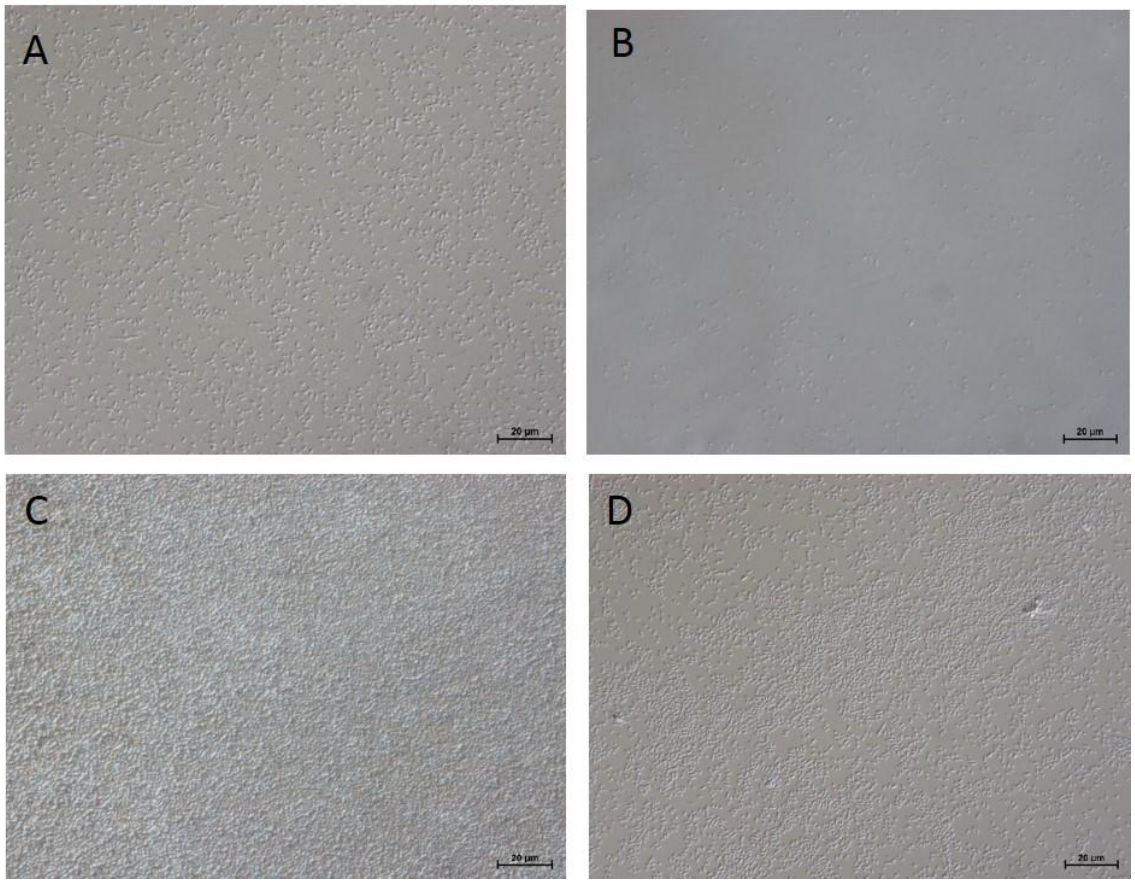

Figure 4-17 Optical microscopy images of biofilm formation on cover slips by *A. hydrophila* (A), *A. hydrophila* with MIP NPs (B), *A. hydrophila* with AHL (C) and *A. hydrophila* with MIP NPs and AHL (D); after 27 hours of biofilm formation at 30 ºC. Magnification 40 x.

4.4 Conclusions

In this study MIP NPs specific for lactones (AHLs) were successfully synthesised using the solid-phase approach that allows easy isolation of high affinity NPs. The MIP NPs were characterised by DLS and TEM to evaluate their homogeneity, dispersion and size. This characterisation indicates that the majority of nanoparticles are around 100 nm. The affinity of the nanoparticles for AHLs was evaluated by SPR using BIAcore chips with the template immobilised on their surface. BIAcore chips with melamine immobilised instead of the lactones were used for an assessment of the specificity. The results demonstrated high affinity (K_D = 20-30 nM) and specificity (K_D for melamine surface was 2-3 µM) of MIP NPs for AHLs.

The MIP NPs were synthesised to sequestrate the QS signal molecules (AHLs), therefore decreasing the density of these molecules around the bacterial cells. These would prevent the expression of genes regulated QS, corresponding with phenotypes such as bioluminescence for *V. fischeri* and biofilms for *A. hydrophila.* The results have shown the capability of MIP NPS to interfere with QS by sequestration of AHLs, since bioluminescence in *V. fischeri* and biofilm production in *A. hydrophila* were significantly reduced.

Importantly, at the levels used, MIP NPs are not cytotoxic, as demonstrated by verotoxicity assays. The biocompatible nature of these MIP NPs and their specificity make them interesting candidates for several applications where the control of bacterial growth and biofilm production are critical.

Chapter 5

General Discussion

5 General Discussion

The control of bacterial virulence *via* QS has been strongly encouraged and several natural or synthetic compounds have been selected as a strategy to fight bacterial infections (Bhardwaj *et al.* 2013, Defoirdt *et al.* 2013, Rampioni *et al.* 2014). However, in order to have more pronounced effects in real environments, the applications of these compounds still need improvement (Glinel *et al.* 2012, Romero *et al.* 2012). It has been already shown in literature that synthetic antimicrobials can be applied as coatings to protect surfaces from the colonisation of bacteria (Glinel *et al.* 2012, Flores *et al.* 2013). In this study, novel synthetic polymers (i.e. linear polymers or copolymers and molecularly imprinted polymers nanoparticles, MIP NPs) were developed to reduce QS-phenotypes, this aim was achieved through bioluminescence and biofilm formation assays. Linear polymers, which were copolymers based on methyl methacrylate (MMA), and MIP NPs can contribute to the control of bacterial infections. In a previous work, Piletska and colleagues (2010) have reported the synthesis of rational designed polymers (cross-linked polymer) with capability to reduce QS-phenotypes, namely bioluminescence of *V. fischeri.* The monomers IA and MAA were chosen among others, from a molecular screening, because they showed the highest interactions with 3-oxo-C_6-HSL (*V. fischeri* AHLs), C_4-HSL and C_6-HSL (*A. hydrophila* AHLs).

The inhibition of QS by natural compounds or synthetic compounds reported in literature, the toxicity of the compounds is usually assessed. In this work, we also have evaluated the toxicity of the materials developed. Using the metabolic activity by resazurin (alamar blue), which is a sensitivity method; we have demonstrated that there is no cytotoxicity associated to the materials. In addition, in our study the target molecules are well defined, contrasting to other approaches where natural compounds are exploited as QS inhibitors but the mechanism used to affect QS is unknown and the target molecules are not identified (Defoirdt *et al.* 2013).

5.1 Linear Polymers and Quorum Sensing

The linear polymers were developed based on the interactions of the two functional monomers, itaconic acid (IA) and methacrylic acid (MAA), with AHLs of *V. fischeri* (3-oxo-C_6-HLS) and *A. hydrophila* (C_4-HSL). These two functional monomers were identified by molecular modelling as producing strong non covalent interactions with the bacterial signal molecule. These monomers have been previously used to synthesise polymers for drug delivery (Coelho *et al.* 2010), and have been incorporated into hydrogels for the prevention of bacterial adhesion on intraocular lens (McCoy *et al.* 2012). In fact, methacrylate/acrylate polymers have been already shown to be a determinant factor for avoiding bacterial adhesion (Hook *et al.* 2012). The binding between AHLs and these types of monomers has been shown to be mainly due to electrostatic interactions.

Cross-linked polymers were synthesised in a bulk format using a cross-linker (EGDMA) in the polymerisation process. The cross-linked polymer with 5% of IA showed to be efficient in the reduction of bioluminescence and biofilm formation of *V. fischeri* (Piletska *et al.* 2010). In the present work the same monomers were used to synthesise (in absence of the cross-linker) linear polymers (*$pMAA_{25}$-co-$pMMA_{75}$* and *pIA_{25}-co-$pMMA_{75}$)* and they also demonstrated an ability to reduce *V. fischeri* QS-phenotype. In the presence of *pIA_{25}-co-$pMMA_{75}$* *V. fischeri* bioluminescence was effectively reduced. The presence of both linear polymers did not affect the growth curve of bacteria, evidencing the lack of toxicity for the microorganisms. Our results are corroborated by Hook and colleagues (2012) who tested several combinations of polymers to prevent bacterial adhesion on surfaces. Their results also showed that bacterial growth was not affected by the methacrylate/acrylate polymers (Hook *et al.* 2012).

Despite the fact that *pIA_{25}-co-$pMMA_{75}$* led to a slight decrease in cell viability in the first 24 hours, Vero cells could completely recovered as confirmed after 48 hours in culture. The initial effect could be due to the acidity of the polymer, which initially was capable to affect the pH of the environment and delays

bacterial growth. However as the number of microorganism increased and the system ‘matured’, the neutral pH was re-established and cell viability was restored. The biocompatibility of synthetic polymers, when are used for coating surfaces, is an important point, because the material can inhibit bacterial films formation without damaging the cells. In the literature, examples of synthetic polymers based on methacrylic acid, where no cytotoxicity was observed for eukaryotic cells, can be found (Hoffmann *et al.* 1997, El Khadali *et al.* 2002, Cooperstein and Canavan 2013).

Recently, Jahid and collaborators reported that biofilm formation and exoprotease production, both QS-phenotypes of *A. hydrophila,* were influenced by 0.05% of glucose (Jahid *et al.* 2013). In another study, it has been demonstrated that the presence of vanillin in membranes was able to reduce biofilm formation of *A. hydrophila* (Ponnusamy *et al.* 2013). Other compounds such as clove oil (Husain *et al.* 2013) and chestnut honey (Truchado *et al.* 2009) have also shown influence on biofilm formation. Most recently a polymeric material, polyethylene (used in the water industry and in medicine) modified with activated organosilanes was tested to verify the impact on biofilm formation and bacterial cell attachment of *A. hydrophila*. The results showed that surfaces modified with the material demonstrated better antibacterial and anti-adhesive properties for *A. hydrophila* when compared with the control (Kregiel and Niedzielska 2014).

Compounds such as cinnamaldehyde were used in some species of *Vibrio* to interfere with the AI-2 signal molecule. The results showed an influence on bioluminescence, inhibition of biofilm formation and reduction of protease production, without inhibiting the bacterial growth (Brackman *et al.* 2008). Another type of antimicrobial chemotherapy used against *V. fischeri* is the photodynamic therapy through a photosensitize (Alves *et al.* 2011).

Despite the encouraging results, in most of the studies reported above, contrary to our approach, the mechanism of the antibacterial compounds was not fully clear and the QS targets were not identified (Defoirdt *et al.* 2013).

5.2 MIP NPs and Quorum Sensing

The template used for the synthesis of MIP NPs (S)-(−)-α-Amino-γ-butyrolactone hydrobromide) was a lactone derivative, allowing to imprint the lactone structure on the MIP nanoparticles. The MIP NPs developed in this study revealed to have a strong ability to sequestrate AHLs from *V. fischeri* and *A. hydrophila*. The MIP NPs were tested both in suspension and coated on glass cover slips, and in both cases they did not show any effect on bacterial growth for *V. fischeri* and *A. hydrophila.* The effect of MIP NPs on QS-phenotypes was also tested in suspension and coated on glass cover slips. This latter coating approach has been already utilised by Chianella and colleagues, and it has shown to be a simple and straightforward technique suitable for several testing formats, including the enzyme-linked immunosorbent assay (ELISA) (Chianella *et al.* 2013).

The QS-phenotypes bioluminescence of *V. fischeri* and biofilm formation of *A. hydrophila* were both affected by MIP NPs, even though very diluted solutions and therefore tiny amounts of the material were used (0.1 nmol for suspension experiments, 2-4 pmol for coatings). By increasing the concentration of these polymeric materials in the environment even better results can be achieved.

In literature, studies where nanoparticles have showed ability to disrupt QS have been reported. A different type of nanoparticles, specifically silver nanoparticles was used to test the bacterial effect on *P. aeruginosa* and *Staphylococcus aureus*. The adhesion of both bacteria decreased in the presence of silver nanoparticles. However osteoblast cells showed low viability at higher concentration of these nanoparticles (Flores *et al.* 2013). In *A. hydrophila* silver nanoparticles showed to have antimicrobial activity when used at the highest concentration tested (Mahanty *et al.* 2013). Titanium dioxide nanoparticles have also demonstrated an antimicrobial activity against *A. hydrophila* (Jayaseelan *et al.* 2013).

Here cytotoxicity of MIP NPs in a fibroblast-like cell line was evaluated and the result showed that MIP NPs were not cytotoxic. The fact that cell viability of mammalian cells are not affected by the MIP NPs opens the way to the application and incorporation of this type of material to several fields from medicine to agriculture and the environment

5.3 Linear Polymers and MIP NPs: which one?

In this work, although the linear polymers produced here showed promising results in reducing QS-phenotypes of *V. fischeri* and *A. hydrophila*, we started looking for more specific, versatile and easy to synthesise material, which could be implemented in diverse ways. Linear polymers can be dissolved in organic solvents and could be integrated into paints. Nevertheless their binding action could be limited by the lack of specificity. Therefore we wanted to take polymers' capacity for QS inhibition to another level, where affinity and specificity are prominent. Molecular imprinting is a versatile and reliable technique, where specificity and affinity are the two major features (Piletsky, Subrahmanyam, *et al.* 2001). However when molecularly imprinted polymers (MIPS) are synthesised in a bulk format, they cannot be easily integrated with real systems. When MIPs are prepared as films, reproducibility and mass production could become an issue. The molecularly imprinted nanoparticles (MIP NPs) are the polymer format that solves the problem. In fact polymers with high affinity and specificity highly dispersed in water and organic solvents and therefore easily integrated are obtained. MIP NPs are specific and have high affinity for the chosen target (Guerreiro *et al.* 2009). In addition the synthesis of MIP NPs using a solid support with the template immobilised, possesses enormous advantages, as the synthesis of the material can be automated and therefore easily mass produced in a cost effective way (Poma *et al.* 2010).

Table 5-1 Comparison in performance of linear polymers and MIP NP

Polymers	Polymer Concentration in solution	Maximum reduction (%)* of *V. fischeri* Bioluminescence	Polymer Concentration on slide	Maximum reduction (*) of *A. hydrophila* Biofilm
pIA$_{25}$-co-pMMA$_{75}$	10 mg/ml (3.4×10^{-4} M)$^{\#}$	90% (4-12 hours after incubation)	100 µg (3.4×10^{-9} mol)$^{\#}$	37%
pMAA$_{25}$-co-pMMA$_{75}$	10 mg/ml (2.4×10^{-4} M)$^{\#}$	90%-40% (4-12 hours after incubation)	100 µg (2.4×10^{-9} mol)$^{\#}$	30%
MIP NPs	2×10^{-8} M	90%-75% (2-6 hours)	2×10^{-12} mol	20%

(*) The calculation of the percentage of reduction was performed by considering 100% the signal of the control.
(#) Molar concentration of the linear polymers was calculated using the average molecular mass (Mn) assessed by GPC.

Regarding the performances, Table 5.1 summarised the results obtained with the different polymers tested in this study. The table shows that the effects of the linear polymers and the MIP NP on QS are similar. However the amount of linear polymers used in the experiments was higher than the amount of nanoparticles, implying that MIP NP are more effective, which means that less material would be required for real applications. This makes nanoparticles more attractive both from an environmental and financial point of view.

Chapter 6

Conclusions and Future Perspectives

6 Conclusions and Future Perspectives

In this work we were able to develop two types of polymeric materials with the ability of sequestering AHLs, and consequently reduce QS-phenotypes. The linear polymers and the MIP NPs have been shown to be effective in the inhibition of QS-phenotypes of *V. fischeri* and *A. hydrophila*.

The *pMAA$_{25}$-co-pMMA$_{75}$* and *pIA$_{25}$-co-pMMA$_{75}$* copolymers were synthesised by free radical polymerisation and characterised by NMR, GPC evaluating the size and the composition. Their binding capacity for AHLs was also evaluated. The MIP NPs specific for lactone (AHLs) were synthesised using the immobilised template approach, using glass beads. The nanoparticles were then characterised by TEM and DLS.

The capacity to interfere with QS-phenotypes was performed with both polymeric materials using *V. fischeri* and *A. hydrophila*. In addition to suspension experiments, linear polymers were coated in a multiwell plate and MIP NPs were coated in glass cover slips. The cytotoxicity in a fibroblast-like cell line was also evaluated for both polymeric materials.

The results showed that even though *pMAA$_{25}$-co-pMMA$_{75}$* had the higher binding capacity for AHLs, *pIA$_{25}$-co-pMMA$_{75}$* showed a greater effect on *V. fischeri* bioluminescence. In addition, whereas both linear polymers affected the biofilm formation of *A. hydrophila*, they did not significantly affect the cell viability.

When the specificity of the MIP NPs was studied by BIAcore, the nanoparticles showed higher affinity for AHLs rather than other molecules (i.e. melamine). In cytotoxicity studies, Vero cells were not affected by MIP NPs demonstrating their lack of toxicity in the condition tested. In QS experiments, MIP NPs were capable of reducing bioluminescence of *V. fischeri* at the early stages of bacterial growth. In addition they were able to significantly reduce biofilm of *A. hydrophila*.

The characterisation and evaluation of both polymeric materials (linear polymers and MIP NPs) has indicated that they are promising materials as QS inhibitors. These polymers could be integrated within biological systems and be used as a strategy to prevent bacterial diseases.

Both materials (linear polymers and MIP NPs) did not interfere with bacterial growth of *V. fischeri* and *A. hydrophila*, showing that they should not promote the development of bacterial resistance.

The linear polymers can be used for several applications, like paints or membranes. These polymers are soluble in organic solvents, so they can be easily integrated and their use could be vast. For example, the coating of surfaces might be an excellent strategy to prevent adhesion and biofilm formation of pathogens as *A. hydrophila.*

MIP NPs can be used in solution or in coating surfaces. The major advantages of MIP NPs, synthesised by the solid approach, are the automated synthesis for their production and the possibility to re-use the solid phase with the template immobilised for multiple syntheses. This makes the mass production of MIP NPs cheap and easily achievable. The MIP NPs can be also modified simply with other functional groups to attach them to other compounds or to films.

The use of these polymeric materials could represent a new solution to mitigate diseases' outbreaks.

As future work, tests *in vivo* should be performed to verify the efficiency and the toxicity of both materials in real environments. In addition, an *in vivo* test should give indication whether the removal of AHLs from the environment does not change behaviour of other bacterial species. Moreover, further optimisation of the concentration and the amount of polymers used *in vivo* experiments might be necessary to obtain optimal results.

Furthermore, a solution addressing the saturation of the polymeric material should be found. In fact, eventually both the linear polymers and the MIP NPs

will be saturated by the AHLs produced by the bacteria. At this point, if they are not removed from the environment, they will start releasing signal molecules promoting instead of inhibiting QS-phenotypes.

Replacement of the surface that contains the polymers (catheters in medicine, painted tank in aquaculture) is only the simplest, but not the most cost effective solution.

In fact, it is well known that MIPs can mimic enzymes and catalyse chemical reactions. Therefore MIP NPs able to hydrolyse the AHLs to harmless products could be developed and combined with the ‘adsorption’ MIPs to obtain a polymeric system that never gets saturated and needs replacement only (and if) the catalytic MIPs stop working.

Chapter 7

References

7 References

Alexander, C., Andersson, H.S., Andersson, L.I., Ansell, R.J., Kirsch, N., Nicholls, I. A, O'Mahony, J., and Whitcombe, M.J., 2006. Molecular imprinting science and technology: a survey of the literature for the years up to and including 2003. *Journal of molecular recognition: JMR*, 19 (2), 106–180.

Allen, M.P. and Tildesley, D.J., 1987. *Computer simulation of liquid.* Oxford University Press.

Alves, E., Neves, M.G.P.M.S., Tome, A.C., Faustino, M.A.F., Cavaleiro, A.S., Cunha, A., Gomes, N.C.M., and Almeida, A., 2011. Photodynamic antimicrobial chemotherapy in aquaculture : photoinactivation studies of *Vibrio fischeri*. *PloS One*, 6 (6).

Ammerman, N.C., Beier-Sexton, M., and Azad, A.F., 2008. Growth and maintenance of Vero cell lines. *Current protocol microbiolology*, 1–10.

Andersson, L.I., Nicholls, I.A., and Mosbach, K., 1996. Molecular imprinting: the current status and future development of polymer-based recognition systems. *In*: B. (Eds. . E. Edward Bittar, B.D. Lelf, ed. *Advances in molecules and cell biology*, 651–670.

Annous, B.A.A., Ratamico, P.I.N.A.M.F., and Mith, J.L.S., 2009. Quorum sensing in biofilms: why bacteria behave the way they do overview of biofilms. *Journal of food science*, 74 (1).

Antunes, L.C.M. and Ferreira, R.B.R., 2009. Intercellular communication in bacteria. *Critical reviews in microbiology*, 35 (2), 69–80.

Antunes, L.C.M., Ferreira, R.B.R., Buckner, M.M.C., and Finlay, B.B., 2010. Quorum sensing in bacterial virulence. *Microbiology*, 156, 2271–2282.

Aragrag, N., Castiglione, D.C., Davies, P.R., Davis, F.J.D., and Patel, S.I., 2004. General procedures in chain-growth polymerisation. *In*: *Polymer chemistry: a pratical approach*. Oxford University Press, UK.

Asad, S. and Opal, S.M., 2008. Bench-to-bedside review: quorum sensing and the role of cell- to-cell communication during invasive bacterial infection. *Critical care*, 12 (236).

Atkinson, S. and Williams, P., 2009. Quorum sensing and social networking in the microbial world. *Journal of the royal society interface*, (6), 959–978.

Azevedo, J.S.N., Araújo, S., Oliveria, C.S., Correia, A., and Henriques, I., 2013. Analysis of antibiotic resistance in bacteria isolated from the surface microlayer and underlying water of an estuarine environment. *Microbial drug resistance*, 19, 64–71.

Bassler, B.L., 1999. How bacteria talk to each other: regulation of gene expression by quorum sensing. *Current opinion in microbiology*, 2(6), 582–587.

Bassler, B.L. and Losick, R., 2006. Bacterially speaking. *Cell*, 125 (2), 237–246.

Beceiro, A., Tomás, M., and Bou, G., 2013. Antimicrobial resistance and virulence: a successful or deleterious association in the bacterial world? *Clinical microbiology reviews*, 26 (2), 185–230.

Bhardwaj, A.K., Vinothkumar, K., and Rajpara, N., 2013. Bacterial quorum sensing inhibitors: attractive alternatives for control of infectious pathogens showing multiple drug resistance. *Recent patents on anti-infective drug discovery*, 8 (1), 68–83.

Bomo, A.M., Storey, M. V, and Ashbolt, N.J., 2004. Detection, integration and persistence of aeromonads in water distribution pipe biofilms. *Journal of water and health*, 2 (2), 83–96.

Boyen, F., Eeckhaut, V., Van Immerseel, F., Pasmans, F., Ducatelle, R., and Haesebrouck, F., 2009. Quorum sensing in veterinary pathogens: mechanisms, clinical importance and future perspectives. *Veterinary microbiology*, 135 (3-4), 187–195.

Boylan, M., Miyamoto, C., Wall, L., Graham, A., and Meighen, E., 1989. LuxC, D and E genes of the Vibrio fischeri luminescence operon code for the reductase, transferase and synthetase enzymes involved in aldehyde biosynthesis. *Photochemistry and photobiology*, 49, 681–688.

Brackman, G., Defoirdt, T., Miyamoto, C., Bossier, P., Van Calenbergh, S., Nelis, H., and Coenye, T., 2008. Cinnamaldehyde and cinnamaldehyde derivatives reduce virulence in Vibrio spp. by decreasing the DNA-binding activity of the quorum sensing response regulator LuxR. *BMC microbiology*, 8, 149.

Branda, S.S., Vik, S., Friedman, L., and Kolter, R., 2005. Biofilms: the matrix revisited. *Trends in microbiology*, 13 (1), 20–26.

Cámara, M., Williams, P., and Hardman, A., 2002. Controlling infection by tuning in and turning down the volume of bacterial small-talk. *The Lancet*, 2, 667–676.

Camilli, A. and Bassler, B.L., 2006. Bacterial small-molecule signaling pathways. *Science*, 311 (5764), 1113–1116.

Chen, R., Zhou, Z., Cao, Y., Bai, Y., and Yao, B., 2010. High yield expression of an AHL-lactonase from Bacillus sp. B546 in Pichia pastoris and its application to reduce *Aeromonas hydrophila* mortality in aquaculture. *Microbial cell factories*, 9 (39).

Chianella, I., Guerreiro, A., Moczko, E., Caygill, J.S., Piletska, E. V, De Vargas Sansalvador, I.M.P., Whitcombe, M.J., and Piletsky, S.A., 2013. Direct replacement of antibodies with molecularly imprinted polymer nanoparticles in ELISA-development of a novel assay for vancomycin. *Analytical chemistry*, 85 (17), 8462–8468.

Chianella, I., Lotierzo, M., Piletsky, S.A, Tothill, I.E., Chen, B., Karim, K., and Turner, A.P.F., 2002. Rational design of a polymer specific for microcystin-LR using a computational approach. *Analytical chemistry*, 74 (6), 1288–1293.

Chianella, I., Piletsky, S.A, Tothill, I.E., Chen, B., and Turner, A.P.F., 2003. MIP-based solid phase extraction cartridges combined with MIP-based sensors for the detection of microcystin-LR. *Biosensors & bioelectronics*, 18 (2-3), 119–127.

Chopra, A.K., 2008. *Characterisation of waterborne Aeromonas species for their virulence potential.*

Clark, M., Cramer, R.D., and Van Opdenbosch, N., 1989. Validation of the general purpose tripos 5.2 force field. *Journal of computational chemistry*, 10 (8), 982–1012.

Coelho, J.F., Ferreira, P.C., Alves, P., Cordeiro, R., Fonseca, A.C., Góis, J.R., and Gil, M.H., 2010. Drug delivery systems: advanced technologies potentially applicable in personalized treatments. *The EPMA journal*, 1 (1), 164–209.

Cole, D.W., Cole, R., Gaydos, S.J., Gray, J., Hyland, G., Jacques, M.L., Powell-Dunford, N., Sawhney, C., and Au, W.W., 2009. Aquaculture: environmental, toxicological, and health issues. *International journal of hygiene and environmental health*, 212 (4), 369–377.

Cooperstein, M.A. and Canavan, H.E., 2013. Assessment of cytotoxicity of (N-isopropyl acrylamide) and poly(N-isopropyl acrylamide)-coated surfaces. *Biointerphases*, 8 (19).

Costerton, J., 1995. Overview of microbial biofilms. *Journal of industrial microbiology*, 15, 137–140.

Costerton, J.W., Stewart, P.S., and Greenberg, E.P., 1999. Bacterial biofilms: a common cause of persistent infections. *Science*, 284, 1318–1322.

Cruz, A., Areias, D., Duarte, A., Correia, A., Suzuki, S., and Mendo, S., 2013. *Aeromonas molluscorum* Av27 is a potential tributyltin (TBT) bioremediator: phenotypic and genotypic characterization indicates its safe application. *Antonie van Leeuwenhoek*, 104 (3), 385–396.

Daniels, R., Vanderleyden, J., and Michiels, J., 2004. Quorum sensing and swarming migration in bacteria. *FEMS microbiology reviews*, 28 (3), 261–289.

Davey, M.E. and O'Toole, G.A, 2000. Microbial biofilms: from ecology to molecular genetics. *Microbiology and molecular biology reviews: MMBR*, 64 (4), 847–867.

Davies, D.G., Parsek, M.R., Pearson, J.P., Iglewki, B.H., Costerton, J.W., and Greenberg, E.P., 1998. The involvement of cell-to-cell signals in the development of bacterial biofilm. *Science*, 10 (280), 295–298.

Davis, F.J., 2004. *Polymer chemistry: a practical approach.* University Press, UK.

Decho, A.W., Norman, R.S., and Visscher, P.T., 2010. Quorum sensing in natural environments: emerging views from microbial mats. *Trends in microbiology*, 18 (2), 73–80.

Defoirdt, T., Boon, N., and Bossier, P., 2010. Can bacteria evolve resistance to quorum sensing disruption? *PLoS pathogens*, 6 (7).

Defoirdt, T., Boon, N., Bossier, P., and Verstraete, W., 2004. Disruption of bacterial quorum sensing: an unexplored strategy to fight infections in aquaculture. *Aquaculture*, 240 (1-4), 69–88.

Defoirdt, T., Brackman, G., and Coenye, T., 2013. Quorum sensing inhibitors: how strong is the evidence? *Trends in microbiology*, 21 (12), 619–624.

Defoirdt, T., Verstraete, W., and Bossier, P., 2008. Luminescence, virulence and quorum sensing signal production by pathogenic *Vibrio campbellii* and *Vibrio harveyi* isolates. *Journal of applied microbiology*, 104 (5), 1480–1487.

Dickschat, J.S., 2010. Quorum sensing and bacterial biofilms. *Natural product reports*, 27 (3), 343–369.

Diggle, S.P., Crusz, S.A., and Cámara, M., 2007. Quorum sensing. *Current Biology*, (17), R907–R910.

Djordjevic, D., Wiedmann, M., and Mclandsborough, L.A., 2002. Microtiter plate assay for assessment of *Listeria monocytogenes* biofilm formation. *Applied and Environmenta Microbiology*, 68 (6), 2950–2958.

Dobretsov, S., Teplitski, M., and Paul, V., 2009. Mini-review: quorum sensing in the marine environment and its relationship to biofouling. *Biofouling*, 25 (5), 413–427.

Dong, Y.H., Wang, L.H., Xu, J.L., Zhang, H.B., Zhang, X.F., and Zhang, L.H., 2001. Quenching quorum-sensing-dependent bacterial infection by an N-acyl homoserine lactonase. *Nature*, 411 (6839), 813–827.

Van den Driessche, F., Rigole, P., Brackman, G., and Coenye, T., 2014. Optimization of resazurin-based viability staining for quantification of microbial biofilms. *Journal of microbiological methods*, 98, 31–34.

Dunlap, P. V, 1999. Quorum regulation of luminescence in *Vibrio fischeri*. *Journal of molecular microbiology and biotechnology*, 1 (1), 5–12.

Elhariry, H., Gherbawy, Y., El-Deeb, B., and Altalhi, A., 2012. Molecular identification and biofilm-forming ability of culturable aquatic bacteria in microbial biofilms formed in drinking water distribution networks. *Geomicrobiology journal*, 29 (6), 561–569.

Engebrecht, J., Nealson, K., and Silverman, M., 1983. Bacterial bioluminescence: Isolation and genetic analysis of functions from *Vibrio fischeri*. *Cell*, 32 (3), 773–781.

EPA, 2006. *Aeromonas: human health criteria document.*

Finch, R.G., Pritchard, D.I., Bycroft, B.W., Williams, P., and Stewart, G.S.A.B., 1998. Quorum sensing: a novel target for anti-infective therapy. *Journal of antimicrobial chemotherapy*, 42, 569–571.

Flores, C.Y., Miñán, A.G., Grillo, C.A, Salvarezza, R.C., Vericat, C., and Schilardi, P.L., 2013. Citrate-capped silver nanoparticles showing good bactericidal effect against both planktonic and sessile bacteria and a low cytotoxicity to osteoblastic cells. *ACS applied materials & interfaces*, 5 (8), 3149–3159.

Francolini, I., Donelli, G., and Stoodley, P., 2004. Polymer designs to control biofilm growth on medical devices. *Reviews in environmental science and biotechnology*, 2, 307–319.

Francolini, I., Norris, P., Piozzi, A., Donelli, G., and Stoodley, P., 2004. Usnic acid, a natural antimicrobial agent able to inhibit bacterial biofilm formation

on polymer surfaces. *Antimicrobial Agents and Chemotherapy*, 48 (11), 4360–4365.

Fuqua, C., Parsek, M.R., and Greenberg, E.P., 2001. Regulation of gene expression by cell-to-cell communication: acyl-homoserine lactone quorum sensing. *Annual review of genetics*, 35, 439–468.

Fuqua, C., Winans, S.C., and Greenberg, E.P., 1996. Census and consensus in bacterial ecosystems: the LuxR-LuxI family of quorum-sensing transcriptional regulators. *Annual review of microbiology*, 50, 727–751.

Fuqua, W.C., Winans, S.C., and Greenberg, E.P., 1994. Quorum sensing in bacteria: LuxR-LuxI family of cell denisty-responsive transcriptional regulators. *Journal of bacteriology*, 176 (2), 269–275.

Galindo, C.L., Sha, J., Fadl, A.A., Pillai, L.L., and Chopra, A.K., 2006. Host immune responses to Aeromonas virulence factors. *Current immunology reviews*, 2, 13–26.

Gao, D.M., Zhang, Z.P., Wu, M.H., Xie, C.G., Guan, G.J., and P, W.D., 2007. A surface functional monomer-directing strategy for highly dense imprinting of TNT at surface of silica nanoparticles. *Journal of the american chemistry society*, 129, 7859–7866.

Garde, C., Bjarnsholt, T., Givskov, M., Jakobsen, T.H., Hentzer, M., Claussen, A., Sneppen, K., Ferkinghoff-Borg, J., and Sams, T., 2010. Quorum sensing regulation in Aeromonas hydrophila. *Journal of molecular biology*, 396 (4), 849–857.

Gera, C. and Srivastava, S., 2006. Quorum-sensing : The phenomenon of microbial communication. *Current Science*, 90 (5), 666–677.

Girod, M., Antoine, R., Lemoine, J., Dugourd, P., and Charles, L., 2013. Structural characterization of a poly(methacrylic acid)/poly(methylmethacrylate) copolymer by activated electron photo-detachment dissociation. *International journal of mass spectrometry*, 333, 27–33.

Glinel, K., Thebault, P., Humblot, V., Pradier, C.M., and Jouenne, T., 2012. Antibacterial surfaces developed from bio-inspired approaches. *Acta biomaterialia*, 8 (5), 1670–1684.

Gottenbos, B., Grijpma, D.W., van der Mei, H.C., Feijen, J., and Busscher, H.J., 2001. Antimicrobial effects of positively charged surfaces on adhering Gram-positive and Gram-negative bacteria. *The journal of antimicrobial chemotherapy*, 48 (1), 7–13.

Gowda, L.K. and Marie, M.A.M., 2014. Role of quorum-sensing molecules in infections caused by Gram-negative bacteria and host cell response. *Reviews in medical microbiology*, (January), 1.

Gray, K.M., Passador, L., Iglewski, B.H., and Greenberg, E.P., 1994. Interchangeability and specificity of components from the quorumsensing regulatory systems of Vibrio fischeri and *Pseudomonas aeruginosa*. *Journal of bacteriology*, 176, 3076–3080.

Greenberg, E.P., 2000. Acyl-homoserine lactone quorum sensing in bacteria, 38 (3), 117–121.

Gudding, R., Lillehaug, A., and Evensen, O., 1999. Recent developments in fish vaccinology. *Veterinary immunology and immunopathology*, 72 (1-2), 203–212.

Guerreiro, A., Soares, A., Piletska, E., Mattiasson, B., and Piletsky, S., 2008. Preliminary evaluation of new polymer matrix for solid-phase extraction of nonylphenol from water samples. *Analytica chimica acta*, 612 (1), 99–104.

Guerreiro, A.R., Chianella, I., Piletska, E., Whitcombe, M.J., and Piletsky, S.A, 2009. Selection of imprinted nanoparticles by affinity chromatography. *Biosensors & bioelectronics*, 24 (8), 2740–2743.

Haginaka, J., 2008. Monodispersed, molecularly imprinted polymers as affinity-based chromatography media. *Journal of chromatography. B, Analytical technologies in the biomedical and life sciences*, 866 (1-2), 3–13.

Haupt, K., Noworyta, K., and Kutner, W., 1999. Imprinted polymer-based enantioselective acoustic sensor using a quartz crystal microbalance. *Anal. Commun.*, 36 (11-12), 391–393.

He, Z., Whale, E.A., and Davis, F.J., 2004. Step-growth polymerization-basics and development of new materials. *In*: *Polymer chemistry: a pratical approach*. Oxford University Press, UK.

Hentzer, M. and Givskov, M., 2003. Pharmacological inhibition of quorum sensing for the treatment of chronic bacterial infections. *The Journal of Clinical Investigation*, 112 (9).

Van Herk, A.M. and Monteiro, M., 2003. *Heterogeneous systems. In handbook of radical polymerisation.* Hohn Wiley & Sons.

Hoffmann, F., Cinatl, J., Kabicková, H., Kreuter, J., and Stieneker, F., 1997. Preparation, characterization and cytotoxicity of methylmethacrylate copolymer nanoparticles with a permanent positive surface charge. *International journal of pharmaceutics*, 157 (2), 189–198.

Holmes, P. and Nicolls, L.M., 1995. Aeromonads in drinking-water supplies: their occurrence and significance. *Water and environment Journal*, 9 (5), 464–469.

Hong, K., Zhang, H., Mays, J.W., Visser, A.E., Brazel, C.S., Holbrey, D., Matthew, W., and Rogers, R.D., 2002. Conventional free radical polymerization in room temperature ionic liquids: a green approach to commodity polymers with practical advantages. *Chem. Commun.*, 1368–1369.

Hook, A.L., Chang, C.Y., Yang, J., Luckett, J., Cockayne, A., Atkinson, S., Mei, Y., Bayston, R., Irvine, D.J., Langer, R., Anderson, D.G., Williams, P., Davies, M.C., and Alexander, M.R., 2012. Combinatorial discovery of polymers resistant to bacterial attachment. *Nature biotechnology*, 30 (9), 868–875.

Hoshino, Y., Haberaecker, W.W., Kodama, T., Zeng, Z., Okahata, Y., and Shea, K.J., 2010. Affinity purification of multifunctional polymer nanoparticles. *Journal of the american chemical society*, 132 (39), 13648–13650.

Hoshino, Y., Kodama, T., Okahata, Y., and Shea, K.J., 2008. Peptide imprinted polymer nanoparticles: a plastic antibody. *Journal of the american chemical society*, 130 (46), 15242–15243.

Hoshino, Y., Koide, H., Urakami, T., Kanazawa, H., Kodama, T., Oku, N., and Shea, K.J., 2010. Recognition, neutralization, and clearance of target peptides in the bloodstream of living mice by molecularly imprinted polymer nanoparticles: a plastic antibody. *Journal of the american chemical society*, 132 (19), 6644–6645.

Hosier, I.L., Vaughan, A.S., Mitchell, G.R., Siripitayananon, J., and Davis, F.J., 2004. Polymer characterisation. *In*: *Polymer chemistry: a pratical approach*. Oxford University Press, UK.

Husain, F.M., Ahmad, I., Asif, M., and Tahseen, Q., 2013. Influence of clove oil on certain quorum-sensing-regulated functions and biofilm of *Pseudomonas aeruginosa* and *Aeromonas hydrophila*. *Journal of Biosciences*, 759, 1–10.

Irie, Y. and Parsek, M.R., 2008. Quorum sensing and microbial biofilms. *Current topics in microbiology and immunology*, 322, 67–84.

Jahid, I.K., Lee, N.Y., Kim, A., and Ha, S.D., 2013. Influence of glucose concentrations on biofilm formation, motility, exoprotease production, and quorum sensing in *Aeromonas hydrophil*a. *Journal of food protection*, 76 (2), 239–247.

Janda, J.M. and Abbott, S.L., 2010. The genus Aeromonas: taxonomy, pathogenicity, and infection. *Clinical microbiology reviews*, 23 (1), 35–73.

Jangid, K., Kong, R., Patole, M.S., and Shouche, Y.S., 2007. luxRI homologs are universally present in the genus Aeromonas. *BMC microbiology*, 7, 93.

Jayaraman, A. and Wood, T.K., 2008. Bacterial quorum sensing: signals, circuits, and implications for biofilms and disease. *Annual review of biomedical engineering*, 10, 145–167.

Jayaseelan, C., Rahuman, A.A., Roopan, S.M., Kirthi, A.V., Venkatesan, J., Kim, S.K., Iyappan, M., and Siva, C., 2013. Biological approach to synthesize TiO2 nanoparticles using *Aeromonas hydrophila* and its antibacterial activity. *Spectrochimica acta. Part A, Molecular and biomolecular spectroscopy*, 107, 82–89.

Jiang, G. and Su, M., 2009. Quorum-sensing of bacteria and its application. *Journal of ocean university of china*, 8 (4), 385–391.

Kalia, V.C. and Purohit, H.J., 2011. Quenching the quorum sensing system: potential antibacterial drug targets. *Critical reviews in microbiology*, 37 (2), 121–140.

Karatan, E. and Watnick, P., 2009. Signals, regulatory networks, and materials that build and break bacterial biofilms. *Microbiology and molecular biology reviews: MMBR*, 73 (2), 310–347.

Kendall, M. and Sperandio, V., 2007. Quorum sensing by enteric pathogens. *Current opinion in gastroenterology*, 23 (1), 10–15.

El Khadali, F., Hélary, G., Pavon-Djavid, G., and Migonney, V., 2002. Modulating fibroblast cell proliferation with functionalized poly(methyl methacrylate) based copolymers: chemical composition and monomer distribution effect. *Biomacromolecules*, 3 (1), 51–66.

Khajanchi, B.K., Sha, J., Kozlova, E. V, Erova, T.E., Suarez, G., Sierra, J.C., Popov, V.L., Horneman, A.J., and Chopra, A.K., 2009. N-acylhomoserine lactones involved in quorum sensing control the type VI secretion system, biofilm formation, protease production, and in vivo virulence in a clinical isolate of *Aeromonas hydrophila*. *Microbiology*, 155, 3518–3531.

Kievit, T.R.D.E., Gillis, R., Marx, S., and Brown, C., 2001. Quorum-sensing genes in Pseudomonas aeruginosa biofilms: their role and expression patterns. *Applied and environmental microbiology*, 67 (4), 1865–1873.

De Kievit, T.T. and Iglewski, B.H., 2000. Bacterial quorum sensing in pathogenic relationships. *Infection and Immunity*, 68, 4839–4849.

Kirby, A.E., Garner, K., and Levin, B.R., 2012. The relative contributions of physical structure and cell density to the antibiotic susceptibility of bacteria in biofilms. *Antimicrobial agents and chemotherapy*, 56 (6), 2967–2975.

Kirke, D.F., Swift, S., Lynch, M.J., and Williams, P., 2004. The *Aeromonas* hydrophila LuxR homologue AhyR regulates the N-acyl homoserine lactone synthase, AhyI positively and negatively in a growth phase-dependent manner. *FEMS Microbiology Letters*, 241 (1), 109–117.

Koch, B., Liljefors, T., Persson, T., Nielsen, J., Kjelleberg, S., and Givskov, M., 2005. The LuxR receptor: the sites of interaction with quorum-sensing signals and inhibitors. *Microbiology*, 151, 3589–3602.

Kollef, M.H., Golan, Y., Micek, S.T., Shorr, A.F., and Restrepo, M.I., 2011. Appraising contemporary strategies to combat multidrug resistant gram-negative bacterial infections--proceedings and data from the Gram-Negative Resistance Summit. *Clinical infectious diseases : an official publication of the Infectious Diseases Society of America*, 53 Suppl 2 (Suppl 2), S33–55; quiz S56–8.

Komnatnyy, V. V, Chiang, W.-C., Tolker-Nielsen, T., Givskov, M., and Nielsen, T.E., 2014. Bacteria-triggered release of antimicrobial agents. *Angewandte chemie,* 53 (2), 439–441.

Korposh, S., Chianella, I., Guerreiro, A., Caygill, S., Piletsky, S., James, S.W., and Tatam, R.P., 2014. Selective vancomycin detection using optical fibre long period gratings functionalised with molecularly imprinted polymer nanoparticles. *The analyst*, 139 (9), 2229–2236.

Kozlova, E. V, Khajanchi, B.K., Sha, J., and Chopra, A.K., 2011. Quorum sensing and c-di-GMP-dependent alterations in gene transcripts and virulence-associated phenotypes in a clinical isolate of *Aeromonas hydrophila*. *Microbial pathogenesis*, 50 (5), 213–223.

Kozlova, E. V, Popov, V.L., Sha, J., Foltz, S.M., Erova, T.E., Agar, S.L., Horneman, A.J., and Chopra, A.K., 2008. Mutation in the S-ribosylhomocysteinase (luxS) gene involved in quorum sensing affects biofilm formation and virulence in a clinical isolate of *Aeromonas hydrophila*. *Microbial pathogenesis*, 45 (5-6), 343–354.

Kregiel, D. and Niedzielska, K., 2014. Effect of plasma processing and organosilane modifications of polyethylene on *Aeromonas hydrophila* biofilm formation. *BioMed research international*, 2014.

Labanowski, J., Motoc, I., Naylor, C.B., Mayer, D., and Dammkoehler, R., 1986. Three-dimensional quantitative structure-activity relationships. 2.

Conformational mimicry and topographical similarity of flexible molecules. *Quantitative structure-activity relationships*, 5, 138–152.

De Lamo Marin, S., Xu, Y., Meijler, M.M., and Janda, K.D., 2007. Antibody catalyzed hydrolysis of a quorum sensing signal found in Gram-negative bacteria. *Bioorganic & medicinal chemistry letters*, 17 (6), 1549–1552.

Landini, P., Antoniani, D., Burgess, J.G., and Nijland, R., 2010. Molecular mechanisms of compounds affecting bacterial biofilm formation and dispersal. *Applied microbiology and biotechnology*, 86 (3), 813–823.

Lupp, C., Urbanowski, M., Greenberg, E.P., and Ruby, E.G., 2003. The *Vibrio fischeri* quorum-sensing systems ain and lux sequentially induce luminescence gene expression and are important for persistence in the squid host. *Molecular microbiology,* 50, 319–331.

Lynch, M.J., Swift, S., Kirke, D.F., Keevil, C.W., Dodd, C.E.R., and Williams, P., 2002. The regulation of biofilm development by quorum sensing in *Aeromonas hydrophila*. *Environmental microbiology*, 4 (1), 18–28.

Lyon, G.J. and Novick, R.P., 2004. Peptide signaling in *Staphylococcus aureus* and other Gram-positive bacteria. *Peptides*, 25 (9), 1389–403.

Mahanty, A., Mishra, S., Bosu, R., Maurya, U., Netam, S.P., and Sarkar, B., 2013. Phytoextracts-synthesized silver nanoparticles inhibit bacterial fish pathogen Aeromonas hydrophila. *Indian Journal of Microbiology*, 53 (4), 438–446.

Mariscal, A., Lopez-Gigosos, R.M., Carnero-Varo, M., and Fernandez-Crehuet, J., 2009. Fluorescent assay based on resazurin for detection of activity of disinfectants against bacterial biofilm. *Applied microbiology and biotechnology*, 82 (4), 773–783.

Martin, C.A., Hoven, A.D., and Cook, A.M., 2008. Therapeutic frontiers: preventing and treating infectious diseases by inhibiting bacterial quorum sensing. *European journal of clinical microbiology & infectious diseases : official publication of the European Society of Clinical Microbiology*, 27 (8), 635–642.

Martin-Carnahan, A. and Joseph, S.W., 2005. Family I. Aeromonadaceae. *In*: N.Y. Springer, ed. *Bergey's manual of systematic bacteriology, vol. 2, the proteobacteria, part B, the Gammaproteobacteria*. 556–558.

Mayes, a G. and Whitcombe, M.J., 2005. Synthetic strategies for the generation of molecularly imprinted organic polymers. *Advanced drug delivery reviews*, 57 (12), 1742–1778.

McCoy, C.P., Craig, R.A., Mcglinchey, S.M., Carson, L., Jones, D.S., and Gorman, S.P., 2012. Biomaterials surface localisation of photosensitisers on intraocular lens biomaterials for prevention of infectious endophthalmitis and retinal protection. *Biomaterials*, 33, 7952–7958.

Meighen, E.A., 1993. Bacterial bioluminescence: organization, regulation, and application of the lux genes. *FASEB journal : official publication of the Federation of American Societies for Experimental Biology*, 7 (11), 1016–1022.

Meng, Z., Wang, J., Zhou, L., Wnag, Q., and Zhu, D., 1999. New cocktail functional monomers in making molecule imprinting polymer with high chiral selectivity. *Progess in natural science*, 9 (794-795).

Merritt, J.H., Kadouri, D.E., and Toole, G.A.O., 2011. Growing and analyzing static biofilms, (August), 1–18.

Michailof, C., Manesiotis, P., and Panayiotou, C., 2008. Synthesis of caffeic acid and phydroxybenzoic acid molecularly imprinted polymers and their application for the selective extraction of polyphenols from olive mill waste waters. *Journal of chromatography A*, 1182, 25–33.

Miller, M.B. and Bassler, B.L., 2001. Quorum sensing in bacteria. *Annual review in microbiology*, 55, 169–199.

Miyashiro, T. and Ruby, E.G., 2012. Shedding light on bioluminescence regulation in *Vibrio fischer*i. *Molecular microbiology*, 84 (5), 795–806.

Moczko, E., Poma, A., Guerreiro, A., Perez de Vargas Sansalvador, I., Caygill, S., Canfarotta, F., Whitcombe, M.J., and Piletsky, S., 2013. Surface-modified multifunctional MIP nanoparticles. *Nanoscale*, 5 (9), 3733–3741.

Moons, P., Michiels, C.W., and Aertsen, A., 2009. Bacterial interactions in biofilms. *Critical reviews in microbiology*, 35 (3), 157–168.

Mosbach, K., 1994. Molecular imprinting. *Trends in Biochemical Sciences*, 19, 9–14.

Moxley, R.A, 2004. *Escherichia coli* 0157:H7: an update on intestinal colonization and virulence mechanisms. *Animal health research reviews / Conference of research workers in animal diseases*, 5 (1), 15–33.

Muniesa, M., Hammerl, J.A., Hertwig, S., and Appel, B., 2012. Shiga toxin-producing *Escherichia coli* O104:H4: a new challenge for microbiology. *Applied and Environmental Microbiology*, 78 (12), 4065–4073.

Nadell, C.D., Xavier, J.B., Levin, S.A., and Foster, K.R., 2008. The evolution of quorum sensing in bacterial biofilms. *PLoS biology*, 6 (1).

Nealson, K.H., 1978. Isolation, identification and manipulation by luminous bacteria. *Methods in Enzymology*, LVI.

Nealson, K.H., Platt, T., and Hastings, J.W., 1970. Cellular control of the synthesis and activity of bacterial luminescent system. *Journal of bacteriology*, 104 (1), 313–322.

Neiditch, M.B., Federle, M.J., Miller, S.T., Bassler, B.L., and Hughson, F.M., 2005. Regulation of LuxPQ receptor activity by the quorum-sensing signal autoinducer-2. *Molecular cell*, 18 (5), 507–518.

Ng, W.L. and Bassler, B.L., 2009. Bacterial quorum-sensing network architectures. *Annual review of genetics*, 43, 197–222.

Nicholson, J.W., 1997. *The chemistry of polymers.* 2nd Edition. UK: The Royal Society of Chemistry.

Nijvipakul, S., Wongratana, J., Suadee, C., Entsch, B., Ballou, D.P., and Chaiyen, P., 2008. Shedding light on bioluminescence regulation in *Vibrio fischeri. Journal of bacteriology*, 190 (5), 1531–1538.

Novick, R.P., 2003. Autoinduction and signal transduction in the regulation of staphylococcal virulence. *Molecular Microbiology*, 48 (6), 1429–1449.

Novick, R.P. and Geisinger, E., 2008. Quorum sensing in staphylococci. *Annual review of genetics*, 42, 541–564.

Novick, R.P. and Muir, T.W., 1999. Virulence gene regulation by peptides in staphylococci and other Gram-positive bacteria. *Current opinion in microbiology*, 2 (1), 40–5.

O'Brien, J., Wilson, I., Orton, T., and Pognan, F., 2000. Investigation of the Alamar Blue (resazurin) fluorescent dye for the assessment of mammalian cell cytotoxicity. *European journal of biochemistry / FEBS*, 267 (17), 5421–5426.

Odian, G., 2004. *Principles of polymerization.* Canada: Wiley-Interscince, John Wiley & Sons, Inc.

Pan, J. and Ren, D., 2009. Quorum sensing inhibitors: a patent overview. *Expert opinion on therapeutic patents*, 19 (11), 1581–1601.

Parsek, M.R. and Fuqua, C., 2004. Biofilms 2003: emerging themes and challenges in studies of surface-associated microbial life. *Journal of bacteriology*, 186 (14), 4427–4440.

Parsek, M.R. and Greenberg, E.P., 2005. Sociomicrobiology: the connections between quorum sensing and biofilms. *Trends in microbiology*, 13 (1), 27–33.

Parsek, M.R., Val, D.L., Hanzelka, B.L., Cronan, J.E., and Greenberg, E.P., 1999. Acyl homoserine-lactone quorum-sensing signal generation. *Proceedings of the national academy of sciences of the United States of America*, 96 (8), 4360–5.

Paul, D., Kim, Y.S., Ponnusamy, K., and Kweon, J.H., 2009. Application of quorum quenching to inhibit biofilm formation. *Environmental engineering science*, 26 (8), 1319–1324.

Peeters, E., Nelis, H.J., and Coenye, T., 2008. Comparison of multiple methods for quantification of microbial biofilms grown in microtiter plates. *Journal of microbiological methods*, 72 (2), 157–165.

Pérez-Moral, N. and Mayes, A.G., 2002. Molecular imprinting of polymeric core-shell nanoparticles. *Materials Research Society Symposium Proceedings*, 14, 667–670.

Pérez-Moral, N. and Mayes, A.G., 2006. MIP formats for analytical applications. *In*: S.A. Piletsky and A. Turner, eds. *Molecular imprinting of polymers*. Eurekah.com/Landes Biosciences, Georgetown, USA, 1–11.

Pettit, R.K., Weber, C.A., Kean, M.J., Hoffmann, H., Pettit, G.R., Tan, R., Franks, K.S., and Horton, M.L., 2005. Microplate alamar blue assay for *Staphylococcus epidermidis* biofilm susceptibility testing. *Antimicrobial agents and chemotherapy*, 49 (7), 2612–2617.

Pichon, V. and Chapuis-Hugon, F., 2008. Role of molecularly imprinted polymers for selective determination of environmental pollutants-a review. *Analytica chimica acta*, 622 (1-2), 48–61.

Pichon, V. and Haupt, K., 2006. Affinity separations on molecularly imprinted polymers with special emphasis on solid-phase extraction. *Journal of liquid chromatography & related technologies*, 29 (7), 989–1023.

Piletska, E. V and Piletsky, S.A, 2010. Size matters: influence of the size of nanoparticles on their interactions with ligands immobilized on the solid surface. *Langmuir : the ACS journal of surfaces and colloids*, 26 (6), 3783–3785.

Piletska, E. V, Stavroulakis, G., Karim, K., Whitcombe, M.J., Chianella, I., Sharma, A., Eboigbodin, K.E., Robinson, G.K., and Piletsky, S.A, 2010. Attenuation of *Vibrio fischer*i quorum sensing using rationally designed polymers. *Biomacromolecules*, 11 (4), 975–80.

Piletska, E. V, Stavroulakis, G., Larcombe, L.D., Whitcombe, M.J., Sharma, A., Primrose, S., Robinson, G.K., and Piletsky, S.A, 2011. Passive control of quorum sensing: prevention of *Pseudomonas aeruginosa* biofilm formation by imprinted polymers. *Biomacromolecules*, 12 (4), 1067–1071.

Piletsky, S.A, Turner, N.W., and Laitenberger, P., 2006. Molecularly imprinted polymers in clinical diagnostics-future potential and existing problems. *Medical engineering & physics*, 28 (10), 971–977.

Piletsky, S.A., Subrahmanyam, S., and Turner, A.P.F., 2001. Application of molecularly imprinted polymers in sensors for the environment and biotechnology. *Sensor review*, 21 (4), 292–296.

Piletsky, S.A., Karim, K., Piletska, E. V, Day, C.J., Freebairn, K.W., Legge, C., and Turner, A.P.F., 2001. Recognition of ephedrine enantiomers by molecularly imprinted polymers designed using a computational approach. *The analyst*, 126, 1826–1830.

Piletsky, S.A., Mijangos, I., Guerreiro, A., Piletska, E. V, Chianella, I., Karim, K., and Turner, A.P.F., 2005. Polymer cookery: influence of polymerization time and different initiation conditions on performance of molecularly imprinted polymers. *Macromolecules*, 38 (4), 1410–1414.

Pina, S., Vieira, S.I., Torres, P.M.C., Goetz-Neunhoeffer, F., Neubauer, J., da Cruz E Silva, O.A.B., da Cruz E Silva, E.F., and Ferreira, J.M.F., 2010. In vitro performance assessment of new brushite-forming Zn- and ZnSr-substituted beta-TCP bone cements. *Journal of biomedical materials research. Part B, Applied biomaterials*, 94 (2), 414–420.

Polowinski, S., 1997. *Template polymerization*. Canada: ChemTec Publishing.

Poma, A., 2012. Automatic solid-phase synthesis of molecularly imprinted nanoparticles (MIP NPs). Cranfield University 2012.

Poma, A., Guerreiro, A., Whitcombe, M.J., Piletska, E. V., Turner, A.P.F., and Piletsky, S.A., 2013. Solid-phase synthesis of molecularly imprinted polymer nanoparticles with a reusable template -“plastic antibodies”. *Advanced functional materials*, 23 (22), 2821–2827.

Poma, A., Turner, A.P.F., and Piletsky, S.A, 2010. Advances in the manufacture of MIP nanoparticles. *Trends in biotechnology*, 28 (12), 629–637.

Ponnusamy, K., Kappachery, S., Thekeettle, M., Song, J.H., and Kweon, J.H., 2013. Anti-biofouling property of vanillin on *Aeromonas hydrophila* initial biofilm on various membrane surfaces. *World journal of microbiology & biotechnology*, 29, 1695–1703.

Poobalane, S., Thompson, K.D., Ardó, L., Verjan, N., Han, H.-J., Jeney, G., Hirono, I., Aoki, T., and Adams, A., 2010. Production and efficacy of an Aeromonas hydrophila recombinant S-layer protein vaccine for fish. *Vaccine*, 28 (20), 3540–7.

Rahman, M., Huys, G., Rahman, M., Albert, M.J., Kühn, I., and Möllby, R., 2007. Persistence, transmission, and virulence characteristics of *Aeromonas* strains in a duckweed aquaculture-based hospital sewage water recycling plant in Bangladesh. *Applied and environmental microbiology*, 73 (5), 1444–1451.

Raina, S., De Vizio, D., Odell, M., Clements, M., Vanhulle, S., and Keshavarz, T., 2009. Microbial quorum sensing: a tool or a target for antimicrobial therapy? *Biotechnology and applied biochemistry*, 54 (2), 65–84.

Rampioni, G., Leoni, L., and Williams, P., 2014. The art of antibacterial warfare: Deception through interference with quorum sensing-mediated communication. *Bioorganic chemistry*, 1–9.

Ramström, O., Ye, L., and Gustavsson, P.E., 1998. Chiral recognition by molecularly imprinted polymers in aqueous media. *Chromatographia*, 48 (3/4), 197–202.

Rasch, M., Buch, C., Austin, B., Slierendrecht, W.J., Ekmann, K.S., Larsen, J.L., Johansen, C., Riedel, K., Eberl, L., Givskov, M., and Gram, L., 2004. An inhibitor of bacterial quorum sensing reduces mortalities caused by Vibriosis in rainbow trout (*Oncorhynchus mykiss*, Walbaum). *Systematic and applied microbiology*, 27 (3), 350–359.

Rasmussen, T.B. and Givskov, M., 2006. Quorum-sensing inhibitors as anti-pathogenic drugs. *International journal of medical microbiology : IJMM*, 296 (2-3), 149–161.

Reading, N.C. and Sperandio, V., 2006. Quorum sensing: the many languages of bacteria. *FEMS microbiology letters*, 254 (1), 1–11.

Rezzonico, F. and Duffy, B., 2008. Lack of genomic evidence of AI-2 receptors suggests a non-quorum sensing role for luxS in most bacteria. *BMC microbiology*, 8, 154.

Romero, D., Traxler, M.F., López, D., and Kolter, R., 2011. Antibiotics as signal molecules. *Chemical Reviews*, 111 (9), 5492–5505.

Romero, M., Acuña, L., and Otero, A., 2012. Patents on quorum quenching: interfering with bacterial communication as a strategy to fight infections. *Recent patents on biotechnology*, 6 (1), 2–12.

Rostamizadeh, K., Abdollahi, H., and Parsajoo, C., 2013. Synthesis, optimization, and characterization of molecularly imprinted nanoparticles. *International nano letters*, 3 (20).

Rutherford, S.T. and Bassler, B.L., 2012. Bacterial quorum sensing: its role in virulence and possibilities for its control. *Cold spring harbor perspectives in medicine*, 2 (11).

Santos, P.G., Santos, P.A, Bello, A.R., and Freitas-Almeida, A.C., 2011. Association of *Aeromonas caviae* polar and lateral flagella with biofilm formation. *Letters in applied microbiology*, 52 (1), 49–55.

Schauder, S., Shokat, K., Surette, M.G., and Bassler, B.L., 2001. The LuxS family of bacterial autoinducers: biosynthesis of a novel quorum-sensing signal molecule. *Molecular microbiology*, 41 (2), 463–476.

Schirhagl, R., Lieberzeit, P.A., and Dickert, F.L., 2010. Chemosensors for viruses based on artificial immunoglobulin copies. *Advanced Materials*, 22, 2078–2081.

Sellergren, B. and Greibrook, T., 2009. Molecular imprinting in separation science. *Journal Separation Science*, 32, 3263–3264.

Sellergren, B., Lepisto, M., and Mosbach, K. (1988).Highly enantioselective and substrate-selective polymers obtained by molecular imprinting utilizing noncovalent interactions-NMR and chromatographic studies on the nature of recognition", *Journal of the American Chemical Society*, 110, 5853-5860.

Sellergren, B. and Shea, K.J., 1993. Influence of polymer morphology on the ability of imprinted network polymers to resolve enantiomers. *Journal of chromatography A*, 635, 31–49.

Sergeyeva, T. A, Slinchenko, O. A, Gorbach, L. A, Matyushov, V.F., Brovko, O.O., Piletsky, S.A, Sergeeva, L.M., and Elska, G. V, 2010. Catalytic molecularly imprinted polymer membranes: development of the biomimetic sensor for phenols detection. *Analytica chimica acta*, 659 (1-2), 274–279.

Seshadri, R., Joseph, S.W., Chopra, A.K., Sha, J., Shaw, J., Graf, J., Haft, D., Wu, M., Ren, Q., Rosovitz, M.J., Madupu, R., Tallon, L., Kim, M., Jin, S., Vuong, H., Stine, O.C., Ali, A., Horneman, A.J., and Heidelberg, J.F., 2006. Genome sequence of *Aeromonas hydrophila* ATCC 7966T: jack of all trades. *Journal of bacteriology*, 188 (23), 8272–8282.

Shutov, R. V, Guerreiro, A., Moczko, E., de Vargas-Sansalvador, I.P., Chianella, I., Whitcombe, M.J., and Piletsky, S. a, 2014. Introducing MINA - the molecularly imprinted nanoparticle assay. *Small*, 10 (6), 1086–1089.

Smith, R.S. and Iglewski, B.H., 2003. *Pseudomonas aeruginosa* quorum sensing as a potential antimicrobial target. *The Journal of Clinical Investigation*, 112 (10).

Spoering, A.L. and Gilmore, M.S., 2006. Quorum sensing and DNA release in bacterial biofilms. *Current opinion in microbiology*, 9 (2), 133–137.

Stoodley, P., Sauer, K., Davies, D.G., and Costerton, J.W., 2002. Biofilms as complex differentiated communities. *Annual review of microbiology*, 56, 187–209.

Swift, S., Karlyshev, a V, Fish, L., Durant, E.L., Winson, M.K., Chhabra, S.R., Williams, P., Macintyre, S., and Stewart, G.S., 1997. Quorum sensing in *Aeromonas hydrophila* and *Aeromonas salmonicida*: identification of the LuxRI homologs AhyRI and AsaRI and their cognate N-acylhomoserine lactone signal molecules. *Journal of bacteriology*, 179 (17), 5271–5281.

Swift, S., Lynch, M.J., Fish, L., Kirke, D.F., Tomás, J.M., Stewart, G.S., and Williams, P., 1999. Quorum sensing-dependent regulation and blockade of exoprotease production in *Aeromonas hydrophila*. *Infection and immunity*, 67 (10), 5192–5199.

Swift, S., Throup, J.P., Williams, P., Salmond, G.G.P., and Stewart, G.S.A.B., 1996. Quorum sensing: a population density component in the determination of bacterial phenotype. *TIBS*.

Tacão, M., Moura, A., Correia, A., and Henriques, I., 2014. Co-resistance to different classes of antibiotics among ESBL-producers from aquatic systems. *Water research*, 48, 100–107.

Takeuchi, T. and Matsui, J., 1996. Feature Article Molecular imprinting : an approach to “ tailor-made ” synthetic polymers with biomimetic functions, 471480, 471–480.

Tan, C.J. and Tang, Y.W., 2007. Molecularly imprinted beads by surface imprinting. *Analytical Bioanalytical Chemistry*, 389, 369–376.

Tay, S.B. and Yew, W.S., 2013. Development of quorum-based anti-virulence therapeutics targeting gram-negative bacterial pathogens. *International journal of molecular sciences*, 14 (8), 16570–16599.

Teegarden, D.M., 2004. *Polymer chemistry: introduction to an indispensable science.* Arlington: National Science Teachers Association.

Tenover, F.C., 2006. Mechanisms of antimicrobial resistance in bacteria. *America journal of infection control*, 34, S3–S10.

Tokonami, S., Shiigi, H., and Nagaoka, T., 2009. Review: micro- and nanosized molecularly imprinted polymers for high-throughput analytical applications. *Analytica chimica acta*, 641 (1-2), 7–13.

Toole, G.O., Kaplan, H.B., and Kolter, R., 2000. Biofilm formation as microbial development. *Annual review in microbiology*, 54, 49–79.

Truchado, P., Gil-Izquierdo, A., Tomás-Barberán, F., and Allende, A., 2009. Inhibition by chestnut honey of N-acyl-L-homoserine lactones and biofilm formation in *Erwinia carotovora*, *Yersinia enterocolitica*, and *Aeromonas hydrophila*. *Journal of agricultural and food chemistry*, 57 (23), 11186–11193.

Tsao, C.-Y., Quan, D.N., and Bentley, W.E., 2012. Development of the quorum sensing biotechnological toolbox. *Current opinion in chemical engineering*, 1 (4), 396–402.

USEPA, 1998. *Announcement of the drinking water contaminant list notice.*

Vaihinger, D., Landfester, K., Krauter, I., Brunner, H., and Tovar, G.E.M., 2002. Molecularly imprinted polymers nanospheres as synthetic affinity receptors obtained by miniemulsion polymerisation. *Chemistry and physics*, 203, 1965–1973.

Verma, S.C. and Miyashiro, T., 2013. Quorum sensing in the squid-Vibrio symbiosis. *International journal of molecular sciences*, 14 (8), 16386–16401.

Vila, J., Ruiz, J., Gallardo, F., Vargas, M., Soler, L., Figueras, M.J., and Gascon, J., 2003. Aeromonas spp. and traveler's diarrhea: clinical features and antimicrobial resistance. *Emerging infectious diseases*, 9 (5), 552–555.

Vivas, J., Razquin, B.E., López-Fierro, P., Naharro, G., and Villena, A., 2004. Correlation between production of acyl homoserine lactones and proteases in an *Aeromonas hydrophila* aroA live vaccine. *Veterinary microbiology*, 101 (3), 167–176.

Waters, C.M. and Bassler, B.L., 2005a. Quorum Sensing : Communication in Bacteria.

Waters, C.M. and Bassler, B.L., 2005b. Quorum sensing: cell-to-cell communication in bacteria. *Annual review of cell and developmental biology*, 21, 319–46.

Watnick, P. and Kolter, R., 2000. Biofilm, city of microbes. *Journal of Bacteriology*, 182 (10), 2675–2679.

Webb, S. a R. and Kahler, C.M., 2008. Bench-to-bedside review: Bacterial virulence and subversion of host defences. *Critical care,* 12 (6), 234.

Weiss R., Freudenschuss, M., Krska, R., and Mizaikoff, B. (2003). Improving methods of analysis for mycotoxins: molecularly imprinted polymers for deoxynivalenol and zearalenone. *Food Additives and Contaminants*, 20, 386-395.

Whitcombe, M.J. and Vulfson, E.N., 2001. Imprinted polymers. *Advanced materials*, 13 (7), 467–478.

Whitehead, N.A, Barnard, A.M., Slater, H., Simpson, N.J., and Salmond, G.P., 2001. Quorum-sensing in Gram-negative bacteria. *FEMS microbiology reviews*, 25 (4), 365–404.

Williams, P., 2002. Quorum sensing: an emerging target for antibacterial chemotherapy? *Expert opinion on therapeutic targets*, 6 (3), 257–274.

Williams, P., 2007a. Quorum sensing, communication and cross-kingdom signalling in the bacterial world. *Microbiology*, (153), 3923–3938.

Williams, P., 2007b. Quorum sensing, communication and cross-kingdom signalling in the bacterial world. *Microbiology (Reading, England)*, 153 (Pt 12), 3923–3938.

Williams, P., Camara, M., Hardman, A., Swift, S., Milton, D., Hope, V.J., Winzer, K., Middleton, B., Pritchard, D.I., and Bycroft, B.W., 2000. Quorum sensing and the population-dependent control of virulence. *Philosophical transactions of the Royal Society of London. Series B, Biological sciences*, 355 (1397), 667–680.

Winzer, K., Hardie, K.R., and Williams, P., 2002. Bacterial cell-to-cell communication: sorry, can ' t talk now — gone to lunch! *Current opinion in Microbiology*, 5, 216–222.

Winzer, K. and Williams, P., 2001. Quorum sensing and the regulation of virulence gene expression in pathogenic bacteria. *International journal of medical microbiology : IJMM*, 291 (2), 131–143.

Wulff, G., 1995. Molecular imprinting in cross-linked materials with the aid of molecular templates - a way towards artificial antibodies. *Angewandte Chemie International Edition in English*, 34, 1812–1832.

Xavier, K.B. and Bassler, B.L., 2003. LuxS quorum sensing: more than just a numbers game. *Current opinion in microbiology*, 6 (2), 191–197.

Ye, L. and Mosbach, K., 2001. The technique of molecular imprinting – principle, state of the art, and future aspects. *Journal of inclusion phenomena and macrocylic chemistry*, 41, 107–113.

Ye, L., Weiss, R., and Mosbach, K., 2000. Synthesis and characterization of molecularly imprinted microspheres. *Macromolecules*, 33 (22), 8239–8245.

Young, Robert J., and Lovell, Peter A., 2011. *Introduction to polymers*. Third edition. CRC Press Taylor & Francis Group.

Yilmaz, E., Haupt, K., and Mosbach, K., 2000. The use of immobilized templates-a new approach in molecular imprinting. *Angewandte chemie*, 39 (12), 2115–2118.

Zhang, L., Murphy, P.J., Kerr, A., and Tate, M.E., 1993. *Agrobacterium* conjugation and gene regulation by N-acyl-L-homoserine lactones. *Nature*, 362, 446–448.

Appendices

8 Appendices

A.1 Appendix A: NMR characterisation

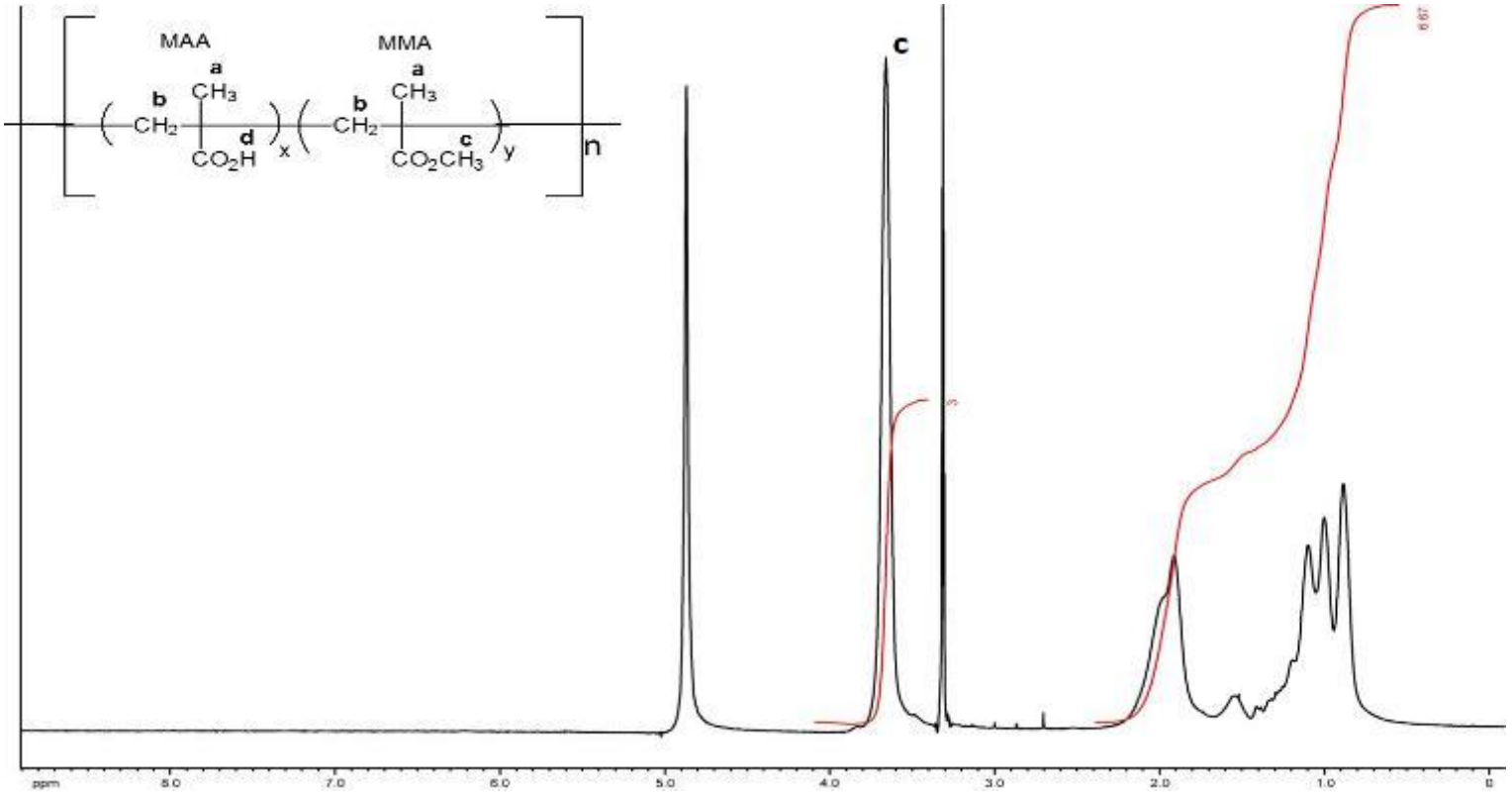

Figure_Apx A-1 1 ^{1}H NMR spectrum of *pMAA$_{25}$-co-pMMA$_{75}$* (400 MHz) in methanol-d4 (CD3OD) (integral values in red)

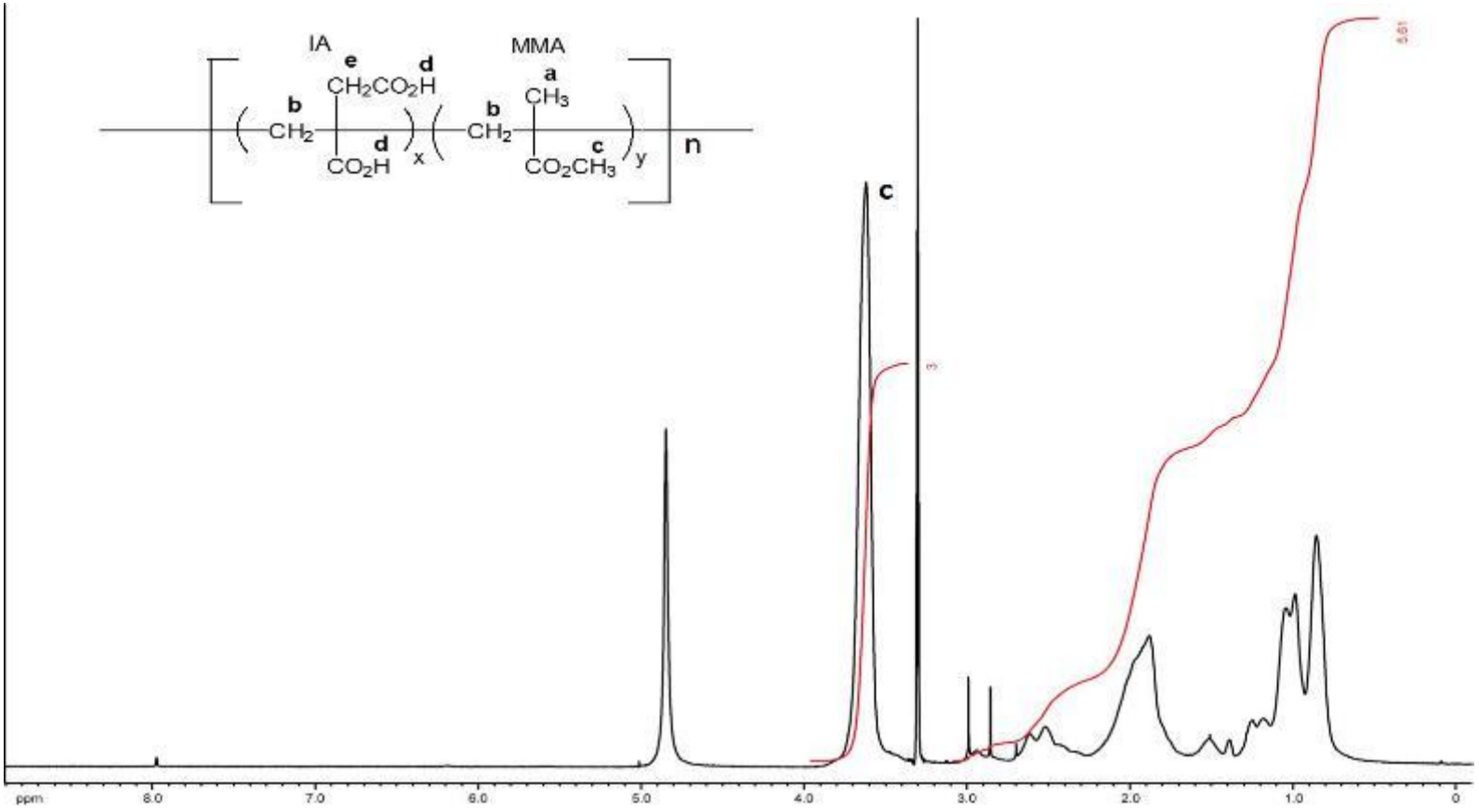

Figure_Apx A-1 2 ^{1}H NMR spectrum of *pIA$_{25}$-co-pMMA$_{75}$* (400 MHz) in methanol-d4 (CD3OD) (integral values in red)

A.2 Appendix B: Optical Density of Linear Polymers

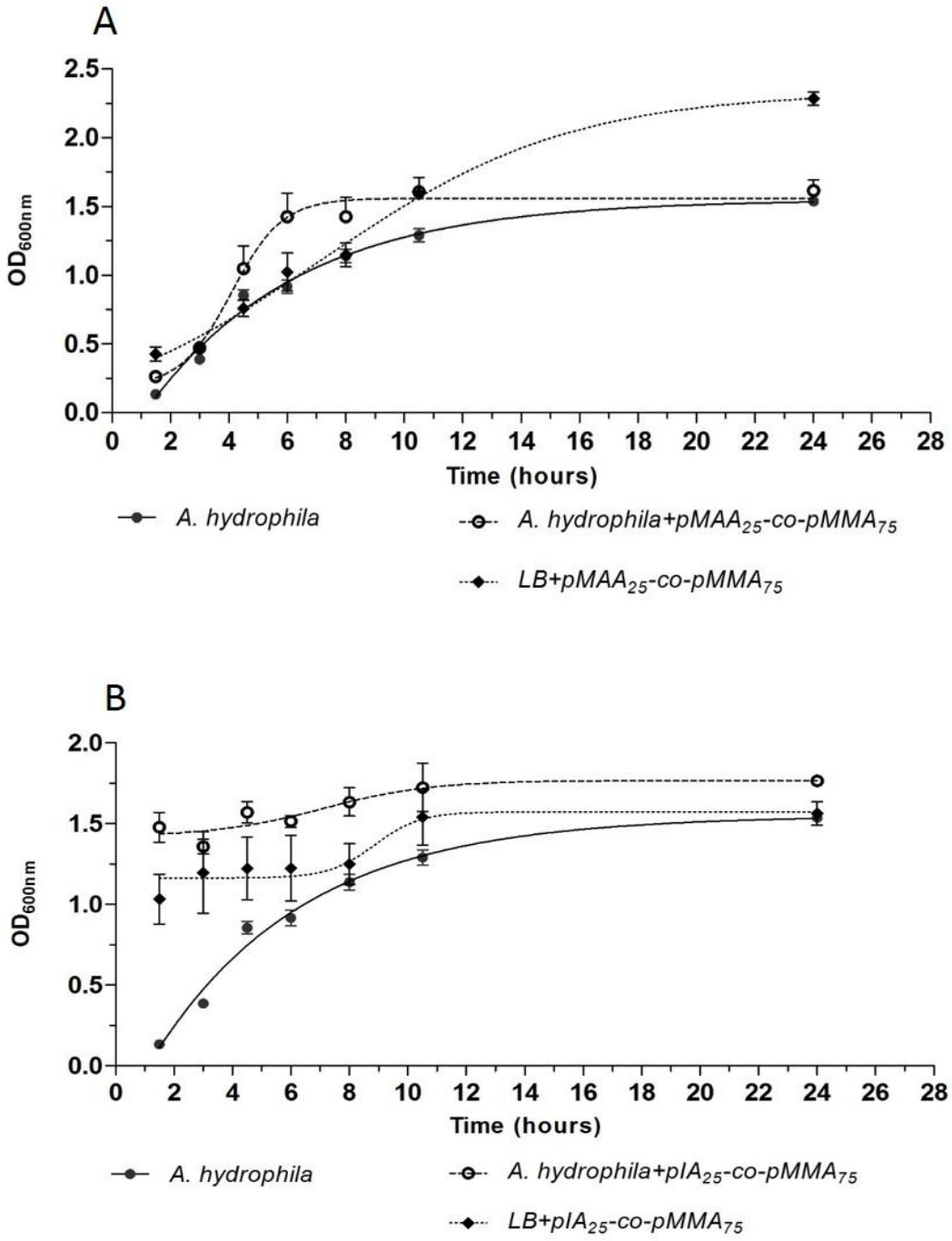

Figure_Apx B-1 3 Bacterial growth (OD at 600 nm) of *A. hydrophila* in the presence of $pMAA_{25}$-*co*-$pMMA_{75}$ (A) and pIA_{25}-*co*-$pMMA_{75}$ (B). The data represent means (standard deviations) of three independent experiments performed in triplicate

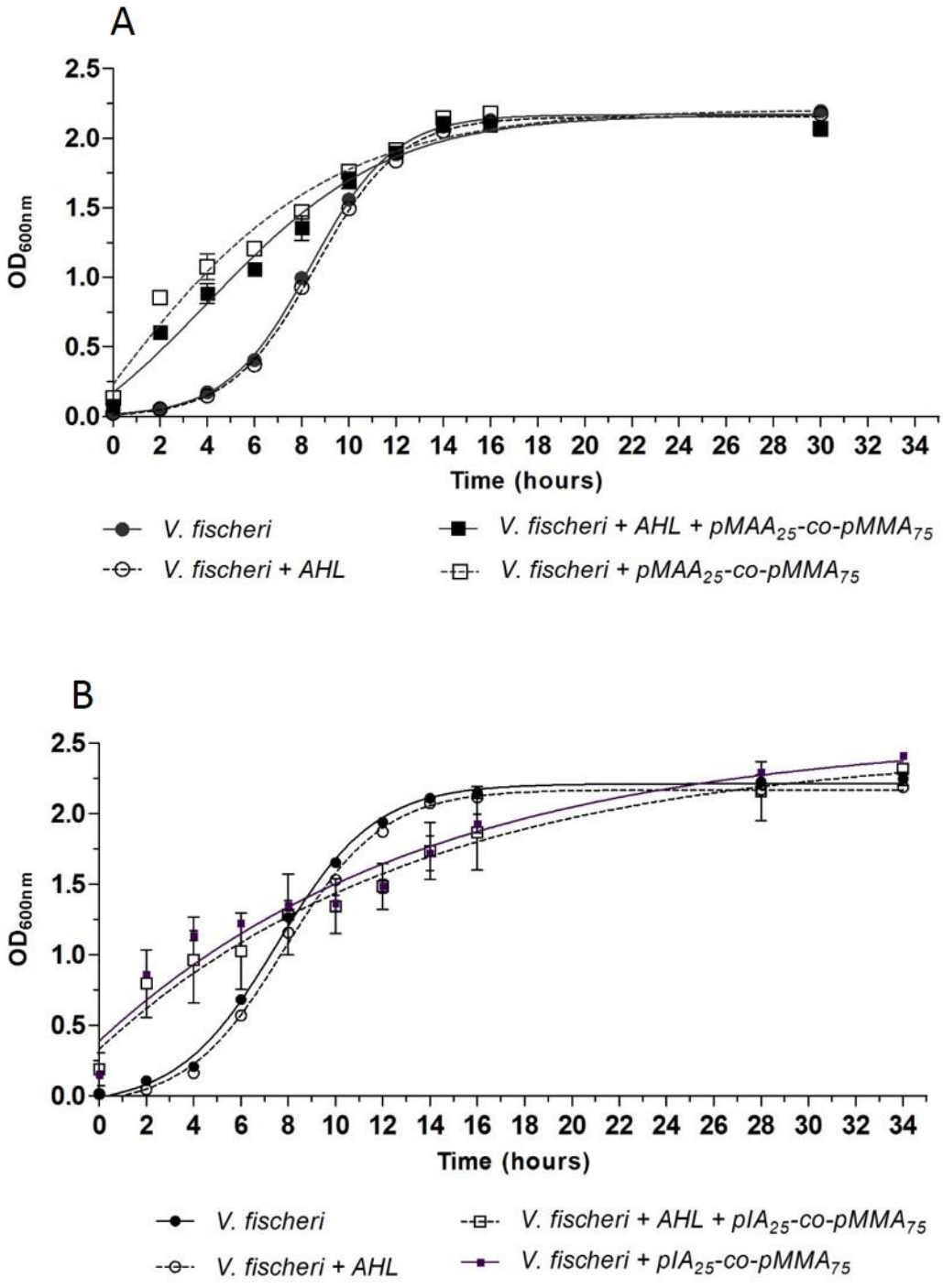

Figure_Apx B-1 4 Bacterial growth (OD at 600 nm) of *V. fischeri* in the presence of *pMAA$_{25}$-co-pMMA$_{75}$* (A) and *pIA$_{25}$-co-pMMA$_{75}$* (B). The data represent means (standard deviations) of three independent experiments performed in triplicate

A.3 Appendix C: Biofilm formation

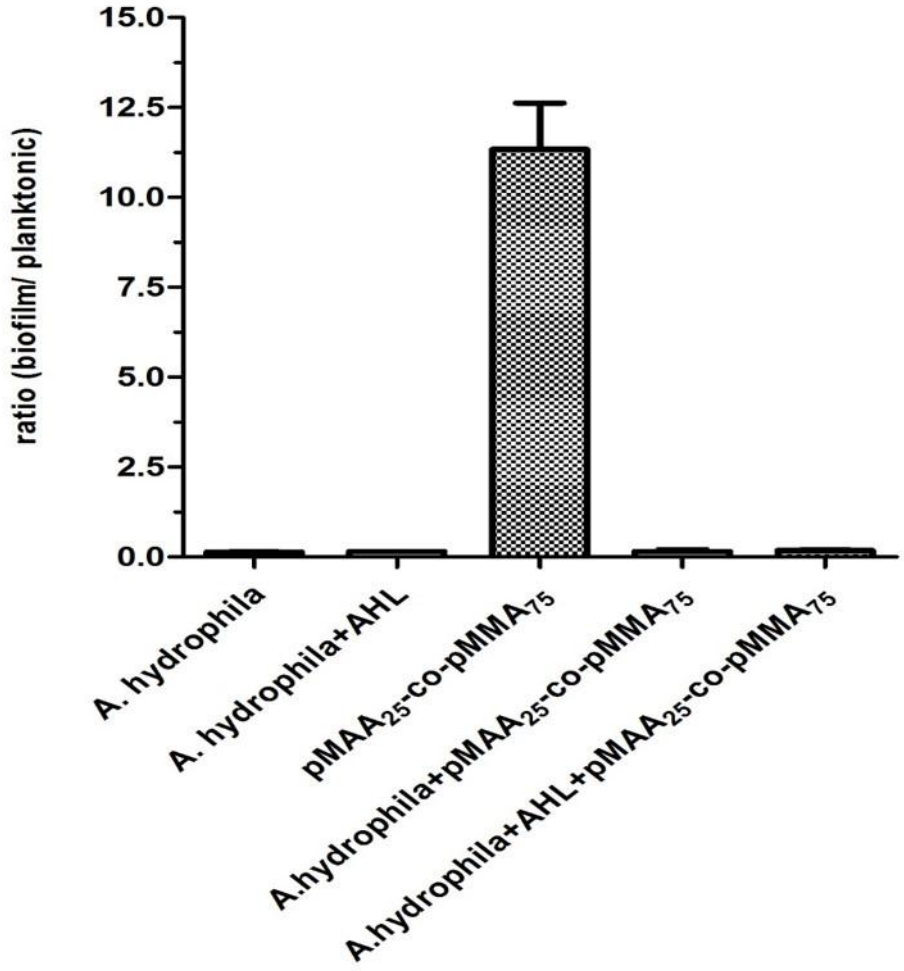

Figure_Apx C-1 5 ***Biofilm detection of A. hydrophila with pMAA$_{25}$-co-pMMA$_{75}$ through crystal violet.***

A.4 Appendix D: Biofilm Stain

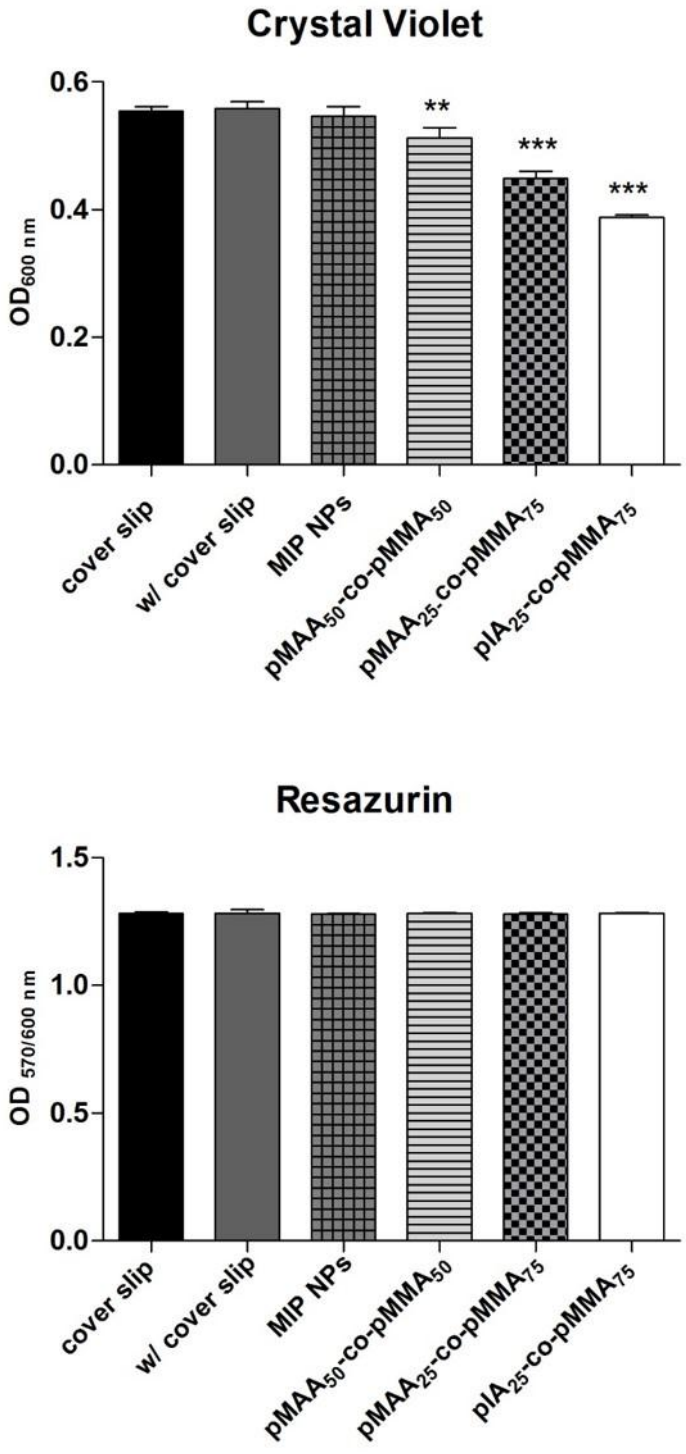

Figure_Apx D-1 6 Stain of polymeric materials in cover slips, respectively with crystal violet and resazurin.